# Investigation of antibody-mediated neutralization and protection against wild-type yellow fever virus by human monoclonal antibodies

by

Danielle R. D. Saunders

B.S., University of Colorado, Colorado Springs, 2008
M.S., University of Colorado, Colorado Springs, 2017

AN ABSTRACT OF A DISSERTATION

submitted in partial fulfillment of the requirements for the degree

DOCTOR OF PHILOSOPHY

Department of Diagnostic Medicine/Pathobiology
College of Veterinary Medicine

KANSAS STATE UNIVERSITY
Manhattan, Kansas

2022

# Abstract

Yellow fever virus (YFV) is the prototype flavivirus that causes severe viscerotropic disease. The disease yellow fever (YF) leads to a high mortality rate in immunologically naïve humans and New World primates in tropical South America. While the safe and effective live-attenuated 17D vaccine is available for disease control, recent outbreaks and vaccine shortages has led to a growing interest in the development of therapeutics and second-generation YF vaccines. To rationally design candidate vaccines that are not inferior to the 17D vaccine, a thorough understanding of the mechanisms of protection against wild-type (wt) strains of YFV is needed, especially neutralizing antibodies that are the correlate of protection elicited by the YF 17D vaccine. Although previous studies have indicated neutralizing antibody responses elicited by the 17D vaccine are type-specific (i.e., only neutralize YFV and does not cross-react with other flaviviruses) and mainly target the envelope (E) protein, few studies have investigated human monoclonal antibodies (mAbs). Therefore, a significant gap in knowledge exists on how a single dose of the 17D vaccine can confer long-lasting immune protection against the seven known genotypes of wt YFV in humans. The research described in this dissertation was undertaken to investigate the antibody-mediated neutralization and protection against wt YFV through the characterization of two YFV type-specific neutralizing human mAbs isolated from 17D vaccinees.

Three approaches were taken to test the central hypothesis that YFV type-specific neutralizing human mAbs isolated from 17D vaccinees recognize epitope(s) on the E protein and can neutralize and protect against wt YFV infection. First, the neutralizing potency of two human anti-YFV mAbs isolated from 17D vaccinees (mAb-29 and mAb-32) were quantified against the 17D-204 vaccine substrain and the representative strains of four genotypes of wt YFV including

West Africa I genotype (BA-55 strain), West Africa II genotype (Asibi strain), South America I genotype (JSS strain), and South America II genotype (1899/81 strain) to demonstrate both mAbs exhibit YFV type-specific neutralizing activities. The four-fold difference in neutralizing titers between the 17D-204 and wt Asibi strains was observed and provided the basis for the epitope characterization using the recombinant 17D-204 strain, Asibi strain, and four chimeras constructed to replace three individual domains of the E protein (ED) of the Asibi strain with the corresponding region in the 17D strain. The antigenic sites recognized by mAb-29 and mAb-32 were delineated by examining the neutralizing potency against recombinant Asibi strain, 17D strain, and Asibi-17D chimeras. The simultaneous replacement of EDI and EDII from the 17D strain altered the sensitivity of the Asibi strain to the neutralization of mAb-29 and mAb-32. Therefore, both mAbs target conformational epitope(s) consisting of amino acids across the EDI and EDII.

Lastly, the prophylactic passive protection of mAb-29 and mAb-32 against neurotropic and viscerotropic YF disease in mice was determined. Both mAbs conferred full protection against neurotropic disease caused by intracerebral challenge of the 17D vaccine strain in outbred CD-1 mice. MAb-29 and mAb-32 were further shown to partially protect against neurotropic disease caused by intracerebral challenge of the wt Asibi strain in CD-1 mice by increasing the median survival time and decreasing the brain viral load compared to the control group. Importantly, mAb-29 and mAb-32 demonstrated partial protection against viscerotropic disease caused by intraperitoneal challenge of the wt Asibi strain in C57BL/6 mice lacking type-I and type-II interferon receptors (C57BL/6-IFNAR$^{-/-}$-IFNGR$^{-/-}$), referred to as AG6 mice, by increasing the median survival time and significantly reducing the tissue viral load in the brain, liver, kidneys, spleen, and mesenteric draining lymph nodes compared to the control group.

Collectively, the completion of these projects advances our understanding of antibody-mediated neutralization and protection against wt YFV in humans. Both human anti-YFV mAbs belong to the YFV type-specific neutralizing antibody group relevant to the protective immunity elicited by YF 17D vaccines. The mAbs target multiple domains in the E protein, suggesting that at least one conformational epitope is responsible for eliciting neutralizing antibody responses in 17D vaccinees. Significantly, passive transfer of mAb-29 and mAb-32 confers protection against the wt YFV Asibi strain, directly demonstrating the involvement of human YFV type-specific neutralizing antibodies in the protective immunity against wt YFV challenge *in vivo*. Results from this dissertation research demonstrated the utility of human anti-YFV mAbs isolated from 17D vaccinees for the investigation of protective immunity against wt YFV and identified two anti-YFV mAbs that can potentially be evaluated as candidate therapeutic antibodies.

# Investigation of antibody-mediated neutralization and protection against wild-type yellow fever virus by human monoclonal antibodies

by

Danielle R. D. Saunders

B.S., University of Colorado, Colorado Springs, 2008
M.S., University of Colorado, Colorado Springs, 2017

A DISSERTATION

submitted in partial fulfillment of the requirements for the degree

DOCTOR OF PHILOSOPHY

Department of Diagnostic Medicine/Pathobiology
College of Veterinary Medicine

KANSAS STATE UNIVERSITY
Manhattan, Kansas

2022

Approved by:

Major Professor
Dr. Dana L. Vanlandingham

# Abstract

Yellow fever virus (YFV) is the prototype flavivirus that causes severe viscerotropic disease. The disease yellow fever (YF) leads to a high mortality rate in immunologically naïve humans and New World primates in tropical South America. While the safe and effective live-attenuated 17D vaccine is available for disease control, recent outbreaks and vaccine shortages has led to a growing interest in the development of therapeutics and second-generation YF vaccines. To rationally design candidate vaccines that are not inferior to the 17D vaccine, a thorough understanding of the mechanisms of protection against wild-type (wt) strains of YFV is needed, especially neutralizing antibodies that are the correlate of protection elicited by the YF 17D vaccine. Although previous studies have indicated neutralizing antibody responses elicited by the 17D vaccine are type-specific (i.e., only neutralize YFV and does not cross-react with other flaviviruses) and mainly target the envelope (E) protein, few studies have investigated human monoclonal antibodies (mAbs). Therefore, a significant gap in knowledge exists on how a single dose of the 17D vaccine can confer long-lasting immune protection against the seven known genotypes of wt YFV in humans. The research described in this dissertation was undertaken to investigate the antibody-mediated neutralization and protection against wt YFV through the characterization of two YFV type-specific neutralizing human mAbs isolated from 17D vaccinees.

Three approaches were taken to test the central hypothesis that YFV type-specific neutralizing human mAbs isolated from 17D vaccinees recognize epitope(s) on the E protein and can neutralize and protect against wt YFV infection. First, the neutralizing potency of two human anti-YFV mAbs isolated from 17D vaccinees (mAb-29 and mAb-32) were quantified against the 17D-204 vaccine substrain and the representative strains of four genotypes of wt YFV including

West Africa I genotype (BA-55 strain), West Africa II genotype (Asibi strain), South America I genotype (JSS strain), and South America II genotype (1899/81 strain) to demonstrate both mAbs exhibit YFV type-specific neutralizing activities. The four-fold difference in neutralizing titers between the 17D-204 and wt Asibi strains was observed and provided the basis for the epitope characterization using the recombinant 17D-204 strain, Asibi strain, and four chimeras constructed to replace three individual domains of the E protein (ED) of the Asibi strain with the corresponding region in the 17D strain. The antigenic sites recognized by mAb-29 and mAb-32 were delineated by examining the neutralizing potency against recombinant Asibi strain, 17D strain, and Asibi-17D chimeras. The simultaneous replacement of EDI and EDII from the 17D strain altered the sensitivity of the Asibi strain to the neutralization of mAb-29 and mAb-32. Therefore, both mAbs target conformational epitope(s) consisting of amino acids across the EDI and EDII.

Lastly, the prophylactic passive protection of mAb-29 and mAb-32 against neurotropic and viscerotropic YF disease in mice was determined. Both mAbs conferred full protection against neurotropic disease caused by intracerebral challenge of the 17D vaccine strain in outbred CD-1 mice. MAb-29 and mAb-32 were further shown to partially protect against neurotropic disease caused by intracerebral challenge of the wt Asibi strain in CD-1 mice by increasing the median survival time and decreasing the brain viral load compared to the control group. Importantly, mAb-29 and mAb-32 demonstrated partial protection against viscerotropic disease caused by intraperitoneal challenge of the wt Asibi strain in C57BL/6 mice lacking type-I and type-II interferon receptors (C57BL/6-IFNAR$^{-/-}$-IFNGR$^{-/-}$), referred to as AG6 mice, by increasing the median survival time and significantly reducing the tissue viral load in the brain, liver, kidneys, spleen, and mesenteric draining lymph nodes compared to the control group.

Collectively, the completion of these projects advances our understanding of antibody-mediated neutralization and protection against wt YFV in humans. Both human anti-YFV mAbs belong to the YFV type-specific neutralizing antibody group relevant to the protective immunity elicited by YF 17D vaccines. The mAbs target multiple domains in the E protein, suggesting that at least one conformational epitope is responsible for eliciting neutralizing antibody responses in 17D vaccinees. Significantly, passive transfer of mAb-29 and mAb-32 confers protection against the wt YFV Asibi strain, directly demonstrating the involvement of human YFV type-specific neutralizing antibodies in the protective immunity against wt YFV challenge *in vivo*. Results from this dissertation research demonstrated the utility of human anti-YFV mAbs isolated from 17D vaccinees for the investigation of protective immunity against wt YFV and identified two anti-YFV mAbs that can potentially be evaluated as candidate therapeutic antibodies.

# Table of Contents

# List of Figures

# List of Tables

# Acknowledgements

First, I would like to thank my major professor, Dr. Dana Vanlandingham, for her support and giving me the opportunity to gain experience and grow as a scientist. I am also incredibly grateful to Dr. Yan-Jang (Scott) Huang for his endless dedication to the research and myself. Lastly, I would like to thank my committee members Dr. Stephen Higgs and Dr. Brandon DeKosky for their invaluable advice, reagents, and review of my work.

I sincerely thank all the staff at the Biosecurity Research Institute, especially the lab coordinators and animal care team. I would also like to thank the Comparative Medicine Group personnel at Kansas State University College of Veterinary Medicine for their assistance. I would like to acknowledge and thank the Kansas State University College of Veterinary Medicine Intramural Grant Program for the research support. Thank you to the past and present members of the Vanlandingham Lab for your support, knowledge, friendship, and laughter during this time. Lastly, I would like to acknowledge the support from the Air Force Academy.

Importantly, I want to express my gratitude and love to my family for their support during this endeavor. Thank you to my mom, dad, and sister for your constant encouragement and laughter. Thank you to my husband and two children for your understanding, patience, laughter, and love.

**Disclaimer:** The views expressed in this article are those of the author and do not necessarily reflect the official policy or position of the Air Force, the Department of Defense, or the U.S. Government.

# Dedication

To Lena and Brody, may you find your passion in life, dream big, and foster the natural curiosity within you. I love you.

# Chapter 1 - Yellow fever virus

## 1.1 Overview of yellow fever virus

### A. History of yellow fever virus

Yellow fever virus (YFV) is a re-emerging zoonotic pathogen that causes viral hemorrhagic fever. The first account attributed to yellow fever (YF) disease was as early as 1648 in Guadeloupe and Yucatan (Hindle 1932). During the 17$^{th}$ century, YF was one of the most dreaded diseases, spreading between West Africa and tropical America by ship. Over the next 250 years, devasting epidemics occurred in the tropical and subtropical Americas with outbreaks on the North American coastline and in Europe. Outbreaks of YF were also recorded in the West Indies and West Africa. In 1848, Josiah Clark Nott was the first to suggest YF was spread by mosquitoes, but it was Cuban physician C.J. Finlay who published in 1881 the first theory of YF mosquito transmission (Finlay 1912).

During the Spanish-American war, YF caused significant morbidity and mortality for the American Army in Cuba, leading to the appointment of Army surgeon Walter Reed as head of the Yellow Fever Commission. In 1900, the work of the Reed Commission proved mosquitoes were the vector of YF (Strode et al. 1951). This also resulted in the first demonstration that a filterable virus caused a specific human disease (Strode et al. 1951). A breakthrough in YF research came in 1927, when Drs. A.F. Mahaffy and J.H. Bauer of the Yellow Fever Commission staff infected a rhesus monkey with blood from a YFV-infected 28-year-old Ghanian man named Asibi (Stokes, Bauer, and Hudson 1928). The propagation of YFV by monkey/monkey passage led to the isolation of the Asibi strain that was ultimately used to develop the vaccine strain in the 1930s.

While YF cases have significantly decreased since implementation of the YF vaccine program, YFV is considered as a re-emerging pathogen due to recent increases in the number of outbreaks. Infection with YFV causes an estimated 109,000 severe infections and 51,000 deaths in Africa and South America annually (Gaythorpe et al. 2021). Due to the large demand for outbreak control coupled with the inability to rapidly produce the vaccine in large quantities, there are recurring YF vaccine shortages (Gaythorpe et al. 2021). For example, during the 2016-2017 Angola/Democratic Republic of Congo outbreak, 6 million doses of the YF vaccine stockpile were depleted twice in the first half of 2016 and a fractional-dosage strategy had to be implemented (Barrett 2020). Therefore, there is a growing interest in producing second-generation YF vaccines by understanding how the 17D vaccine protects against wild-type (wt) YFV. Although it is well accepted that neutralizing antibodies are the correlate of protection for the YFV 17D vaccine strain based on direct challenge of nonhuman primates (NHPs) (Mason et al. 1973), the mechanism of antibody-mediated neutralization is poorly understood. Thus, it is important to investigate how neutralizing antibodies elicited by the YFV 17D vaccine strain protect recipients against wt YFV infections. Understanding this information is critical for designing therapeutics and rationally designing second-generation YF vaccines.

## B. Classification

The International Committee on Taxonomy of Viruses classifies YFV as a positive, single-stranded, enveloped RNA virus in the *Flaviviridae* family under the genus *Flavivirus* (International Committee on Taxonomy of Viruses, 2021). Yellow fever virus is the prototype species of the family *Flaviviridae*, genus *Flavivirus*, and the virus after which the family and genus names are derived: *flavus* – Latin for “yellow” due to YF disease affecting the liver leading to jaundice. Members of the *Flaviviridae* family are arthropod-borne viruses

(arboviruses), referring to a group of viral infections transmitted among vertebrate hosts by hematophagous (blood feeding) vectors including mosquitoes, ticks, or other biting flies. Of the 500 arboviruses recognized, more than 130 are associated with causing human disease.

The genus *Flavivirus* consists of approximately 70 members that infect a range of hosts that are capable of replicating in vertebrate and/or invertebrate cells (Cook and Holmes 2006). Flaviviruses are transmitted by mosquitoes, ticks, or have no known vectors and the viruses are found world-wide. More than 50% of flaviviruses are associated with human disease, ranging from asymptomatic to severe disease such as meningitis, encephalitis, or hemorrhagic disease (International Committee on Taxonomy of Viruses, 2021).

Flaviviruses are serologically related, which has been demonstrated by antibody binding assays (International Committee on Taxonomy of Viruses, 2021). Cross-neutralization tests using polyclonal antisera have been used to distinguish at least eight antigenic complexes to assign closely related flaviviruses (Calisher et al. 1989). The assignment of flaviviruses to their antigenic complexes is summarized in **Table 1.1**. The neutralization epitopes of YFV, however, are sufficiently distinct from other flaviviruses so the virus is excluded from an assigned complex and all strains of YFV belong to a single serotype (Monath 1999b; Marfin and Monath 2008).

**Table 1.1 Assignment of pathogenic flaviviruses in distinct serocomplexes.**
Cross-neutralization tests using polyclonal antisera have identified at least eight serocomplexes. Flaviviruses with insufficient cross-reactivity are not assigned to an antigenic complex. Reference: (Calisher et al. 1989).

| Antigenic complex | Viruses in complex | Virus examples |
|---|---|---|
| Tick-borne encephalitis | 12 | Tick-borne encephalitis, Powassan, Omsk hemorrhagic fever virus |
| Japanese encephalitis | 10 | Japanese encephalitis, Murray Valley encephalitis, St Louis encephalitis, Usutu, West Nile, Kunjin |
| Dengue | 4 | Dengue serotypes 1, 2, 3, and 4 |
| Not assigned due to insufficient cross-reactivity | 17 | Yellow fever, Zika, Spondweni |

## C. Transmission cycle and geographic distribution

Yellow fever is endemic in regions of sub-Saharan Africa and tropical South America where the enzootic transmission cycle of YFV involves mosquitoes and NHPs (Marfin and Monath 2008). Yellow fever virus is transmitted primarily through the bite of infected *Aedes* (*Ae.*) or *Haemagogus (Hg.)* spp. mosquitoes and amplified by both humans and NHPs (World Health Organization, 2021). Yellow fever virus has three transmission cycles: jungle (sylvatic), intermediate (savannah) that is only found in Africa, and urban (**Figure 1.1**). During the jungle cycle, transmission of YFV occurs between NHPs by mosquito species found in the forest canopy. Mosquito species maintaining the jungle cycle in sub-Saharan Africa include *Ae. africanus* mosquitoes whereas *Hg. janthinomys* and *Sabethes chloropterus* mosquitoes maintain the cycle in South America (Degallier et al. 1992; Barrett and Monath 2003). Spillover of YFV by mosquitoes from NHPs to humans can occur when humans are working or visiting the jungle.

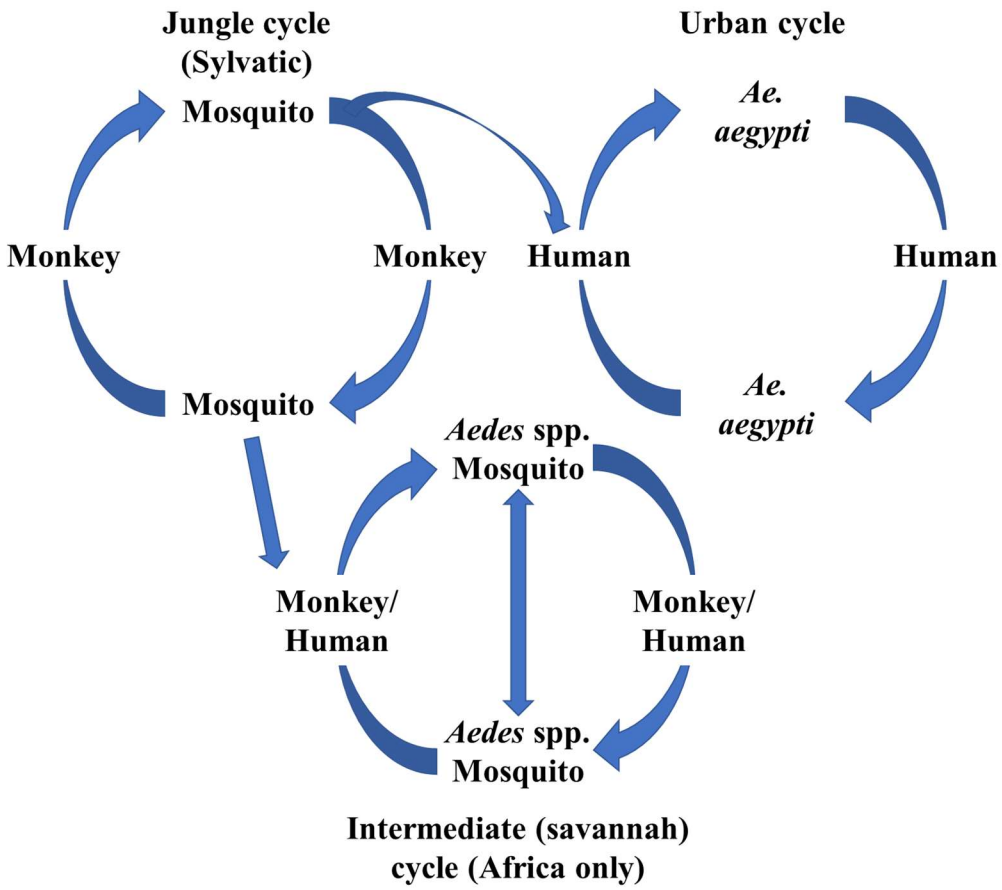


**Figure 1.1 Transmission cycle of YFV in Africa and South America.**
In both Africa and South America, the virus is primarily maintained in the jungle cycle by transmission among monkeys and the *Ae. africanus* or *Haemagogus* and *Sabethes* genera mosquitoes, respectively. Spillover occurs from the jungle cycle to either the urban or intermediate (savannah) cycle (Africa only). In the urban cycle, *Ae. aegypti* mosquitoes maintain the YFV transmission cycle with humans. In the sylvatic cycle, YFV is maintained by transmission among both monkeys and humans by several *Aedes* spp. mosquitoes. References: (Monath 2001; Mutebi and Barrett 2002).

The intermediate (savannah) cycle exists in Africa, supporting transmission of YFV from mosquitoes to humans living or working in jungle border areas. Human-to-human or NHP-to-human transmission can occur by mosquitoes during this cycle. Tree-hole breeding mosquitoes primarily of the *Aedes* spp. are responsible for transmission during the intermediate cycle in Africa (Germain et al. 1980). Lastly, the urban cycle involves transmission of YFV between humans and urban *Ae. aegypti* mosquitoes (Barrett and Monath 2003). The urban cycle is typically the result of humans infected with YFV in the jungle or savannah bringing the virus

back to an urban environment. While still reported in Africa, the last urban outbreak of YFV in South America occurred in Bolivia in the late 1990s (Monath 1999a; Barrett and Monath 2003).

During the early 1900s, regions in Central and North America, the Caribbean, and Southern Europe were infested with *Ae. aegypti* mosquitoes and had periodic outbreaks of YFV (Marfin and Monath 2008). These areas are at risk of YF should the virus be reintroduced. Yellow fever has not been reported in Asia or Australia despite the presence of susceptible mosquitoes such as *Ae. aegypti* (Aitken, Downs, and Shope 1977; Lataillade et al. 2020). Australian strains of *Ae. aegypti* and *Ae. notoscriptus* had similar infection, dissemination, and transmission rates compared to an *Ae. aegypti* strain (RexD Higgs white-eye strain) used extensively in YFV susceptibility studies (van den Hurk et al. 2011). Likewise, experimental infections indicate Asian strains of *Ae. aegypti* can transmit YFV but are less competent compared to other strains and evidence of geographical variation in this mosquito species has been observed (Beaty and Aitken 1979; Carrington and Auguste 2013). While the absence of YFV in Asia is not fully understood, there are several proposed hypotheses. Demographic factors including a lack of ideal ecological conditions (absence of a sylvan cycle) or cross protective immunity due to other predominant flaviviruses in the region (dengue or Japanese encephalitis virus) have been proposed (Baroian and Lozinskaia 1958; Saron et al. 2018).

The geographic distribution of YFV reflects the primary mosquito vectors. As shown in **Figure 1.2**, countries in Africa and South America that recommend vaccination correlates with the geographic distribution of YFV (CDC, 2019). According to the World Health Organization, YF is endemic in Africa from 15° north to 15° south of the Equator. The YF endemic region in Africa includes three climatic regions: equatorial rain forest, the moist savannah, and the dry savannah (Barrett and Higgs 2007). Many YF outbreaks occur in the moist savannah due to

heavy agricultural activity in this region. The vast majority of YF cases occur in Africa with an estimated global disease burden of 92.2% of annual cases (Gaythorpe et al. 2021). In South America, YFV is primarily found in the Orinoco, Amazon, and Araguaia river basins (Barrett and Higgs 2007). Here, YF occurs from December to May when *Haemagogus* spp. mosquitoes are prevalent due to the rainy season.

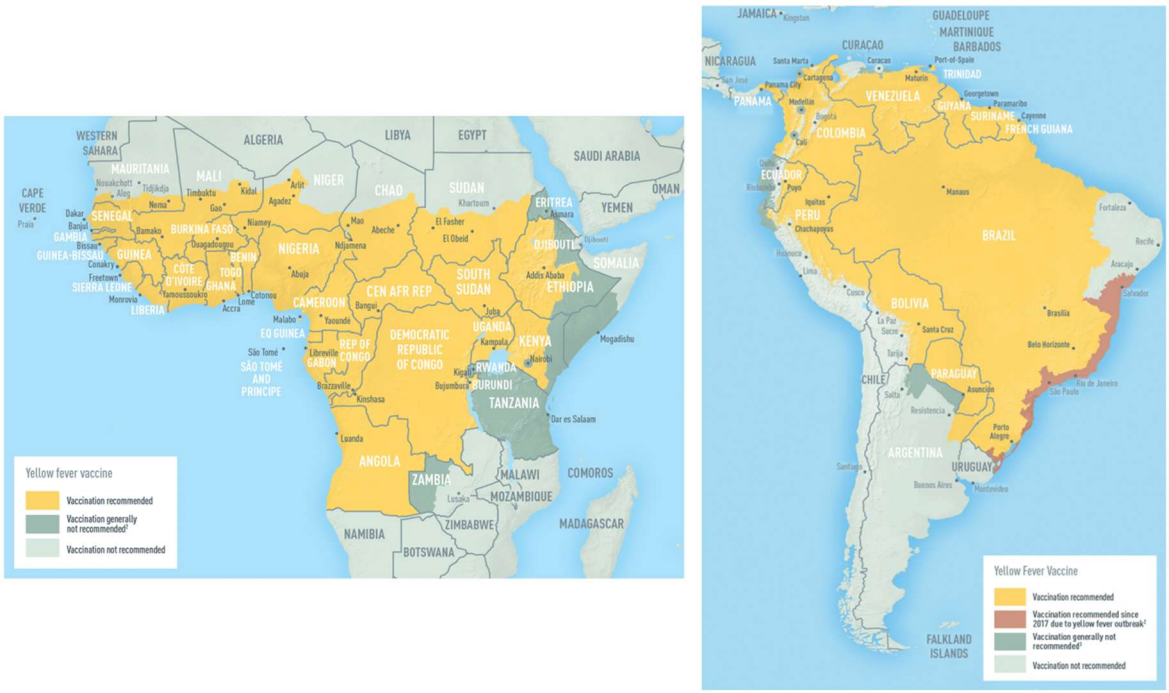


**Figure 1.2 Global distribution of YFV.**
Yellow fever virus is endemic in regions of sub-Saharan Africa and tropical South America and reflects the distribution of mosquito vectors. The highlighted regions are areas with risk of YFV transmission that recommend vaccination. Image taken from the CDC, www.cdc.gov; contributed by U.S. government employees and published in the public domain.

## D. Clinical disease

Yellow fever remains a major public health threat, particularly in Africa, despite the availability of an effective and safe vaccine. Wild-type YFV strains cause viscerotropic disease and rarely, neurotropic disease in humans (Marfin and Monath 2008). Clinical manifestations range from asymptomatic or mild infection to fatal hemorrhagic fever. While the majority of YF

infections are asymptomatic or mild, approximately 15% of symptomatic patients will develop severe disease (Mutebi and Barrett 2002). Yellow fever is an acute disease that includes two phases of development separated by a period of remission (WHO 1986). The two main phases of YF disease are the period of infection and the period of intoxication.

The incubation period is 3 to 6 days after the bite of a YFV-infected mosquito (Vainio, Cutts, and Organization 1998). Disease onset is sudden with symptoms including fever, chills, headache, back pain, nausea, dizziness, and myalgia (WHO 1986). Congestion of the conjunctivae and face as well as the unusual slow pulse in relation to a high fever (Faget's signs) are common during this phase. During the first 3 to 4 days after the onset of symptoms, the person is viremic and therefore infectious to mosquitoes (Government of Kenya, Ministry of Health 1996). After several days in this period of infection, patients may enter a "period of remission" that can last up to 24 hours and includes a disappearance of fever and symptoms (Tomori 1999). During remission, the virus is cleared by the cellular immune response and antibodies (Monath 2001). Some patients may recover after this stage with no further symptoms, however 15-25% of patients progress to a more severe form of the disease known as the "period of intoxication" (Monath 2001).

During the period of intoxication, or hepatorenal phase, patients experience fever, vomiting that may contain digested blood, jaundice, albuminuria, a reduction in urine production, and hemorrhagic signs such as bleeding of the gums, nose, and hematuria (WHO 1986; Vainio, Cutts, and Organization 1998). Additionally, serum transaminase levels rise and jaundice worsens (Tuboi et al. 2007). These correlate with the severity of illness. In the terminal stage of illness, hypoglycemia and hypotension contribute to metabolic acidosis as well as renal dysfunction (Monath 1987). Patients may also experience central nervous system signs such as

delirium, stupor, convulsive seizures, or coma (Monath 1987). Blood from patients in the toxic phase of YF infection do not contain virus, however, anti-YFV antibodies are detected during this phase (Mutebi and Barrett 2002). The fatality rate in cases that progress to the toxic phase can be between 20% and 50%, or higher, with death usually occurring 7 to 10 days after the onset of symptoms (WHO 1986). Patients who survive YF infection are immune for life (Mutebi and Barrett 2002).

## 1.2 Molecular virology and disease pathogenesis of YF

### A. Virus structure and genome

Yellow fever virus virions are small (40-60 nm in diameter), spherical, and contain a lipid envelope (Zhang et al. 2003; Marfin and Monath 2008). A mature YFV virion structure is currently not available; therefore, the cryo-electron microscopic structure of a mature dengue virus (DENV) particle is shown (**Figure 1.3**). The nucleocapsid core is surrounded by a host-derived lipid bilayer and an outer protein shell consisting of 180 copies of heterodimers that constitute the membrane (M) and envelope (E) proteins (Kuhn et al. 2002). The M protein is a molecular chaperone that guides the folding of the E protein during virion morphogenesis but is largely unexposed on the virion surface. The E protein is the major structural protein that occupies most of the virion surface. Two neighboring monomers of the E protein are antiparallel to each other, while the homodimers of the E protein form a "herringbone-like" pattern (Kuhn et al. 2002). Ninety copies of the E protein homodimers are assembled on the virion, creating 2-fold, 3-fold, and 5-fold asymmetry axes unique to flaviviruses (Pierson et al. 2007). The assembly of the E protein on the virion surface has significant implications for the binding of virions to various molecules, including cellular receptors and antibodies. This is because the same residue in the E protein may be presented differently in varying asymmetrical units. The

nucleocapsid core of the mature virion contains the single-stranded, positive sense RNA genome approximately 11-kilobases (kb) in length.

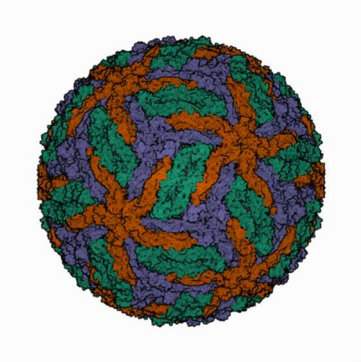

**Figure 1.3 Cryo-electron microscopic structure of a mature DENV particle.**
The structure of a mature YFV virion is currently not available, therefore the cryo-electron microscopic structure of a native, mature DENV particle is shown. Like YFV, DENV causes viral hemorrhagic fever and is transmitted by *Ae. aegypti* mosquitoes. The virion surface consists of membrane (M) and envelope (E) proteins; however, the E protein constitutes most of the virion surface. The M and E proteins are color-coded in the same color. Ninety copies of the E protein homodimers are assembled on the virion, creating 2-fold (green), 3-fold (blue), and 5-fold (red) asymmetry axes. Image from the Research Collaboratory for Structural Bioinformatics Protein Data Bank (RCSB PDB, rcsb.org) of PDB ID 3J27 (Zhang et al. 2013). Data files contained in the archive are free of all copyright restrictions.

The YFV genome is composed of a 5′ untranslated region (UTR) preceded by a type I cap structure (m7GpppAmp), a long single open reading frame (ORF), and a 3′ UTR. The cap structure increases viral genome stability by protecting against exonuclease activity and has an immunomodulatory role through evasion of intrinsic cellular defense mechanisms (Furuichi, LaFiandra, and Shatkin 1977; Daffis et al. 2010). Like all mosquito-borne viruses, YFV lacks a 3′-terminal poly(A) tail and instead terminates with the conserved dinucleotide CU. The 5′ and 3′ UTR contain conformational structures and complementary sequences necessary for replication and encapsidation of the genome (Marfin and Monath 2008).

The single ORF of 10,223 nucleotides (nt) encodes three structural and seven nonstructural (NS) proteins (Marfin and Monath 2008) (**Figure 1.4**). Beginning at the 5′ end, three structural proteins form the virion and include the capsid (C), pre-membrane/membrane

(prM/M), and E proteins. The C protein forms the nucleocapsid core, the prM facilitates folding and trafficking of the E protein during viral replication, and the E protein is responsible for receptor binding, fusion of the viral and endosomal membrane, and viral assembly (Konishi and Mason 1993; Kaufmann and Rossmann 2011). Additionally, the prM protects the E protein from premature fusion during virion morphogenesis while the E protein is the main antigenic target of neutralizing antibodies (Zhang et al. 2003; Carbaugh and Lazear 2020).

During the maturation process, the prM is cleaved by furin in the secretary pathway prior to release. The membrane-anchored M and E glycoproteins each contribute 180 copies to form the outer protein shell. The NS proteins NS1, NS2a, NS2b, NS3, NS4a, NS4b, and NS5 proceed the structural proteins. The NS proteins have enzymatic functions critical for RNA replication, translation, and protein cleavage, as well as serve as antagonists of the host innate immune response (Marfin and Monath 2008).

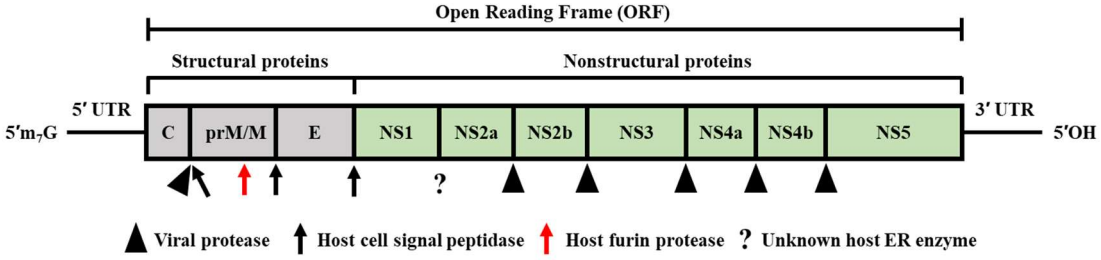


**Figure 1.4 Schematic diagram of the YFV genome and the proteolytic processing.** Yellow fever virus is a positive sense RNA virus flanked by a 5′ and 3′ UTR. The ORF is translated into a large viral polyprotein that is processed into structural proteins C, prM, and E, and NS proteins NS1, NS2a, NS2b, NS3, NS4a, NS4b, and NS5. The genome is capped on the 5′ end with a $N^7$ methylated guanosine cap (5′$m_7$G) and on the 3′ end forms a hairpin loop. Symbols indicate the viral and host enzymes that cleave the YFV proteins during processing.

## B. Virus replication cycle

The YFV life cycle begins with entry into mammalian host cells by receptor-mediated endocytosis. These interactions may be between the asparagine-linked sugars on the viral

structural proteins with various cellular C-type lectins such as the dendritic-cell-specific intercellular adhesion molecule-3-grabbing non-integrin (DC-SIGN) or mannose receptors, binding of E protein to glycosaminoglycans on the cell surface (e.g. heparin sulfate), or interactions with the T-cell immunoglobulin domain and mucin domain (TIM) and Tyro3, Axl, and Mertk (TAM) family of phosphatidylserine receptors (Chen et al. 1997; Tassaneetrithep et al. 2003; Meertens et al. 2012). Once the YFV virions are attached to cells, they are internalized by clathrin-dependent endocytic vesicles (van der Schaar et al. 2008).

During cellular entry, the conformational change of the YFV E protein triggers the fusion between viral and cellular (endosomal) membranes (Harrison 2008). The surface of the YFV particles is covered with 90 copies of E protein homodimers. The E protein is organized into three structurally distinct domains: envelope domain I, II, and III (EDI, EDII, and EDIII). Prior to viral membrane fusion, two neighboring copies of the E protein form an antiparallel dimer to protect the fusion loop at the tip of EDII. Upon acidification of the endosome, the dimers dissociate and the EDII of each monomer swing away from the viral membrane to expose the fusion loop. The fusion loop inserts into the target membrane to form an unstable trimeric intermediate structure. The EDIII rotates in each monomer to stabilize the post-fusion trimer, subsequently leading to the release of the viral genome into the cytoplasm (Harrison 2008).

Penetration of the YFV genome into the cytoplasm permits the cap-dependent translation of the viral polyprotein in association with the endoplasmic reticulum (ER) membrane. This initiation of translation is also enhanced by structures in the 5′ and 3′ UTRs (Ruiz-Linares et al. 1989; Li and Brinton 2001). The polyprotein is co- and post-translationally cleaved by viral and cellular proteases into the structural and NS proteins, and to initiate viral RNA replication (**Figure 1.4**). The structural proteins are incorporated into the virion while the non-enzymatic NS

proteins, including NS1, NS2a, NS4a, and NS4b proteins, are critical for virus replication, assembly, and immunomodulation (Muñoz-Jordán et al. 2003; Xie et al. 2013; Macdonald et al. 2005; Kümmerer and Rice 2002; Roosendaal et al. 2006). The enzymatic protein NS3 contains serine protease, nucleoside 5′ triphosphatase (NTPase), RNA helicase, and 5′ RNA triphosphatase (RTPase) activities, while NS2b serves as a cofactor to NS3 (Falgout et al. 1991; Wengler and Wengler 1991; Li et al. 1999). Lastly, the functional domains of the NS5 protein includes methyltransferase and RNA-dependent RNA polymerase (RdRp) activities necessary for genome replication and capping of RNA (Koonin 1991; Zhou et al. 2007).

Once the polyprotein is processed, the replication complex (RC) is formed on ER membranes. Evidence suggests the NS1 protein is on the luminal side of the ER; NS2a, NS2b, NS4a, and NS4b are integrated within the ER membrane; and NS3, NS5, and the viral RNA are on the cytoplasmic side of the membrane (Westaway et al. 1997; Welsch et al. 2009). The RC synthesizes negative-sense RNA that then serves as a template for the synthesis of genomic RNA progeny. While still in the ER, the genomic RNA progeny combine with newly synthesized viral proteins to form immature, fusion-incompetent virus particles (Kaufmann and Rossmann 2011). Once assembled, the immature virions traverse from the ER through the trans-Golgi network (TGN) to the cell surface. Acidification of the TGN exposes the furin cleavage site and the prM is cleaved but the protein stays with the virion to prevent membrane fusion (Yu et al. 2008). Upon release of the virus particles into the neutral pH extracellular milieu, the pr dissociates allowing for the formation of the mature virus particle (Yu et al. 2008). The cleavage of pr from M protein also causes the E proteins to rearrange on the particle surface that facilitates a metastable conformation to allow a low pH-triggered membrane fusion (Stiasny and Heinz

2006). Ultimately, the mature, infectious virions pass through the secretory pathway and progeny viruses are exocytosed from the cell.

## C. Genotypes of YFV

Yellow fever virus genotypes are defined based on their geographic distribution. Genomic sequence analyses of YFV structural and NS genes have identified at least seven distinct genotypes with a high degree of homology (Chang et al. 1995; Mutebi et al. 2001). Yellow fever virus was divided into West and East African genotypes prior to its introduction into the Americas. Five African genotypes are now recognized: West Africa I, West Africa II, East Africa, East/Central Africa, and Angola (**Figure 1.5.A**). South American YFV is subdivided into two genotypes: South America I (Brazil) and South America II (western portion of the continent) (Marfin and Monath 2008) (**Figure 1.5.B**).

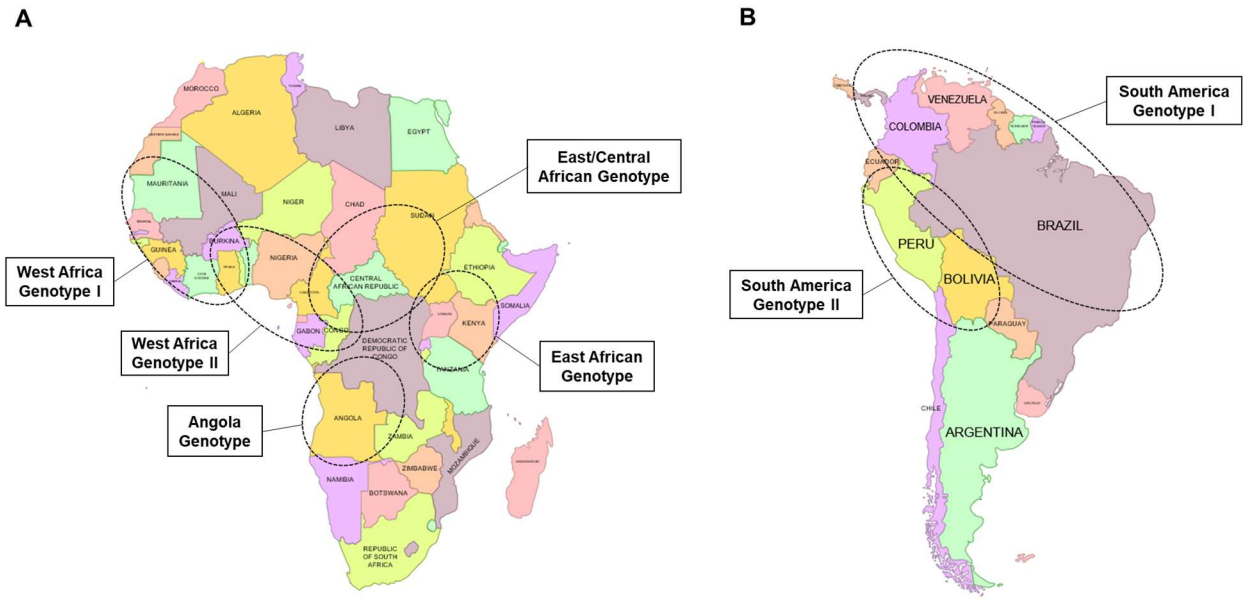


**Figure 1.5 Recognized geographic distribution of the seven YFV genotypes.**
Yellow fever virus is divided into five African genotypes including West Africa I, West Africa II, East Africa, East/Central Africa, and Angola (**A**). South America is divided into two genotypes including South America I and South America II (**B**).

The West Africa genotype I is distributed from eastern Côte d'Ivoire to Cameroon and Nigeria (Lepiniec et al. 1994; Mutebi et al. 2001). The West Africa genotype II is primarily

found from the western part of the Côte d'Ivoire and Mali to Senegal (Lepiniec et al. 1994). The Angola genotype is primarily found in Angola (Mutebi et al. 2001). The Eastern/Central African genotype is distributed in the Central African Republic, portions of Sudan, Uganda, Ethiopia, and the Democratic Republic of the Congo (Mutebi et al. 2001; Barrett and Higgs 2007). Lastly, the East African genotype is primarily found in portions of Kenya, Southern Sudan, Uganda, and Tanzania (Mutebi et al. 2001). The earliest existing strain of YFV was isolated from a man named Asibi in Ghana, West Africa in 1927, termed the "Asibi" strain (Stokes, Bauer, and Hudson 1928). The Asibi strain is West African genotype II and considered the prototype strain. West African genotype I strains circulating in Nigeria and surrounding areas are more genetically heterogeneous compared to other genotypes and are associated with more frequent outbreaks (Mutebi and Barrett 2002).

In South America, genotype I is distributed in Brazil, Panama, Columbia, Ecuador, Venezuela, and Trinidad (de Filippis et al. 2002). The South America genotype II is primarily distributed in Peru and Bolivia, but some isolates have been found in Brazil and Trinidad (Bryant and Barrett 2003). The first South American strain, "JSS," was isolated from a human case in Brazil in 1935. Analysis of 79 YFV isolates collected between 1935 through 2001 showed a single genotype circulating in Brazil, including the JSS strain, with one exception of a South American genotype II isolate (de Filippis et al. 2002). Comparative phylogenies of YF isolates from Brazil and Peru are genetically distinct with some strains persisting within specific locales whereas others are dispersed over thousands of kilometers (Bryant and Barrett 2003).

Based on nucleotide sequences and phylogenetic analysis, it is accepted that YFV originated in Africa because YFV is genetically more heterogeneous in Africa than South America (Lepiniec et al. 1994). South American lineages are monophyletic, originating from the

West African lineages, which indicates a probable source of introduction that is consistent with an African origin of YFV (Marfin and Monath 2008). The subgroups in West Africa may have evolved separately because there is a divergence from the East African and Angolan strains (Lepiniec et al. 1994). The phenotypic correlates of YFV sequence diversity remains to be determined due to the majority of studies using the YFV 17D vaccine strain or the parental wt Asibi strain, with a lack of studies using the other genotypes (Kleinert et al. 2019).

Genetic studies show variation among the YFV genotypes associated with different geographic regions that evolved slowly over time (Deubel et al. 1986). Each YFV genotype is distinct, representing independent evolution of the lineage, and are genetically stable with little nucleotide variation (Deubel et al. 1986; Mutebi et al. 2001). Between the YFV genotypes there is up to 25% nucleotide variation with approximately 7% amino acid divergence (von Lindern et al. 2006). Phylogenetic analysis based on various portions of the YFV genome including the 5′ and 3′ UTR, and fragments from prM/M, E, NS4a, and NS4b proteins gave consistent genotypic results, suggesting different regions of the genome can be used to represent the entire YFV genome (Wang et al. 1996; Mutebi et al. 2001).

Interestingly, the evolutionary divergence of YFV genotypes is associated with changes in the size of the 3′ UTR. The 3′ UTR has the largest size heterogeneity among YFV genotypes that is correlated with geographical distribution (Mutebi et al. 2004; Bryant et al. 2005). These variations are due to one to three deletions and/or duplications, termed repeated nucleotide sequence elements (RYF) (Mutebi et al. 2004). West African genotypes contain three copies of the RYF, Angola and the East/Central African genotypes two, and South American genotypes having only one copy of the RYF (Mutebi et al. 2004). These data may help in distinguishing the different strains of YFV.

## D. Disease pathogenesis in the vertebrate host

Wild-type YFV strains are predominately viscerotropic in humans and NHPs, causing lesions in multiple organs including the liver, spleen, heart, and kidneys (Hudson 1928). While natural infection of YFV-induced encephalitis is rare in primates, YF encephalitis can be artificially induced in mice under laboratory conditions. Even if NHPs are challenged with YFV by the intracerebral (ic) route, they die from hepatitis rather than encephalitis (Marfin and Monath 2008). However, an early study found that when a small amount of antibody was given to monkeys before or concurrently with YFV injected intracerebrally, the animal dies of encephalitis (Findlay and Stern 1935). These outcomes are likely related to the perivascular hemorrhage tendency leading to death during YF infection and not a true encephalitis (Stevenson 1939). While YF pathogenesis and pathophysiology are still only partially defined, studies in NHP models, hamster models, and human tissue biopsies from fatal YF cases have helped to elucidate our understanding of YF disease pathogenesis.

Primates (including humans) develop high viremia and hepatitis following the bite of an infected mosquito, an important feature crucial for YFV transmission by mosquitoes. African NHPs do not normally produce severe disease, although they do develop viremia high enough to maintain transmission (Valentine, Murdock, and Kelly 2019; Mares-Guia et al. 2020). In contrast, some New World and Asian primates develop lethal infection with sudden onset of hepatitis that resembles human disease (Bugher 1951). The pathophysiology of YF is characterized by liver dysfunction, kidney failure, coagulopathy, and shock. Yellow fever-induced pathogenesis begins after the bite of a YFV-infected mosquito. The general steps include 1) viral multiplication at the site in the skin, 2) migration to draining lymph nodes (DLNs), 3) induction of viremia, 4) replication in the liver, and finally 5) triggering a cytokine storm

ultimately leading to vasculopathy and multiorgan dysfunction. Viral replication in the liver is critical to the establishment of disease through the induction of proinflammatory cytokines. Based on *in vitro* studies, wt YFV and YFV 17D vaccine strains have broad tissue tropism. A brief synopsis of each step is discussed in further detail below.

At the site of inoculation, lymphoid cells serve as early replication sites. Dendritic cells (DCs) also serve a vital role during the early stage of infection by processing the viral antigens into immunogenic peptides to present to T cells and secreting immunoregulatory cytokines to activate the innate and adaptive immune responses. Yellow fever virus spreads from the DLNs to the central lymph nodes. While the extent of lymphoid injury directly attributed to YFV replication is unknown, lymphocytic elements in the germinal centers of the spleen, lymph nodes, tonsils, and Peyer's patches are depleted (Klotz and Belt 1930; Monath et al. 1981).

Once YFV is amplified in the DLNs, the virus spreads to the visceral organs. There, its target organ is the liver where the virus targets Kupffer cells and hepatocytes. The infected liver Kupffer cells in the sinusoids lead to hepatocyte infection. The Kupffer cells and hepatocytes undergo eosinophilic degeneration with condensed nuclear chromatin (Councilman bodies) (Vieira et al. 1983). Degeneration of hepatocytes occurs in the late phase of YF infection with 5% to 100% (mean of 80%) of hepatocytes undergoing coagulative necrosis in humans with viscerotropic disease (Klotz and Belt 1930). Lesions may also occur in the kidney, spleen, thymus, and heart in humans and/or animal models (De Brito et al. 1992; Meier et al. 2009; Melo-Lima et al. 2015).

In the terminal stage, system inflammatory response syndrome (SIRS) leads to shock with the appearance of antibody and cellular responses coinciding with the toxic phase. Macrophages and endothelial cells are thought to play an important role in the dysregulation of

cytokine and chemokine responses, as these cells support replication of several other hemorrhagic fever viruses (ter Meulen et al. 2004). In YF-infected patients, increased CD4+ T cells have been detected, leading to the expression of pro-inflammatory cytokines interferon (IFN)-γ and tumor necrosis factor alpha (TNF-α), a mediator of liver injury (Bradham et al. 1998). Elevated levels of TNF-α from both CD4+ T cells and macrophages may enhance CD8+ T cell cytolysis and liver damage (Quaresma et al. 2007; Douam and Ploss 2018). Collectively, this cytokine storm is correlated with hepatoxicity and YF disease, as fatal cases of YF have elevated pro-inflammatory cytokines compared to non-fatal cases, suggesting high levels contribute to lethality (ter Meulen et al. 2004; Marfin and Monath 2008).

### E. Human immune responses to natural YFV infection

Immune responses have the utmost importance in disease pathogenesis and more importantly, protection after either natural infection or vaccination. The scope of this dissertation research is to investigate a crucial part of protective immunity elicited by the 17D vaccine. Therefore, a brief overview of human immune responses to natural YFV infection has a dual purpose: 1) to provide the basis for the discussion of protective immunity of 17D vaccines and 2) to highlight and distinguish the immune responses developed towards the wt YFV strains and the 17D vaccine strain. In this section, an overview of human immune responses to YFV infection will be given in the context of natural infection. The detailed discussion of protective immunity elicited by the vaccine strain will be discussed in Section 1.3.

Most of our knowledge of immune responses to YFV has been derived from 1) the characterization of human immune responses elicited by the YFV vaccine strain, 2) the investigation of murine responses towards wt or vaccine strains of YFV (discussed further in Section 1.5), and 3) the post-mortem examination of specimens collected from individuals

infected with wt YFV. There is a major gap of knowledge in what constitutes the protective immunity against wt YFV strains in humans because most studies are only descriptive in their analysis and failed to demonstrate passive protection achieved by specific immune responses *in vivo*. Natural infection with wt YFV elicits both innate and adaptive immune responses, resembling infection with other pathogenic flaviviruses. It is also generally assumed that protective immunity against wt YFV, or any flavivirus, involves both innate and adaptive immune responses.

***Innate immune responses.*** The activation of innate immune responses against wt YFV involves the detection of viral RNA. Replication of the flavivirus genome produce single-stranded and double-stranded RNA intermediates in the cytoplasm, which are considered pathogen associated molecular patterns (PAMPs) and can be detected by various pattern recognition receptors (PRRs). There are specific classes of PRRs that commonly initiate the anti-viral signaling cascades against YFV and flaviviruses, including toll-like receptors (TLRs) and cytoplasmic retinoic acid inducible gene I (RIG-I)-like receptors (RLRs) (Kato et al. 2006; Loo et al. 2008; Nasirudeen et al. 2011). The detection of viral RNA by TLRs activates the MyD88-mediated immune signaling pathway and RLRs activate signal transduction pathways such as RIG-I and melanoma differentiation-associated protein 5 (MDA5). Both signaling pathways lead to the expression of pro- and anti-inflammatory cytokines.

Cytokines such as type I and type III IFNs are activated during the early phase of YFV infection to drive the transcriptional regulation of hundreds of IFN-stimulated genes (ISGs). Type I IFNs (IFN-α and -β) induce both direct and indirect antiviral states such as the modulation of viral attachment, entry, and trafficking, viral protein production, or viral particle assembly and exocytosis (as reviewed by Schoggins 2019). The importance of type-I IFNs in

controlling flavivirus infections is well recognized, as immunocompromised mice that lack type I-IFN receptors are highly sensitive to a broad range of flaviviruses, including YFV (Shresta et al. 2006; Meier et al. 2009; Sarathy et al. 2018). Type III IFNs (IFN-λ) have direct antiviral effects by binding receptors primarily at the barrier surface (i.e., epithelial cells) and modulating T and B lymphocyte responses (as reviewed by Lazear, Nice, and Diamond 2015).

The early and rapid production of IFNs, complement proteins, and innate immune cells induced by YFV plays a vital role in host protection. This was demonstrated when monkeys given the YFV vaccine were partially protected after challenge with virulent YFV in just one to three days (Smithburn and Mahaffy 1945). The hallmarks of a robust innate immune response to YFV are suppression of further viral replication and shaping the adaptive immune response. It is important to note, however, that there is not a comprehensive list of innate immune responses elicited by YFV or even other flaviviruses.

***Adaptive immune responses.*** Adaptive immune responses develop after the activation of innate immune responses. The onset of adaptive immune responses is at least partially overlapped with the development of severe YF diseases. Therefore, adaptive immune responses against wt YFV may contribute to both protection and disease pathogenesis. Wild-type YFV elicits both T and B lymphocytes for cell-mediated and humoral immune responses, respectively. Most research on the adaptive immune response to natural YFV infection characterizes the humoral response with a focus on neutralizing antibodies. Neutralizing antibodies isolated from patients recovered from severe YF disease have been shown to confer passive protection in mice (Daffis et al. 2005; Lu et al. 2019). Importantly, neutralizing antibodies produced by YFV 17D vaccinees are the correlate of protection (see Section 1.3.C).

There is a limited understanding of the cell-mediated immune response to natural YFV infection, but evidence suggests that wt YFV elicits a different response in humans compared to the vaccine strain. Most studies investigating the human cell-mediated immune response to primary wt YFV infection involve post-mortem or near post-mortem examination of human samples. Consequently, this does not recapitulate the infection process and host responses in detail. Both CD4+ and CD8+ T lymphocyte responses are activated in YF patients. Livers from patients who developed fatal disease show infiltration of primarily CD4+ T lymphocytes but also CD8+ T lymphocytes and B lymphocytes (Quaresma, Duarte, and Vasconcelos 2006; Quaresma et al. 2007). This may suggest patients with fatal outcomes mount a T lymphocyte response that is either ineffective at controlling the spread of YFV or even exacerbate YF disease (Quaresma et al. 2005; Quaresma et al. 2006; Quaresma, Duarte, and Vasconcelos 2006). Lastly, a preferential expression of Th1 profile cytokines (i.e., TNF-α and IFN-γ to increase the cell-mediated immune response) may be implicated in both viral clearance and induction of cell injury or apoptosis (Quaresma et al. 2006). This activation of CD4+ T lymphocytes attributed to immune pathogenesis is not a common phenomenon in YFV vaccinees. Lastly, increased TNF-α enhances CD8+ T lymphocyte cytolytic activity, thus contributing to tissue damage.

The B cell response is vital in controlling infection based on convalescent serum collected from naturally infected humans protecting monkeys from fatal YFV infection (Theiler, Sellards, and Sellards 1928). This suggests neutralizing antibodies provide protection in humans. Despite the importance of antibody-mediated neutralization in immune protection, it is still an understudied area. During the first week of infection, immunoglobulin (Ig) M antibodies appear but decline over the next two months, however some last for several years (WHO 2015). At the end of the first week, specific IgG neutralizing antibodies are detected and can persist over a

person's lifespan (WHO 2015). This was demonstrated when sera of persons naturally infected with YFV as far back as 78 years prior to collection protected monkeys from lethal infection (Sawyer 1931). A detailed discussion of anti-YFV antibodies against the YFV vaccine strain is discussed in Section 1.4.

Collectively, further knowledge of immune responses towards natural wt YFV infection remains to be explored. This is due to the small number of research groups investigating YFV around the world and subsequently, limited published studies. Additionally, wt YFV requires the use of biosafety level 3 containment and there is a scarcity of animal models to study viscerotropic YFV infection (further discussed in Section 1.6).

## 1.3 Yellow fever vaccine strains

### A. Development of YF live-attenuated vaccines

Yellow fever is a zoonotic virus with a high mortality rate, therefore the only reliable way to prevent disease is through vaccination. Two live-attenuated YF vaccines were developed in the 1930s: the French neurotropic vaccine (FNV) and the 17D vaccine. The vaccine strains were derived from the genetically related wt YFV Asibi and French viscerotropic virus (FVV) strains, respectively, isolated during the same outbreak in Senegal, differing by only two amino acids (Beck et al. 2018). French workers in Dakar, Senegal developed the YF FNV strain by serial ic mouse brain passage (238 passages) of the wt FVV isolated from a mild YF case (Peltier 1947). Administration of FNV was through scarification and was highly immunogenic (Peltier 1947). While this inoculation route made it easier to use during larger campaigns, vaccinating up to 5,000 people a day, the FNV had unacceptable rates of post-vaccine complications, especially in children (Frierson 2010). The FNV caused febrile and central nervous system reactions such as

encephalitis. Attempts to decrease the neurotropism of the FNV were made, but failed (Theiler and Smith 1937).

The FNV was used on a large-scale during World War II (primarily in French-speaking African countries) but by the end of the war, neurologic reactions using this vaccine strain were becoming more apparent. In large vaccination campaigns in Nigeria in 1953 and later in Costa Rica and the Congo, multiple cases of encephalitis were observed following vaccination with the YF FNV (Frierson 2010). Additionally, for the first time, virus was isolated from affected brain tissues (Macnamara 1953). By 1982, production of the YF FNV strain was discontinued and only the 17D vaccine was administered (Monath et al. 2013).

### B. Yellow fever 17D strain

In 1937, the YFV 17D vaccine strain was derived from the wt Asibi strain after being initially passaged 53 times in monkeys with intermittent passages in *Ae. aegypti* mosquitoes (Theiler and Smith 1937). The virus was empirically attenuated by undergoing 18 passages in embryonic mouse cultures, 58 passages in minced whole chicken embryo tissues, and finally 128 passages in minced chicken embryos without nervous tissues (Lloyd, Theiler, and Ricci 1936). The virus had a significant change in virulence, including a loss of neurotropism and viscerotropism, ideal for a vaccine candidate (Theiler and Smith 1937).

It is believed that multigenic mutations are responsible for the attenuated phenotype of the 17D vaccine strain, but the detailed attenuation mechanism(s) remain poorly understood. Deep sequencing reveals YFV 17D has attenuating mutations compared to the Asibi strain, indicating the vaccine strain was derived by discrete mutations (Beck et al. 2013). Based on whole genome sequencing between the parental Asibi strain and the 17D vaccine strain passaged 240 total times *in vitro*, a 0.63% nucleotide sequence diversion resulted in 32 amino acid

changes (0.94%) (Hahn et al. 1987). Mutations arising during the serial passage process contribute to the attenuated phenotype of 17D, therefore, the sequencing was undertaken to identify mutations in the consensus sequence between the Asibi and 17D strains throughout the genome (**Table 1.2)**.

**Table 1.2 Genetic comparison between YFV Asibi strain and 17D vaccine strains.**
The genetic differences between the wt YFV Asibi strain and 17D vaccine strains are grouped by the nucleotide (nt) position and amino acid (aa) position. The nucleotide position number begins at the 5′ terminus of the YFV genome. If the nucleotide change(s) results in an amino acid change it is reflected in the second column. Data compiled using the following references: (Beck et al. 2014; Serrão de Andrade et al. 2021).

| Gene | Position (nt) | Asibi | 17D-204 | 17DD | Position (aa) | Asibi | 17D-204 | 17DD |
|---|---|---|---|---|---|---|---|---|
| **C** | 304 | G | A | A | | | | |
| | 370 | U | C | U | | | | |
| **M** | 854 | C | U | U | 36 | L | F | F |
| | 883 | A | G | A | | | | |
| **E** | 1127 | G | A | A | 52 | G | R | R |
| | 1140 | C | U | C | 56 | A | V | A |
| | 1482 | C | U | U | 170 | A | V | V |
| | 1491 | C | U | U | 173 | T | I | I |
| | 1572 | A | C | C | 200 | K | T | T |
| | 1750 | C | U | U | | | | |
| | 1819 | C | U | U | | | | |
| | 1870 | G | A | A | 299 | M | I | I |
| | 1887 | C | U | U | 305 | S | F | F |
| | 1946 | C | U | C | 325 | P | S | P |
| | 1965 | A | G | G | 331 | K | R | R |
| | 2112 | C | G | G | 380 | T | R | R |
| | 2219 | G | A | G | 416 | T | A | T |
| | 2356 | C | U | U | | | | |
| **NS1** | 2687 | C | U | U | 79 | L | F | F |
| | 2704 | A | G | G | | | | |
| | 3274 | G | A | A | | | | |
| | 3371 | A | G | G | 307 | I | V | V |
| | 3613 | G | A | A | | | | |
| **NS2A** | 3817 | G, A | G | G | | | | |
| | 3860 | A | G | G | 61 | M | V | V |
| | 3915 | U, A | U | U | | | | |
| | 4007 | A | G | G | 110 | T | A | A |
| | 4013 | C | U | C | 112 | L | F | L |
| | 4022 | A | G | G | 115 | T | A | T |

| Gene | Position (nt) | Asibi | 17D-204 | 17DD | Position (aa) | Asibi | 17D-204 | 17DD |
|---|---|---|---|---|---|---|---|---|
| **NS2A** | 4054 | C | U | C | | | | |
| | 4056 | C | U | U | 126 | S | F | F |
| **NS2B** | 4289 | A | C | C | 37 | I | L | L |
| | 4387 | A | G | G | | | | |
| | 4505 | A | C | C | 109 | I | L | L |
| | 4507 | U | C | C | | | | |
| **NS3** | 4612 | U | C | U | | | | |
| | 4864 | A, G | G | G | | | | |
| | 4873 | U | G | U | | | | |
| | 5131 | U, G | G | G | 187 | I, M | M | M |
| | 5153 | A | G | A | 195 | I | V | I |
| | 5194 | U | C | C | | | | |
| | 5431 | C | U | U | | | | |
| | 5473 | C | U | U | | | | |
| | 5641 | G | A | G | | | | |
| | 6013 | C | U | U | | | | |
| | 6023 | G | A | A | 485 | D | N | N |
| | 6448 | G | U | U | | | | |
| | 6529 | U | C | C | | | | |
| **NS4A** | 6758 | A | G | A | 107 | I | V | I |
| | 6829 | U | C | C | | | | |
| | 6876 | U | C | C | 146 | V | A | A |
| **NS4B** | 7171 | A | G | G | 95 | I | M | M |
| | 7571 | C | A | C | | | | |
| | 7580 | U | C | C | 232 | Y | H | H |
| **NS5** | 9605 | A | G | A | 657 | N | D | N |
| | 10075 | G, U | G | G | 814 | M, I | M | M |
| | 10142 | G | A | A | 836 | E | K | K |
| | 10243 | G | A | A | | | | |
| | 10285 | U | C | C | | | | |
| | 10312 | A | G | G | | | | |
| | 10316 | U, C | U | U | 894 | S, P | S | S |
| | 10338 | C | U | U | 900 | P | L | L |
| **3′ UTR** | 10367 | U | C | C | | | | |
| | 10418 | U | C | C | | | | |
| | 10454 | A | G | A | | | | |
| | 10550 | U | C | U | | | | |
| | 10800 | G | A | A | | | | |
| | 10847 | A | C | C | | | | |

Specifically, the E protein has the most amino acid substitutions. This is significant because the E protein is targeted by neutralizing antibodies and affects virus-host receptor

binding that leads to the reduced neurotropism and viscerotropism of the 17D vaccine strain (Hahn et al. 1987; Davis and Barrett 2020). Mutations between different substrains of the 17D vaccine is summarized in **Table 1.3.** This is important not only for the pathogenesis of YFV, but for immune responses such as antibody-mediated neutralization. The attenuated phenotype of 17D is also attributed to the loss of genetic diversity (Beck et al. 2013). This is a common process observed among multiple RNA viruses. Most notably, the neurovirulence of polio virus in mice is at least in part due to the highly diverse quasi-species populations due to mutation rates and population dynamics (Vignuzzi et al. 2006).

**Table 1.3 Amino acid changes in the envelope protein between the wild-type parental Asibi strain and vaccine strains of YFV.**
The parental wt YFV Asibi strain was used to generate the YFV vaccine substrains 17D-204, 17DD, and 17D-213. The envelope protein contains the most amino acid substitutions that distinguish the Asibi and 17D strains. Sequences were aligned using BioEdit.

| Amino acid in E protein | Wild-type and vaccine strains of YFV | | | |
|---|---|---|---|---|
| | Asibi | 17D-204 | 17DD | 17D-213 |
| 52 | G | R | R | R |
| 56 | A | V | A | V |
| 153 | N | T | N | T |
| 155 | D | D | S | D |
| 170 | A | V | V | V |
| 173 | T | I | I | I |
| 200 | K | T | T | T |
| 299 | M | I | I | I |
| 305 | S | F | F | F |
| 325 | P | S | P | S |
| 331 | K | R | R | R |
| 380 | T | R | R | R |
| 407 | A | V | V | V |
| 416 | A | T | A | T |

Multiple 17D substrains are used for vaccine production. The 17D vaccine substrains show differences in plaque morphologies and biological properties but all of them are effective and safe vaccine viruses (Liprandi 1981; Barrett and Gould 1986). In the beginning, some of the 17D substrains had enhanced neurotropism with increased incidences of encephalitic type

reactions post-vaccination (Fox and Penna 1943). This prompted the use of a seed-lot system to minimize subcultures necessary for vaccine production. The full genomes of 17D vaccine stocks have been compared to determine sequence variation in order to improve documentation of variations in YF seed vaccine production (Stock et al. 2012). Based on sequence alignments and phylogenetic analysis, the nucleotide sequences of all 17D substrains showed an overall homology of 99.2%, supporting the notion of genetic stability of the vaccine strains (Stock et al. 2012).

The genealogy of the 17D vaccine strains that have been generated and used in the manufacture of YF vaccines is summarized in **Figure 1.6** (WHO 2010). Today, ten producers using three substrains derived from the original 17D strain including 17DD, 17D-204, and 17D-213 are used for the manufacture of the 17D vaccine (Monath et al. 2013). The 17DD substrain was isolated at passage 195. The 17D-204 substrain was derived from the original 17D strain at passage 204 (WHO 2010). The 17D-213 strain, a derivative of 17D-204, gained an E protein glycosylation site (Post et al. 1992). While all three 17D-derived vaccine substrains have slightly different genomic sequences including glycosylation sites of the E protein, they are equally immunogenic and safe in vaccinees (Ferreira et al. 2018).

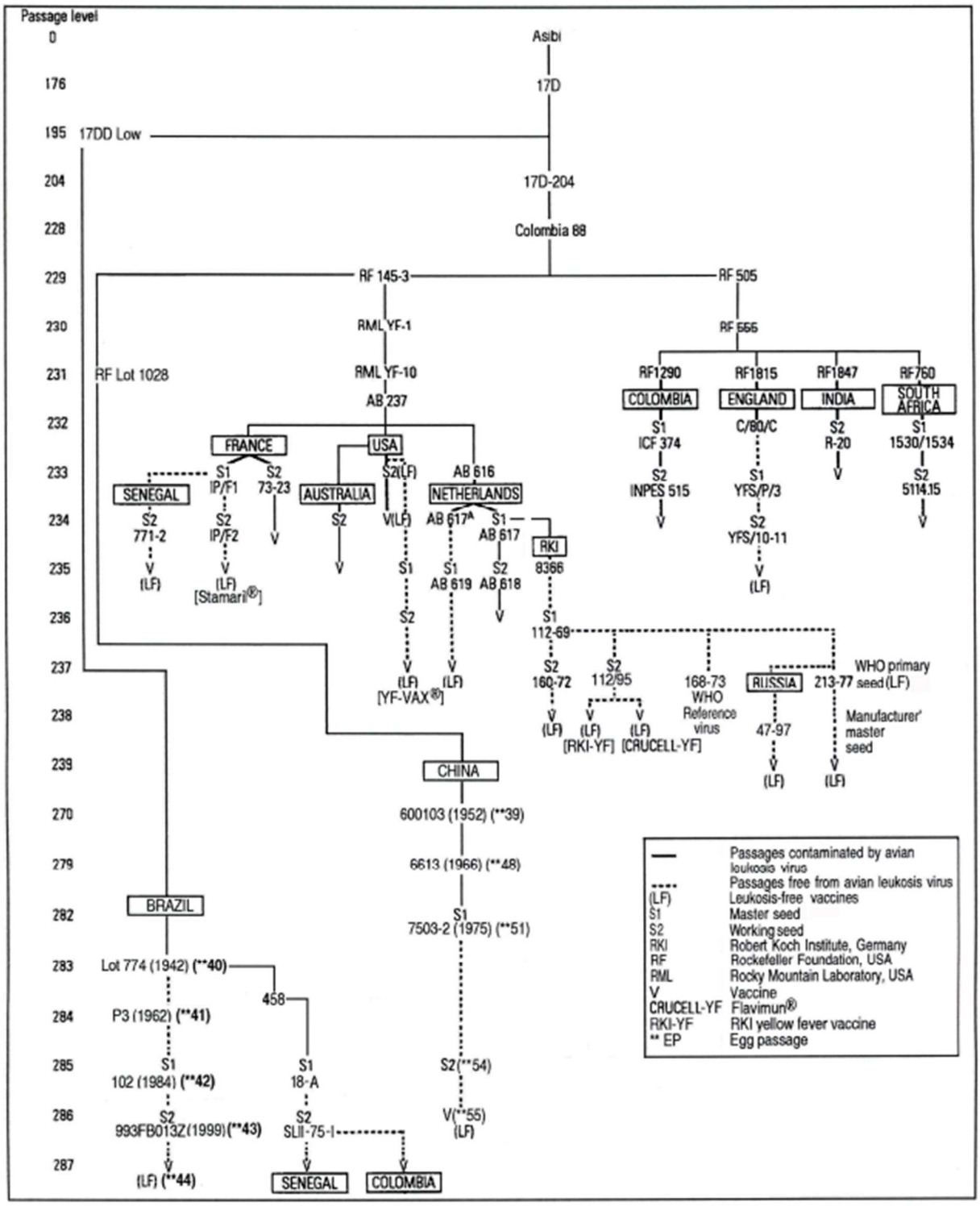


**Figure 1.6 The historical overview and genealogy of YFV 17D vaccine strains.**
The genealogy of the 17D vaccine strains that have been generated and used in the manufacture of YF vaccines. Image courtesy of the World Health Organization (https://www.who.int/biologicals/YF_Recommendations_post_ECBS_FINAL_rev_12_Nov_2010.pdf) (WHO 2010); published under the Creative Commons Attribution License CC BY-NC-SA 3.0 IGO.

Over 850 million doses of the 17D vaccine have been administered since receiving licensing approval in 1938 (Elvidge 2020). The vaccine is recommended for individuals 9 months of age and older. Reactions to the YF vaccine are generally mild with symptoms including headache, muscle ache, or low-grade fevers. The YF vaccine is considered one of the safest vaccines, however reactions causing invasive and disseminated disease with high lethality has been observed in otherwise healthy people. Rarely, people can develop yellow fever vaccine-associated viscerotropic disease (YEL-AVD) or vaccine associated neurotropic disease (YEL-AND). Almost all cases of both YEL-AVD and YEL-AND occur in first-time vaccine recipients (Gershman 2021).

The risk of developing YEL-AVD is estimated to occur in 0.3 cases per 100,000 doses and increases to 1.2 cases per 100,000 in people over the age of 60 (Gershman 2021). Symptoms of YEL-AVD begin one to 18 days post-vaccination with fever, malaise, headache, and myalgia, that progress to hepatitis, hypotension, and multi-organ system failure. The symptoms are similar in people infected with wt YFV. The case fatality rate of people who develop YEL-AVD is 48% (Gershman 2021).

The risk of developing YEL-AND is estimated to occur in 0.8 cases per 100,000 and increases to 2.2 cases per 100,000 in people over the age of 60 (Gershman 2021). Others also at an increased risk of developing YEL-AND include infants, or those that are immunosuppressed or have a thymus disorder. Symptoms of YEL-AND begin from two to 56 days post-immunization with a fever and headache that may progress to meningoencephalitis, Guillain-Barré syndrome, acute disseminated encephalomyelitis, or cranial nerve palsies (although rare) (Gershman 2021). The incidence of YEL-AND is primarily seen in infants presenting as

encephalitis but can occur in people of all ages. The development of YEL-AND is rarely fatal (Gershman 2021).

Viremia following vaccination with the 17D strain is extremely low and can be detected between two- and seven-days following inoculation (Reinhardt et al. 1998; Akondy et al. 2015). Live YFV can be isolated from the blood of vaccinated humans and *Ae. aegypti* are able to become infected with YFV 17D in the midgut, however, the mosquitoes are incapable of transmitting the virus to susceptible animals through a bite (Whitman 1939). This is due to the inability of the 17D strain to disseminate from the midgut to other tissues such as salivary glands, and so fails to be transmitted (Jennings et al. 1994; McElroy et al. 2008).

### C. Immune protection elicited by the YFV 17D vaccine

A single immunization with YFV 17D vaccine elicits long-lasting protection against natural infection. Although extensive reports have described the activation of immune responses after vaccination, the robust innate and adaptive immune response following vaccination with YFV 17D has only been hypothesized to contribute to the efficacy of the vaccine as a strong immunogen to generate long-lived immunity (Monath et al. 2013). While neutralizing antibodies are the correlate of protection of the 17D vaccine, the protective mechanism of the 17D vaccine strain is poorly understood. It is important to highlight the distinction between the identification of human immune responses elicited by the 17D vaccine and the discovery of the mechanism(s) of protection of the 17D vaccine. Most studies only identified specific human immune responses that are activated in response to the immunization with the 17D vaccine. However, this lacks the demonstration of passive protection against wt YFV to prove that specific human immune responses are responsible for the protection of 17D vaccinees and hence are the mechanism(s) of protection. Because this dissertation research is to understand part of the protective immunity

elicited by the 17D vaccine, an overview of the innate and adaptive immune responses induced by the 17D vaccine is provided.

***Innate immune responses.*** Upon vaccination with 17D, the human innate immune response is activated within a few days and peaks on day 7 (Silva et al. 2011; Monath et al. 2013). Like wt YFV infection, the detection of viral RNA through TLRs and RLRs activates signal transduction pathways to modulate pro- and anti-inflammatory cytokines. Vaccination of 17D activates multiple TLRs including TLR-2, -3, -7, -8, and -9 to stimulate a polyvalent immune response (Neves et al. 2009; Querec et al. 2006). A wide array of early innate immune gene expression signatures can be detected within one day following vaccination (Querec et al. 2009). Additional pathways and transcriptional elements leading to the upregulation of natural killer cells, macrophages, and the complement system are detected. The IFN response appears shortly after YFV 17D vaccination to drive Th1-directed CD8+ T and B cell responses (Wheelock and Sibley 1965). The cumulative innate response triggers the production of both CD4+ and CD8+ T cells, and B cell populations (Querec et al. 2006; Monath et al. 2013). This robust innate immune response is key to why 17D generates long-lived immunity through the development of memory T and B cell populations.

***Adaptive immune responses.*** The only adaptive immune response proven to contribute to the protection of 17D vaccinees is neutralizing antibodies. Within 10 days of receiving YFV 17D, 80-100% of vaccine recipients develop protective levels of neutralizing antibodies and 99% develop protective levels within 30 days, with levels persisting for decades (WHO 2015). These values are based on monkey challenge studies, where a log neutralization index (LNI) of >0.7 correlates with immunological protection following vaccination (Mason et al. 1973; WHO 2015). The plaque reduction neutralization test (PRNT), which detects the presence or absence of

neutralizing antibodies by varying the concentrations of antibody and keeping the virus constant, has mostly replaced the LNI. This assay is typically used during clinical trials for flavivirus vaccines with a 50% PRNT value of 1 in 10 considered as the correlate of protection (Hombach et al. 2005; WHO 2007; Roehrig, Hombach, and Barrett 2008).

An early B cell response is mediated by IgM antibodies, which appear between 7- and 14-days post-vaccination (Gibney et al. 2012). Unlike wt YFV infection, IgM neutralizing antibodies can be detected for up to 4 years (Gibney et al. 2012). This persistence is correlated with an earlier onset of viremia and a high neutralizing antibody titer at one month and three to four years after 17D vaccination. IgG neutralizing antibodies develop within the first month of 17D vaccination and may last up to 40 years or longer (Wieten et al. 2016). Details on distinct types of antibodies elicited by YFV 17D vaccines are discussed further in Section 1.4.

The development of broad and polyfunctional YFV-specific CD4+ and CD8+ T cells with highly functional memory are inherent to the 17D vaccine (Akondy et al. 2009; James et al. 2013; Akondy et al. 2017). Mixed CD4+ Th1 and Th2 T cell populations promote CD8+ T cell and B cell/antibody responses, respectively. The CD8+ T cell response correlates with viral load, as CD8+ T cells peak when virus is no longer detected (Akondy et al. 2015). The long-lived memory of CD8+ T cells is evident based on samples collected from 99 17D vaccinees (Wieten et al. 2016). CD8+ T cells were detected by day 12, differentiated to become mostly memory T cells by day 28, and persisted for 18 years. These data suggest the significance of memory CD4+ and CD8+ T cells contributing to the robust protective immunity elicited by the 17D vaccine.

In summary, there is still a major gap of knowledge in the mechanism(s) of protection of the YF 17D vaccine. While the correlate of protection for the 17D vaccine are neutralizing antibodies, how they protect 17D vaccinees is poorly understood. There is a lack of

understanding of the mechanism of human antibody-mediated neutralization of wt YFV. It remains unknown how a single live-attenuated vaccine (LAV) can confer protection against wt YFV strains that differ significantly in antigenicity (Clarke 1960). Because there are differences in the human and murine immune responses towards flaviviruses, the neutralizing antibody responses elicited by the 17D vaccine in mouse models do not reflect how antibody-mediated neutralization of wt YFV takes place in humans, especially 17D vaccinees. A better understanding of neutralizing antibody responses elicited by the 17D vaccine will facilitate the identification of its mechanism(s) of protection against all seven genotypes of wt YFV and be applied to the development of next-generation YF vaccines.

## 1.4 Anti-YFV 17D antibodies

### A. Overview of antibody responses elicited by YFV 17D Vaccine

It is important to note that neutralizing antibodies only constitute part of the antibody repertoire in 17D vaccinees. Replication of the 17D strain leads to the presentation of antigenic structures in several viral proteins. Consequently, polyclonal sera of naturally infected and 17D vaccinees contain antibodies that react with multiple proteins including prM, E, and NS1 proteins (Lennette and Perlowagora 1943; Vratskikh et al. 2013). Each type of antibody varies in the neutralizing activity and hence has different functional importance in antibody-mediated neutralization, the mechanism hypothesized to contribute to the protective immunity of 17D vaccinees against wt YFV.

It is believed that anti-prM and anti-NS1 antibodies play limited roles in antibody-mediated neutralization of wt YFV in 17D vaccinees. This is consistent with the absence of prM and NS1 proteins on the virion surface. Consequently, the direct neutralization of infectious viruses by anti-prM and anti-NS1 antibodies is less likely to occur. Although anti-prM antibodies

have been reported in some vaccinated individuals, the epitope(s) in the prM protein in flaviviruses are not immunodominant and only elicit weak neutralizing activity (Vratskikh et al. 2013). On the contrary, NS1 proteins contain immunodominant epitopes. The majority of anti-YFV NS1 antibodies only exhibit complement fixation activity, which is consistent with its role in complement-mediated cytolysis of infected cells (Schlesinger, Brandriss, and Monath 1983; Schlesinger, Brandriss, and Walsh 1985; Brandriss et al. 1986). Anti-NS1 antibodies are largely absent after primary 17D vaccination but are part of the antibody response to natural YFV infection and can be detected in vaccinated individuals with preexisting immunity to other flaviviruses (Lennette and Perlowagora 1943; Monath et al. 1980). Immunization with purified YFV NS1 protein leads to partial protection against wt YFV in NHPs (Schlesinger et al. 1986). Additionally, passive immunization of anti-YFV NS1 monoclonal antibodies (mAbs) protects mice against lethal 17D YF encephalitis (Schlesinger, Brandriss, and Walsh 1985). The mechanisms of anti-YFV NS1 antibodies in protective immunity remains unclear, however, because there are a limited number of studies demonstrating passive protection against wt YFV.

Most anti-YFV E antibodies physically bind to antigenic structures in the virion, as demonstrated with their ability to block hemagglutination activity of the E protein (Schlesinger, Brandriss, and Monath 1983). It is important to note that physical binding of anti-YFV E antibodies does not always lead to the neutralization of viral infectivity. Therefore, although many anti-YFV E antibodies exhibit hemagglutination inhibition (HI) activity, only a limited number of anti-YFV E antibodies elicit neutralizing activity and have been proven important for protective immunity against wt YFV. The remainder of Section 1.4 discusses the characterization and methods investigating antibody-mediated neutralization of YFV.

## B. Neutralizing anti-YFV E antibodies

Polyclonal sera from 17D vaccinees without previous exposure to other flaviviruses only neutralize YFV (Groot 1962; Wisseman et al. 1962). This observation suggests that antibody-mediated neutralization of wt YFV in 17D vaccinees mainly involves type-specific neutralizing antibodies. The characterization of human polyclonal sera using modern molecular biological techniques consistently shows that flavivirus-reactive neutralizing antibodies are absent or present at very low titers in 17D vaccinees (Vratskikh et al. 2013). However, using polyclonal sera to investigate neutralizing antibody responses elicited by the 17D vaccine precludes the characterization of different clonal populations of neutralizing antibodies and individual antigenic structures in the E protein that are critical for the development of neutralizing antibody responses.

The initial attempt to overcome these limitations was to generate mAbs by repeated immunization of mice with different 17D substrains (Schlesinger, Brandriss, and Monath 1983; Buckley and Gould 1985; Barrett et al. 1989). Five major classes of neutralizing anti-YFV E mouse mAbs have been identified: 1) 17D-specific, 2) vaccine-specific, 3) YFV type-specific, 4) intermediate reactivity with flaviviruses, and 5) broad reactivity with flaviviruses. It is apparent only the YFV type-specific neutralizing anti-YFV E mouse mAbs are relevant to antibody-mediated neutralization in 17D vaccinees. The four other classes of neutralizing anti-YFV E mouse mAbs may be artifacts caused by repeated immunization with 17D strain in mice, which are not naturally susceptible to YFV. For example, albeit the high neutralization titers *in vitro*, 17D-specific mAbs neither neutralize nor confer passive protection against wt YFV (Schlesinger, Brandriss, and Monath 1983; Gould et al. 1985; Sil et al. 1992). Epitope mapping showed the potently neutralizing 17D-204 substrain-specific mAb-864 recognizes antigenic structures in

EDIII, which is often recognized by murine neutralizing antibodies but does not normally elicit neutralizing antibody responses in humans (Cammack and Gould 1986; Daffis et al. 2005; Vratskikh et al. 2013). Mouse mAbs that exhibit intermediate or broad reactivity do not aid in the investigation of neutralizing antibody responses in 17D vaccinees because immunologically naïve individuals do not develop neutralizing antibodies that cross-react with other flaviviruses. Similarly, mouse mAbs that elicit specific neutralizing activity against wt YFV do not represent an important population of neutralizing antibodies in 17D vaccinees. This is consistent with West Nile virus (WNV) and DENV immune responses, where EDIII-specific neutralizing antibodies and broad flavivirus cross-reactive antibodies are present at low titers or absent altogether (Throsby et al. 2006; Oliphant et al. 2007; Wahala et al. 2012).

More recently, the advancement of molecular genomic technologies enables the isolation of neutralizing anti-YFV mAbs from patients that recovered from wt YFV infection or were immunized with the 17D vaccine. The number of type-specific neutralizing anti-YFV E mAbs is still limited though, despite that three mouse mAbs prepared against the 17D strain and three human mAbs isolated from YF patients recognize the overlapped antigenic structures that constitute the quaternary structure of the EDI and EDII (Schlesinger, Brandriss, and Monath 1983; Barrett et al. 1989; Daffis et al. 2005). The available knowledge still does not fully address how antibodies raised against the 17D vaccine strain can neutralize and protect against multiple genotypes of wt YFV.

### C. Neutralizing activity and passive protection of anti-YFV E antibodies

The 17D vaccine protects against all genotypes of wt YFV based on its universal success in preventing disease (WHO 2015). Polyclonal sera from 17D vaccinees neutralizes different genotypes of YFV (Groot and Riberiro 1962; Monath 1971; Daffis et al. 2005). Therefore, it is

important to understand how each clonal population of type-specific antibodies raised against the 17D strain neutralizes and protects against different wt YFV genotypes. Surprisingly, few YFV type-specific mAbs have been investigated for the neutralization and passive protection against multiple genotypes of wt YFV. This creates a gap of knowledge in how neutralizing anti-YFV antibodies contribute to the protective immunity elicited by the 17D vaccine.

To the best of our knowledge, the only type-specific anti-YFV mouse mAb that neutralizes and confers passive protection against wt YFV is mAb-2C9 isolated by Schlesinger *et al*. The humanized mAb-2C9 neutralizes both the 17D strain and the prototype Asibi strain and partially protects against 17D-204 in the immunocompromised AG129 mouse model (Thibodeaux, Garbino, Liss, Piper, Schlesinger, et al. 2012). The mAb was further shown to protect against the hamster-adapted Jimenez p.10 strain in passively immunized hamsters (Julander et al. 2014). Gould *et al*. also demonstrated neutralization of the prototype wt YFV Asibi strain (West African genotype II) and several Brazilian isolates (South American genotype I) via indirect immunofluorescence by type-specific anti-YFV mouse mAb-825 (Gould et al. 1985). However, passive immunization of outbred mice with mAb-825 only conferred partial protection against ic challenge with the 17D strain and failed to protect against the Asibi strain (Gould et al. 1985; Gould et al. 1986). Another type-specific neutralizing anti-YFV mAb-B45 binds epitopes in the E protein of wt YFV strains in the West African II and South American II genotypes via indirect immunofluorescence (Barrett et al. 1989). The neutralization potency of mAb-B45 against the representative strains of wt YFV is unknown though, and passive immunization of outbred mice with mAb-B45 only partially protected against 17D-204 and one of three 17DD substrains (Barrett et al. 1989).

A large panel of YFV type-specific mAbs has been generated but only a handful neutralize both 17D and wt YFV strains *in vitro* and none have shown passive protection against both 17D and wt YFV (Schlesinger, Brandriss, and Monath 1983; Barrett et al. 1989). Even though some type-specific mAbs have demonstrated passive protection regardless of neutralization titers, these studies only challenged mice intracerebrally with YFV 17D (Brandriss et al. 1986). Importantly, these are mouse mAbs and likely target different epitopes on the E protein than what would be observed during human YFV infection. Anti-flavivirus mouse mAbs often use recombinant EDIII as the immunogen and this may skew the immune response toward an artificial immunogen (Davis and Barrett 2020). If used as a treatment option, mouse mAbs could lead to the introduction of YFV escape mutants or result in anti-mouse immune responses. Consequently, mouse mAbs are not the best model to understand the mechanism(s) of protection of the YF 17D vaccine as well as not being a viable option for YF therapeutic treatments.

Three human mAbs were isolated from two patients infected with wt YFV during an epidemic in Guinea, West Africa in 2000 and all are YFV type-specific including mAb-5A, -7A, and -R3 (Daffis et al. 2005). They were generated using human mAb fragments through repertoire cloning from B cells collected approximately 6 months post-acute infection and screened using the 17D vaccine strain. Importantly, all three mAbs neutralized both 17D and wt strains of YFV that belong to the West Africa I, West Africa II, East/Central Africa, and Angola genotypes (Daffis et al. 2005; Lu et al. 2019). Furthermore, mice challenged intracerebrally with YFV 17D were completely protected following immunization with mAb-5A by the intraperitoneal (ip) route one day post-infection (Lu et al. 2019). Wec *et al.* isolated YFV E-specific mAbs from two 17D vaccinees and the antigenic site was mapped to the fusion-loop

proximal epitopes within the YFV EDII, but neutralization potency was only tested against the 17D strain (Wec et al. 2020).

Collectively, the results derived from the three mouse mAbs raised against the 17D strain offer a limited understanding of how type-specific antibodies produced by 17D vaccinees neutralize and protect against wt YFV. While there is considerable overlap in the residues that constitute the epitope recognized by the three mAbs isolated from two YF patients and the neutralizing mAbs isolated from two 17D vaccinees, very few human mAbs have been characterized (Daffis et al. 2005; Wec et al. 2020). Human mAb-5A attaches to highly conserved regions of the YFV EDII at the prefusion step but prevents the fusion loop from interacting with the endosomal membrane during post-fusion, suggesting mAb-5A may prevent both virus attachment and fusion (Lu et al. 2019). Lastly, the functional importance of available neutralizing anti-YFV human mAbs remains to be tested in passive protection studies against wt YFV. The demonstration of passive protection against wt YFV strains is challenging, though, as few animal models are available to recapitulate disease pathogenesis of human YF.

## 1.5 Animal models of YF infection

As stated above, the demonstration of passive protection against wt YFV is essential for the delineation of the protective mechanism of the 17D vaccine. Although wt YFV can cause up to 60% mortality in immunologically naïve individuals, it replicates poorly after peripheral challenge in most model organisms used in biomedical research. Only a few animal models are suitable for investigating the viscerotropism of wt YFV. Importantly, there are significant logistical, economical, and/or regulatory challenges in acquiring model organisms that resemble viscerotropic disease observed in human YF.

## A. Nonhuman primate model of YF infection

Nonhuman primates are generally susceptible to YFV infection and considered the most relevant model for human YF. In addition to the difficulties in conducting NHP studies in BSL-3 laboratories, only a limited number of NHP species have been shown to develop viscerotropic disease, especially hepatitis that resemble wt YFV infection in humans (Stokes, Bauer, and Hudson 1928; Monath et al. 1981; Engelmann et al. 2014).

Asian monkey species including rhesus and cynomolgus macaques and most New World NHPs develop YF disease that is nearly identical to that observed in humans whereas African NHPs are typically asymptomatic, although still viremic (Stokes, Bauer, and Hudson 1928; Bauer and Mahaffv 1930; Lloyd and Mahaffy 1936; Smithburn and Haddow 1949). The prototype wt YFV Asibi strain produces lethal diseases in rhesus monkeys (Hudson and Philip 1929; Engelmann et al. 2014). Remarkably, rhesus monkeys also succumbed to disease 108-135 hours following inoculation with wt YFV DakH 1279 strain, which belongs to the same West African genotype II and was isolated 38 years after the isolation of the Asibi strain (Monath et al. 1981). As in humans, YF disease in rhesus monkeys is characterized by renal failure, coagulopathy, jaundice, and shock, however disease onset and death occur at a much faster rate compared to humans. Clinical disease symptoms including organ dysfunction/failure appears 14-25 hours prior to death with peak viremia at 96-hours post-infection. Pathological changes in the liver, lungs, spleen, and lymph nodes were similar between rhesus monkeys and humans (Hudson 1928).

The outcome of experimental challenge with African and South American wt YFV strains is variable, hinting that the distinct genetic composition may account for the difference in virulence of wt YFV (Davis and Burke 1929; Sawyer et al. 1930). Therefore, it may be difficult

to investigate how the 17D vaccine broadly protects against disease caused by different genotypes of wt YFV. A more practical animal model such as hamsters and mice are necessary to examine the protective immunity elicited by the 17D vaccine.

## B. Immunocompetent mouse model of YF infection

Murine models have been used for studying YFV pathogenesis and immune responses due to a well characterized biology and availability of reagents. Mice are small, inexpensive, and commercially available, therefore larger cohorts can be used. However, immunocompetent or wt mouse strains may be insusceptible to either vaccine or wt strains of YFV depending on the route of inoculation. This challenge was overcome by the application of the ic challenge technique to deliver YFV.

In 1930, the white (Swiss) mouse was first shown to be susceptible to YFV after ic injection (Theiler 1930a). Various inbred and outbred mouse strains at different ages were subsequently proven to succumb to ic or intranasal challenge with either 17D or wt YFV strains (Sawyer and Lloyd 1931; Fitzgeorge and Bradish 1980; Barrett and Gould 1986; Ryman et al. 1998). Susceptibility of mice to YFV is also age-dependent (Fitzgeorge and Bradish 1980). Unlike adult mice, suckling mice are susceptible to lethal YF encephalitis after ic or ip injection (Theiler 1930b). This work effectively demonstrates that YFV exhibits the neuroinvasive and neurovirulence phenotype in mice and murine nervous tissues can support the replication of YFV, especially in mouse brains.

Although the outcome of YFV infection in mice does not resemble human disease, mouse models have a broad utility in supporting virus isolation, producing YF virus stocks for numerous studies, and detecting neutralizing anti-YFV antibodies. Prior to the establishment of techniques that detect neutralizing anti-YFV antibodies *in vitro*, neutralization tests against YFV

were frequently performed in mice by injecting a cocktail of infectious viruses and immune sera via the ic route (Groot and Riberiro 1962). The susceptibility of mouse brains to YFV infection also enables the demonstration of passive protection by neutralizing antibodies. Passive protection studies in mice can be performed by the transfer of neutralizing antibodies via the ip route before or after ic challenge with either 17D or wt YFV strains. This technique was universally applied to the evaluation of mouse and human neutralizing antibodies (Sawyer and Lloyd 1931; Brandriss et al. 1986; Gould et al. 1986; Schlesinger, Brandriss, and Walsh 1985).

To date, YF encephalitis induced by the ic challenge remains a valuable tool for preclinical development of candidate antiviral treatments and vaccines for YFV despite the little resemblance to human disease. The neurovirulence model of YFV in outbred mice can be undertaken in large numbers, providing the statistical power needed for the screening of promising leads before progressing to viscerotropic disease models in immunocompromised mice and NHPs.

### C. Immunocompromised mouse model of YF infection

The utility of mouse models in YF studies is further broadened by the observation that viscerotropic diseases can be induced in immunocompromised mouse strains that constitute either the 129 or C57BL/6 background. To date, mouse strains deficient in antiviral signaling pathways have been proven to be highly susceptible to vaccine and wt YFV strains via the ip or subcutaneous routes. Viscerotropic diseases can be modeled by the challenge of mice that lack IFN receptors or STAT1 transcription factors with wt YFV strains. Importantly, viral genome can be detected in the liver of immunocompromised mice, whereas virus is only detected in brains of immunocompetent mice injected with YFV by the ic or ip route.

Infection with YFV is restricted by the mouse type I IFN response and to a lesser extent the type II IFN response in the 129-mouse strain (Meier et al. 2009). A129 mice lacking receptors for IFN-α/β (IFNAR$^{-/-}$) and AG129 mice lacking both IFN-α/β and IFN-γ (IFNAR$^{-/-}$-IFNGR$^{-/-}$) can both develop lethal viscerotropic disease after challenge with wt YFV strains (Lee and Lobigs 2008; Meier et al. 2009). A129 and AG129 mice infected subcutaneously with wt Asibi or Angola73 YFV result in 100% lethality, with AG129 mice succumbing approximately one day sooner (Meier et al. 2009). Importantly, these mice develop viscerotropic disease that recapitulate YF disease in humans with viral genomes detected in the liver. Mice lacking the STAT1 signaling protein (STAT129) are also susceptible to wt Asibi YFV by the subcutaneous route, confirming the importance of type-I IFN signaling in determining the susceptibility of mice to wt YFV. Importantly, neither A129 or STAT129 mice develop neurological disease proceeding subcutaneous injection of wt Asibi or Angola73 YFV and the detection of viral genomes in liver suggest that the mice succumb to viscerotropic disease caused by wt YFV (Meier et al. 2009). In contrast, G129 mice lacking receptors for IFN-γ (IFNGR$^{-/-}$) are not susceptible to either the wt or vaccine strains of YFV, suggesting IFN-γ plays a minor role in the protection against YFV. However, type-II IFNs are likely involved in limiting replication and dissemination of the 17D strain along with type-I IFNs, as clinical disease is not evident in A129 or G129 mice, but results in 100% mortality in AG129 mice following subcutaneous YFV 17D-204 infection (Meier et al. 2009; Tretyakova et al. 2014).

In IFNAR$^{-/-}$ mice, subcutaneous inoculation of YFV 17D-204 results in viral replication and dissemination, reproducing what is observed during human vaccination. Both A129 and inbred C57BL/6 mice deficient in IFN-α/β (AB6) immunized subcutaneously with YFV 17D-204 develop only minor clinical signs of infection and no lethality (Meier et al. 2009; Watson et

al. 2016). Subsequently, AB6 mice are completely protected against lethal infection with wt Angola71 YFV (Watson et al. 2016). While subcutaneous inoculation of YFV 17D-204 in either A129 mice or AB6 mice results in no mortality, other routes of peripheral inoculation including intramuscular and ip have been shown to result in varying degrees of illness (Erickson and Pfeiffer 2013, 2015). Importantly, AB6 mice inoculated with the 17D strain produce lethality in a dose-dependent manner (Erickson and Pfeiffer 2013, 2015). However, not all AB6 mice receiving the ip challenge with 17D develop lethal viscerotropic disease (Erickson and Pfeiffer 2015). Therefore, it is not a robust model for studying human YF infection.

In contrast, AG129 mice infected subcutaneously with YFV 17D-204 develop signs of neurologic disease with paresis and paralysis (Meier et al. 2009). This suggests the knockout of IFN-α/β and IFN-γ receptor genes contribute to mortality. Subcutaneous inoculation of YFV 17D-204 in AG129 mice is dose-dependent with lower doses resulting in incomplete morbidity and/or mortality (Thibodeaux, Garbino, Liss, Piper, Blair, et al. 2012). On the other hand, ip challenge of AG129 mice with YFV 17D-204 is uniformly lethal in a dose-dependent manner (Thibodeaux, Garbino, Liss, Piper, Blair, et al. 2012; Calvert et al. 2016). Infection in these mice is characterized by high viral loads in both the central nervous system and hepatic tissues, indicating infection is both neurotropic and viscerotropic (Thibodeaux, Garbino, Liss, Piper, Blair, et al. 2012). However, mortality was observed after the peak of tissue viral loads in the liver, suggesting that lethality is due to neurotropic disease rather than viscerotropic disease.

Because of the uniform lethality and consistent production of viscerotropic disease symptoms induced by both wt and vaccine YFV strains in IFNAR$^{-/-}$-IFNGR$^{-/-}$ mice, this is the best model to evaluate the protective efficacy of human anti-YFV mAbs. There is limited research using the IFNAR$^{-/-}$-IFNGR$^{-/-}$ mouse model, specifically C57/BL6 IFNAR$^{-/-}$-IFNGR$^{-/-}$

(AG6) mice, against lethal challenge with wt YFV by the ip route and no passive protection studies against wt Asibi YFV have been conducted. Additionally, there is limited commercial availability of immunocompromised mice. AG6 mice are available in the U.S.A. whereas AG129 mice are not readily commercially available. Therefore, this dissertation research can help elucidate viscerotropic YF disease in AG6 mice and evaluate the protective efficacy of human anti-YFV mAbs against wt Asibi infection.

## D. Hamster model of YF infection

The Syrian golden hamster (*Mesocricetus auratus*) has also been evaluated as the model for disease pathogenesis of YFV. Hamster models exhibit disease like humans under the right laboratory conditions, have intact immune systems, and are small and commercially available, therefore larger cohorts can be used. While the hamster model is appropriate for some YFV pathogenesis studies and vaccine or therapeutic research and development, the model does come with some disadvantages. To induce lethal YFV infection in hamsters, the viral strain must be adapted through serial passage. Furthermore, there is a lack of immunological reagents to study the hamster immune response. This may cast doubt on the sensitivity or specificity of the data.

Hamsters inoculated with the South American Jimenez strain, isolated from a fatal case in Panama in 1974, caused illness and death in a small number of hamsters with moderate viremia (Tesh et al. 2001; Xiao et al. 2001). In contrast, hamsters inoculated with wt YFV Asibi strain showed no outward signs of illness although mild and transient viremia was observed (McArthur et al. 2003). To increase viscerotropic YFV infection in hamsters and generate a model with pathological outcomes like human YF, both the Asibi and Jimenez strains of YFV were serially passaged in hamster livers. The Jimenez strain was serially passaged 10 times in hamster liver resulting in the hamster-adapted Jimenez p.10 strain (Tesh et al. 2001). This hamster adapted

YFV strain increases and prolongs viremia, but only moderately increases morbidity and mortality. Following infection with the Jimenez p.10 strain, hamsters have similar histopathological and clinical laboratory outcomes as observed in severe human cases of YF infection (Sbrana et al. 2006). The Asibi hamster-adapted strain, generated by passaging 7 times in hamster liver (Asibi/hamster p.7 virus), results in robust viremia, severe illness, and 100% death of subadult hamsters (McArthur et al. 2003). The genome of the hamster-adapted Jimenez p.10 and Asibi p.7 strain accumulated two and seven amino acid substitutions, respectively (McArthur et al. 2003; McArthur et al. 2020). These mutations suggest there is a potential difference behind the adaptation process in each strain.

The hamster-adapted Jimenez p.10 strain was used to demonstrate protection of the XRX-001 candidate inactivated YFV vaccine generated with β-propiolactone and the type-specific neutralizing mAb-2C9 (see section 1.4.C) (Julander, Trent, and Monath 2011). Because the inactivated XRX-001 vaccine candidate mainly elicits antibody responses and the protection was proven to correlate with the $PRNT_{50}$ titer, it aided in the establishment of threshold for immune protection against YFV at 1:10 $PRNT_{50}$ titer. The same threshold in the $PRNT_{50}$ titer has been extensively applied to the evaluation of various candidate flavivirus vaccines.

Although it requires the use of YFV variants that contain genetic substitutions, hamsters are considered a biologically relevant model for human YF and hence have the broad utility in YF research. However, they are not a relevant model for understanding protective mechanisms elicited by the 17D vaccine against different genotypes of wt YFV due to the necessity of using a hamster-adapted strain.

## 1.6 Hypothesis and scope

In summary, a single immunization with the 17D vaccine elicits protective immunity against all seven genotypes of wt YFV. However, the mechanism(s) of protection remains poorly understood. Neutralizing antibodies are the only correlate of protection for 17D vaccinees against wt YFV. Importantly, the neutralizing antibody responses elicited by the 17D vaccine are type-specific (i.e., only neutralize YFV and does not cross-react with other flaviviruses). It is also known that the E protein is the major target of neutralizing anti-YFV antibodies. To date, the specific antibody-mediated neutralization process has not been investigated using human mAbs isolated from individuals vaccinated with the 17D vaccine. There is a major gap in knowledge in how human antibodies raised against the 17D vaccine strain neutralize and protect against wt YFV.

The research described in this dissertation aims to: 1) determine the neutralizing activity of two human anti-YFV mAbs isolated from 17D vaccinees against different genotypes of wt YFV, 2) identify residues on the E protein recognized by the human anti-YFV mAbs, and 3) to compare the level of passive protection of each neutralizing human anti-YFV mAb in mice against the 17D strain (the immunogen) and wt YFV. Formulated on the available knowledge, ***the central hypothesis of this dissertation is that human anti-YFV mAbs isolated from 17D vaccinees recognize epitope(s) on the E protein and can neutralize and protect against wt YFV infection***. To test this hypothesis, three approaches were undertaken to determine the neutralizing activity and passive protection of two human mAbs isolated from 17D vaccinees against YFV.

## A. Neutralizing activity of two human anti-YFV mAbs against the vaccine strain and four wild-type strains of YFV

The neutralizing activity of two anti-YFV mAbs isolated from 17D vaccinees were evaluated against the 17D strain and strains representative of four genotypes of wt YFV. The neutralization potency of each human anti-YFV mAb was determined against the 17D vaccine strain, West Africa I genotype (BA-55 strain), West Africa II genotype (Asibi strain), South America I genotype (JSS strain), and South America II genotype (1899/81 strain). The $PRNT_{50}$ titers of the two human anti-YFV mAbs against the YFV strains were determined. Results from these studies are discussed in Chapter 3.

## B. Characterization of YFV type-specific neutralizing epitopes on the envelope protein

The two human anti-YFV mAbs isolated from 17D vaccinees were used to characterize YFV type-specific epitopes on the E protein. This study was based on the premise that the two anti-YFV mAbs exhibit different neutralizing activity against the 17D vaccine strain and the prototype wt YFV Asibi strain. Therefore, the 12 mutations that distinguish the E protein sequence of the 17D-204 vaccine substrain and the Asibi strain, at least in part, constitute the neutralizing epitope(s) recognized by the anti-YFV mAbs. Chimeric viruses were constructed to contain three individual domains of the E protein derived from the 17D vaccine strain and wt Asibi strain. The $PRNT_{50}$ titers of the two human anti-YFV mAbs against the chimeras were measured to identify residues that constitute the neutralizing epitope(s). Data from this study are summarized in Chapter 4.

## C. Passive protection of human anti-YFV mAbs against neurotropic and viscerotropic diseases in mice

The ability of each human anti-YFV mAb to protect mice against neurotropic and viscerotropic YF disease was determined. Firstly, outbred CD-1 mice were prophylactically passively immunized with one of two human anti-YFV mAbs or an isotype control and intracerebrally challenged with the 17D vaccine strain to select mAbs that confers the passive protection *in vivo.* Additionally, the same neurotropic disease model was used to determine the ability of each human anti-YFV mAb to protect against the wt Asibi strain. The second mouse model utilized the C57BL/6 mouse strain lacking type-I and type-II interferon responses (C57BL/6-IFNAR$^{-/-}$-IFNGR$^{-/-}$), referred to as AG6 mice, as a viscerotropic disease model for wt YFV infection. Prophylactic passive immunization of AG6 mice with one of two human anti-YFV mAbs or the isotype control was undertaken to evaluate each mAbs ability to protect against viscerotropic disease induced by ip challenge with the wt YFV Asibi strain. Results from these studies will help demonstrate that antibody-mediated neutralization protects against YFV infection. Data from this study are presented in Chapter 5.

Collectively, the completion of these projects advances our understanding of antibody-mediated neutralization and protection against wt YFV in humans. We have demonstrated that both human anti-YFV mAbs are type-specific, which is consistent with the observations in human polyclonal sera isolated from the 17D vaccinees but investigates the antibody-mediated neutralization of YFV at a higher resolution. The passive protection observed in this study is significant and demonstrates that individual clonal populations of anti-YFV mAbs confer protection against YFV challenge *in vivo*.

# Chapter 2 - Materials and Methods

## 2.1 Introduction

Three complementary approaches were employed to characterize two human anti-YFV mAbs isolated from two 17D vaccinees. The neutralization potency of each mAb against the 17D vaccine strain and the representative strains of four wt YFV genotypes were determined using $PRNT_{50}$ to demonstrate both human mAbs represent YFV type-specific neutralizing antibodies (Section 2.2). The antigenic structure(s) recognized by each mAb based on the different $PRNT_{50}$ titers against the recombinant 17D strain, Asibi strain, and chimeras that exchange the three domains of the E protein between the 17D and Asibi strains was investigated (Section 2.2). Finally, the level of passive protection against the 17D strain and Asibi strain was evaluated in mice to identify mAb(s) that have functional importance in the protection against YFV infection (Section 2.4). Section 2.3 provides the quantification of virus by plaque assay (2.3.A) and PRNT (2.3.B) techniques and materials used throughout all three experiments.

## 2.2 Cell lines, viruses, and anti-YFV mAbs

### A. Cell lines

Two cell lines were used for the preparation of virus stocks and quantification of infectious viruses in this project, including *Aedes albopictus* C6/36 cells and three subclones of African green monkey (*Cercopithecus aethiops*) kidney epithelial Vero cells. Both C6/36 cells and Vero cells are considered standard reagents for flavivirus research. Importantly, Vero cells are recommended by the World Health Organization for plaquing of flaviviruses and are therefore appropriate for $PRNT_{50}$ against both the 17D vaccine strain and wt YFV strains.

C6/36 cells were originally derived from a pool of *Ae. albopictus* larvae and selected to support the multiplication of multiple arboviruses, including several wt YFV genotypes that do

not consistently reach high titers in cultures in mammalian cell lines (Igarashi 1978; Stock et al. 2013; Faye et al. 2020). Therefore, the comparison of neutralization potency between two different human anti-YFV mAbs was performed using virus stocks generated in C6/36 cells. The line of C6/36 cells used in this study was obtained from the World Reference Center for Emerging Viruses and Arboviruses, University of Texas Medical Branch (Vasilakis et al. 2009). All cultures were maintained in high-glucose Dulbecco's Modified Eagle Medium (DMEM) supplemented with 10% heat-inactivated fetal bovine serum (FBS), 10% tryptose phosphate broth (TPB), 2 mM of L-glutamine, 100 U/ml penicillin, and 100 µg/ml streptomycin at 28°C with 5% $CO_2$.

Three different lines of Vero cells were used in this project including Vero, Vero76, and VeroE6 cells. The subtle difference in the biological properties of each line allows the optimization of specific experiments. Vero cells without the clonal selection (ATCC catalogue number CCL-81) is suited as a transfection host and has been used in the production of recombinant live-attenuated viral vaccines (Monath et al. 2000). Therefore, the recovery of all recombinant YFV was performed by the transfection of Vero cells, as described in previously published studies (Huang et al. 2005; Collins et al. 2018). Vero cells were maintained in modified Minimum Essential Medium (MEM-α) supplemented with 10% heat-inactivated FBS, 100 U/ml penicillin, 100 µg/ml streptomycin, 2 mM of L-glutamine mixture, and 1% MEM vitamin solution. The Vero76 cells (ATCC catalogue number CRL-1587), selected from the original Vero cells, is known to develop visible plaques after the infection of flaviviruses and was used for all plaque assay and $PRNT_{50}$ assays in this project (Park et al. 2018; Stone et al. 2018). The growth media for Vero76 cells consists of Leibovitz (L-15) media supplemented with 10% heat-inactivated FBS, 10% TPB, 100 U/ml penicillin, 100 µg/ml streptomycin, and 2 mM

of L-glutamine mixture. The VeroE6 cells, a derivative clone of Vero76 cells (ATCC catalogue number CRL-1586) were used for the propagation of the 17D vaccine strain and the wt YFV Asibi strain for passive protection studies as it has been proven effective in propagating both YFV strains to titers sufficient for lethal challenges (Cong et al. 2016). VeroE6 cells were maintained in DMEM supplemented with 10% heat-inactivated FBS, 10% TPB, 100 U/ml penicillin, 100 μg/ml streptomycin, and 2 mM of L-glutamine mixture. All three lines of Vero cells were maintained at 37°C. Cultures of Vero cells and VeroE6 cells were supplemented with 5% atmospheric $CO_2$ level because of the use of media buffered with sodium bicarbonate. Vero76 cells maintained in HEPES-buffered L-15 media were maintained without the supplementation of $CO_2$.

## B. Yellow fever viruses

The neutralization potency of each human mAb is determined by the $PRNT_{50}$ against the 17D vaccine strain and four wt YFV strains, proving the two anti-YFV mAbs are type-specific neutralizing antibodies relevant to the antibody-mediated neutralization of wt YFV in 17D vaccinees. An additional panel of recombinant YFV chimeras rescued from the cDNA infectious clones was also used to investigate the antigenic structures in the E protein recognized by each mAb. Lastly, the 17D vaccine strain and the wt prototypic Asibi strain were used to investigate the ability of each mAb to confer passive protection *in vivo*.

***Yellow fever virus 17D vaccine strains.*** The 17D-204 substrain was used as a representative of the 17D strain, the immunogen, because of its availability and utility in the manufacturing of the live-attenuated 17D vaccine in the United States. The YFV 17D-204 vaccine strain used in this project was acquired from two sources. For simplicity, the 17D-204 substrain is referred to as the 17D strain in the discussion of all experiments.

Virus stocks used as a control in the $PRNT_{50}$ against different genotypes of wt YFV were prepared from the 17D strain available at the depository of the Biodefense and Emerging Infections (BEI) Research Resources (Lot no. 7496108). Although the passage history is unclear, the 17D strain is known to be genetically stable with a negligible likelihood to differ in the antigenicity and affect the outcome of neutralization tests (Barban et al. 2007). The seed virus from BEI was propagated once in VeroE6 cells and amplified once in C6/36 cells for 7 days. Virus stocks generated from the culture of C6/36 cells were used for $PRNT_{50}$ assays.

The 17D strain used in the passive protection studies was reconstituted from a commercial lot of lyophilized YF-Vax manufactured in embryonated chicken eggs by Sanofi Pasteur (Swift Water, PA) reconstituted in 2006 (Lot no. UE639AA). The 17D strain directly reconstituted from a commercial lot of YF-Vax was used as all YF-Vax vaccines must be characterized for neurovirulence in monkeys prior to market distribution. Stocks of the 17D strain was passaged once in VeroE6 cells for 7 days upon the development of 70-80% of cytopathic effects. All stocks of the 17D strain were stored at -80°C until use.

***Wild-type YFV strains*.** Yellow fever virus type-specific neutralizing antibodies elicit neutralizing activity against both vaccine and wt YFV strains. Therefore, the neutralization potency of each mAb against wt YFV strains that are representative of four genotypes, including BA-55 (West Africa I genotype), Asibi (West Africa II genotype), JSS strain (South America I genotype), and 1899/81 strain (South America II genotype) were determined. Regardless of the passage history, each wt YFV strain was amplified once in C6/36 cells to generate virus stocks used in all $PRNT_{50}$ assays. The Asibi strain was also used to investigate the ability of each mAb to confer the passive protection of CD-1 mice or AG6 mice against the lethal challenge with wt YFV (Section 2.4). Virus stocks used for the challenge of passively immunized CD-1 mice and

AG6 mice were prepared in infected VeroE6 cells to allow the comparison of the results derived from the passive protection studies conducted with the 17D strain.

The Asibi strain is the prototypic wt YFV strain and is made available from three major sources: Yale University (GenBank access number: MT956628.1), London School of Tropical Medicine and Hygiene (LSTMH) (GenBank access number: MT956629.1), and the Division of Vector-Borne Diseases, Centers for Disease Control and Prevention (GenBank access number: MT956630.1) (Davis et al. 2021). It belongs to the West Africa II genotype that contains wt YFV strains circulating in Ghana, Senegal, Burkina Faso, and Guinea-Bissau (Mutebi et al. 2001). The Asibi strain used in this project was obtained from LSTMH. Although the genomic sequence of the Asibi strain-LSTMH differ from the Asibi strains available at the other two institutions, several type-specific anti-YFV mAbs have been characterized using the Asibi strain-LSTMH, making it ideal for the investigation of neutralization potency and passive protection of the two human anti-YFV mAbs. Prior to the passive immunization experiments, the YFV Asibi strain was passaged once in VeroE6 cells. For all neutralization (*in vitro*) experiments, YFV Asibi was passaged one to two times in C6/36 cells. All virus stocks were stored at -80°C until use.

The BA-55 strain was isolated from a fatal YF case during an epidemic in Nigeria in 1987 (Miller et al. 1989). The prM (Genbank access number: AF369684.1), E (Genbank access number: U23572.1), and NS5 (Genbank access number: AY960144.1) genes of the BA-55 strain have been partially sequenced, placing it in the West Africa I genotype and making it a representative strain for wt YFV isolates from Nigeria, Côte d'Ivoire, and Senegal (Chang et al. 1995; Mutebi et al. 2001).

The JSS strain was the oldest strain of wt YFV found in the New World and was isolated from an infected individual in 1935 (Bryant, Holmes, and Barrett 2007). This strain represents the South American genotype I found predominantly in Brazil. The capsid, prM, and E genes of the JSS strain have been sequenced (Genbank access number: U52389.1) (Wang et al. 1996). Similarly, the NS4A gene (Genbank access number: U52391.1) and 3' UTR (Genbank access number: U42390.1) have also been sequenced (Wang et al. 1996). The isolate used in this study has the designated number TVP11 in the WRCEVA collection and the record indicates one passage in mosquitoes, eight passages in suckling mouse brains, and one passage in Vero cells that took place prior to the amplification in C6/36 cells. The 18991/81 strain was isolated in the Apurimac River Valley, Ayacucho, Peru in 1981 (Méndez et al. 1984). The genome of the 1899/81 strain has also been partially sequenced (Genbank access number: D14458.1 and AY161932.1) (Ballinger-Crabtree and Miller 1990; Bryant et al. 2003).

Collectively, all four strains tested in this project were originally derived from humans infected in the urban YF outbreaks and hence are well suited for investigating how human antibodies produced in 17D vaccinees neutralize and protect against wt YFV.

***Recombinant YFV.*** The neutralization potency of each mAb against the recombinant 17D strain, Asibi strain, and YFV chimeras that contain individual domain(s) from the E protein of the 17D and Asibi strains was compared. The recombinant 17D strain represents the immunogen that induces the primary immune response against YFV and the Asibi strain is a surrogate for wt YFV strains. Since the E protein is the primary target of neutralizing antibodies, the individual domains of the E protein from the 17D and Asibi strains are differentially presented in a total of 4 chimeras to identify the putative region(s) recognized by each mAb (**Figure 2.1**).

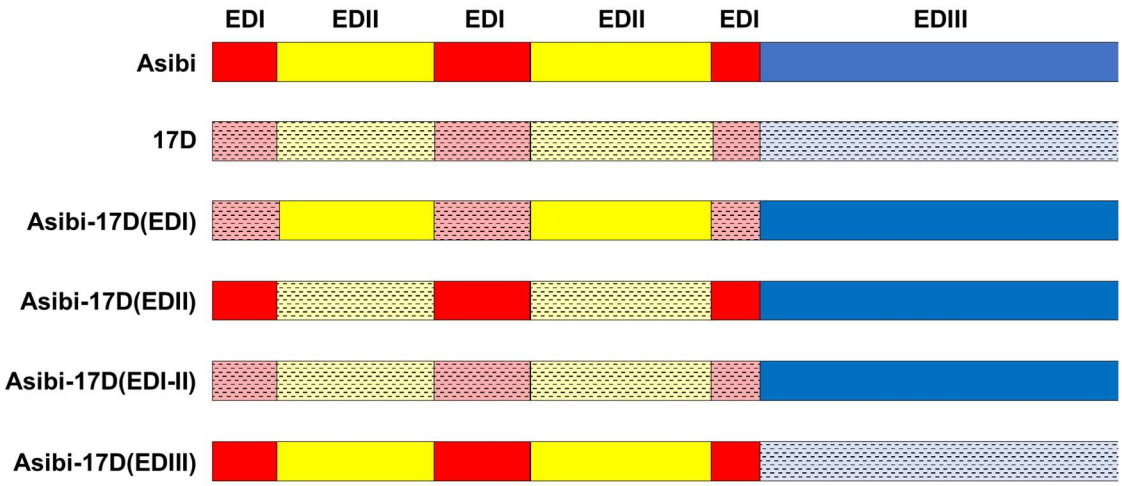


**Figure 2.1 cDNA infectious clones of YFV and chimeras characterized in this study.** The recombinant YFV Asibi strain was used as a backbone and amino acid residues in the EDI, EDII, both EDI and EDII (EDI-II), or EDIII were swapped with 17D to generate chimeras with different domains to determine the antigenic structures recognized by the human anti-YFV mAbs.

Two chimeras were produced by replacing both the EDI and EDII (EDI-II) regions or the EDIII region in the infectious clone of the Asibi strain with the corresponding region from the 17D strain, as previously described (McElroy et al. 2006). The remaining two chimeras were constructed by introducing mutations specific to the EDI or EDII of the 17D strain to the infectious clone of the Asibi strain, using the primer sets listed in **Table 2.1** and following the standard methods of PCR site-directed mutagenesis and In-Fusion cloning.

The cDNA infectious clones of the 17D and Asibi strains were developed using the low-copy pANCR plasmid in previously published studies (Rice et al. 1989; Bredenbeek et al. 2003; McElroy et al. 2005). The infectious clone of 17D strain contains the genome of the 17D-204 strain available at ATCC. The YFV genome in the pANCR-YFV-17D plasmid was replaced with the corresponding region of the Asibi strain-Yale to produce the infectious clone of the Asibi strain. Therefore, the recombinant 17D and Asibi strains differ by 10 amino acids in the EDs as listed in **Table 2.2** and mapped in the crystal structure of YFV E protein (**Figure 2.2**).

**Table 2.1 Primers used for PCR site-directed mutagenesis of the Asibi-17D(EDI) and Asibi-17D(EDII) chimeras.**

| Primer name | Sequence (5′ → 3′) |
|---|---|
| 17D-F2 | ACGGGTGGAGTGACCTTGGTCCGGAAAAACAGATGGTTGC |
| 17D-R3 | AAGACTGCGTCCATGTACAC |
| C1140T-Rev | CTTTCCTCACCTCAGCAGGTCTATC |
| C1140T-Fwd | GATAGACCTGCTGAGGTGAGGAAAG |
| C1482T-Rev | CAATGAACTCGACTTCCTGGGAGCCTG |
| C1482T-Fwd | CTCCCAGGAAGTCGAGTTCATTGG |
| A1572C-Rev | CTATCCAGCTCTCTGTTTCCATCTC |
| A1572C-Fwd | GAGATGGAAACAGAGAGCTGGATAG |

**Table 2.2 Amino acid mutations introduced into the E protein of YFV Asibi to generate YFV Asibi/17D chimeras.**

The amino acid residues mutated from the Asibi strain to the 17D strain were introduced to generate YFV chimeras with different E domains.

| Amino acid | Amino acid change (Asibi → 17D) | Domain in E protein |
|---|---|---|
| 52 | G → R | II |
| 56 | A → V | II |
| 170 | A → V | I |
| 173 | T → I | I |
| 200 | K → T | II |
| 299 | M → I | III |
| 305 | S → F | III |
| 325 | P → S | III |
| 331 | K → R | III |
| 380 | T → R | III |

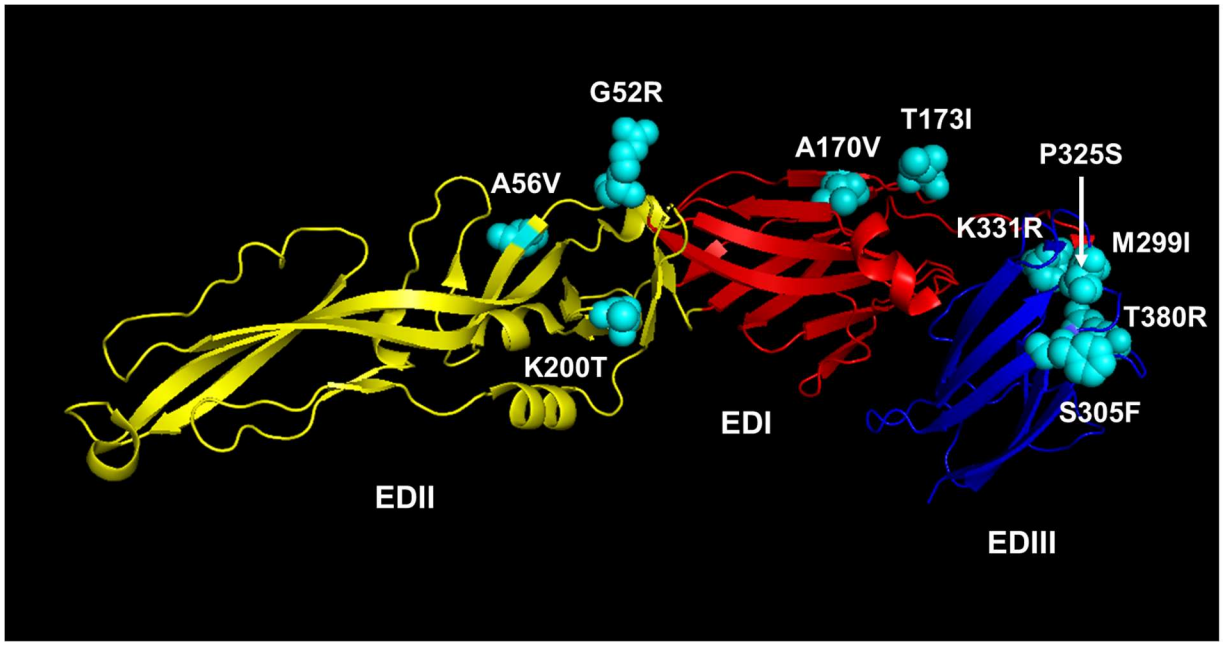


**Figure 2.2 Locations of mutations in the E protein between YFV Asibi and 17D strains in the crystal structure of YFV secreted E protein.**
Locations of amino acid residues in the YFV E protein mutated from Asibi strain to 17D strain for the generation of chimeras is shown. The three domains are labeled in red for EDI, yellow for EDII, and blue for EDIII. Amino acids mutated are shown as cyan spheres. Image adapted from the Research Collaboratory for Structural Bioinformatics Protein Data Bank (RCSB PDB, rcsb.org) of PDB ID 6IW4, YFV-17D E protein monomer in pre-fusion conformation (Lu et al. 2019). Data files contained in the archive are free of all copyright restrictions.

All full-length cDNA infectious clones were propagated in the MC1061 strain of *E. coli* competent cells maintained in terrific broth (TB) supplemented with ampicillin. Briefly, the MC1061 strain was harvested at the log phase of its growth period, washed in prechilled buffer containing 0.01 M MOPS, 0.01 M RbCl at pH 7.0, and permeabilized with the buffer containing 0.1 M MOPS, 0.05 M CaCl2, and 0.01 M RbCl on ice for at least 40 minutes. Each plasmid was transferred by the heat shock method at 43.5°C for 45 seconds, followed by recovery in 250 rpm shaking culture held at 37°C for one hour and plating on 2x YT agar plates (1.6% tryptone, 1% yeast extract, 0.5% NaCl, and 1.2% agar) containing 50 mg/ml of ampicillin for overnight culture at 37°C. After permeabilization the competent cells were used for construction of the YFV 17D and Asibi cDNA infectious clones and generated the cDNA of the full-length YFV

genome. Single colonies of each plasmid were inoculated into 10 ml of TB broth (1.2 % peptone, 2.4% yeast extract, 72 mM $K_2HPO_4$, 17 mM $KH_2PO_4$, and 0.4% glycerol) supplemented with ampicillin at 50 mg/ml to generate starter cultures. Two-hundred-and-fifty ml cultures of each plasmid were initiated by inoculating 1 ml of starter culture, followed by the shaking culture at 250 rpm for approximately 16 hours at 37°C. The purification of plasmids followed the alkaline lysis procedure using the commercially available Neucleobond®XTra Maxi kit (Takara, Mountview, CA). The overnight cultures were pelleted by centrifugation at 4,000 rpm for 10 minutes at 4°C. The liquid was decanted, and the bacterial pellet was gently resuspended in 24 ml of resuspension buffer (RES) and sat for 5 minutes at room temperature. An additional 25 ml of lysis buffer (LYS) was added, inverted several times, and incubated at room temperature for 3-5 minutes for the alkaline lysis reaction. To neutralize the reaction and separate the plasmid DNA from the lysates, 24 ml of neutralization buffer (NEU) was added, inverted several times until the solution turned clear, and centrifuged at 4,000 rpm for 15 minutes at 4°C. The supernatant was filtered using a sterile gauze assembled to 50 ml conical tubes. The liquid flow through from the gauze filter was added to a silica column filter pretreated with 25 ml of equilibration buffer (EQU) and the liquid flow through was discarded. The silica column filter was washed with 15 ml of buffer EQU and the filter was discarded once the buffer EQU had completely flown through, leaving only the silica column. Twenty-five ml of buffer wash (WASH) was added to the column and the flow through was discarded. New 50 ml conical tubes containing 10.5 ml of isopropanol were placed under the silica column. Fifteen ml of elution buffer (ELU) was added and the flow through was retained. A pellet formed and the tube was vortexed until the pellet was dissolved. The mixture was aliquoted into 2.0 ml Eppendorf tubes (one column generated approximately 13 2.0 ml Eppendorf tubes). The 2.0 ml Eppendorf tubes

were centrifuged at 11,800 rpm for 30 minutes at 4°C. Following centrifugation, the isopropanol was removed from each tube and the pellets were resuspended with 1 ml of 70% ethanol, consolidating pellets to 3-4 tubes. The 2.0 ml Eppendorf tubes were centrifuged at 11,800 rpm for 5 minutes at 4°C, the 70% ethanol was removed, and the pellets were resuspended again in 1 ml of 70% ethanol. These steps consolidated all the 2.0 ml Eppendorf tubes into 1 final 2.0 ml Eppendorf tube. A final centrifugation of the remaining tube at 11,800 rpm for 5 minutes at 4°C pelleted the sample. The 70% ethanol was removed, and the pellet was air-dried for 15-30 minutes. The DNA was resuspended in 200 µl of nuclease-free water and vortexed. The DNA was aliquoted into 2 1.5 ml Eppendorf tubes containing 100 µl each and stored at -20°C.

Each plasmid was linearized by a specific restriction endonuclease to generate the template for the SP6 DNA-dependent RNA polymerase. The cDNA infectious clones based on the backbone of the Asibi strain were digested by the *Nru*I restriction endonuclease (New England Biolabs) and the 17D stain infectious clone was digested using the *Xho*I restriction endonuclease (New England Biolabs). Briefly, each plasmid was digested in a 40 µl reaction containing 3-4 µg of plasmid DNA, 4 µl of 10x reaction buffer (NEBuffer 3), 4 µl of 10x bovine serum albumin (BSA), and 1 µl of *Nru*I restriction endonuclease. The cDNA infectious clone of 17D-204 was digested in a 40 µl reaction using 3-4 µg of plasmid DNA, 4 µl of 10x reaction buffer (Cutsmart buffer), and 1 µl of *Xho*I restriction endonuclease. The contents were gently mixed by tapping, briefly centrifuged, and incubated at 37°C for 1 hour. Each reaction was purified using the phenol-chloroform extraction and ethanol precipitation methods. The DNA-enzyme mixture was first diluted with 60 µl of nuclease-free water, mixed with 100 µl of phenol:chloroform:isoamylalcohol (25:24:1) solution by vortexing for 15 seconds and pelleted by centrifugation at 13,500 rpm for 5 minutes. The aqueous layer was collected and transferred

to a new, sterile tube, and the phenol was removed by mixing with 100 µl of chloroform:isoamylalcohol (24:1) for 15 seconds followed by centrifugation at 13,500 rpm for 5 minutes. The aqueous layer was collected and mixed with 220 µl of 70% ethanol and 10 µl of sodium acetate (pH 4.2) by gently tapping. Plasmid DNA was precipitated at -80°C until needed for *in vitro* transcription.

The *in vitro* transcription of linearized DNA plasmids was performed to generate the infectious positive-sense genome using the SP6 mMessage mMachine kit (Life Technologies). Linearized plasmids were removed from -80°C and centrifuged at 15,000 rpm for 10 minutes. The supernatant was removed and 150 µl of 70% ethanol was added to remove the salts. The DNA was centrifuged for 5 minutes at 15,000 rpm and the supernatant (70% ethanol) was removed. The pellet air-dried for 20-30 minutes. The reactions were assembled by combining (in the following order): 10 µl of 2x CAP/NTP mixture, 6 µl of linear DNA, 2 µl of 10x reaction buffer, 2 µl of 20 mM GTP, and 1.4 µl of SP6 enzyme mix and incubated for 60 minutes at 37°C. The integrity of the RNA products was ensured by loading 1 µl of the reaction collected approximately 15 minutes into the reaction time and separated on a 1% agarose gel at 125 volts for 20 minutes. The reaction was aliquoted into 10 µl samples and stored at -80°C for electroporation.

The infectious viral RNA was electroporated into Vero cells. Vero cells were seeded two days prior to electroporation at a concentration of $3.0x10^6$ cells/flask in 25 ml of MEM-α in tissue culture-treated T150 flasks (Corning). The cells were rinsed with 12 ml of Dulbecco's phosphate buffer saline (DPBS) without $Ca^{2+}$ and $Mg^{2+}$ (Corning) and treated with 3 ml of 0.25% trypsin-EDTA for 5-10 minutes at 37°C with 5% $CO_2$. Once the cells were detached from the surface, the reaction was terminated by adding 8 ml of MEM-α. The cells were pelleted by

centrifugation at 1,200 rpm for 5 minutes at 4°C. The cells were resuspended in 10 ml of ice-cold DPBS without $Mg^{2+}/Ca^{2+}$ and pelleted by centrifugation at 1,200 rpm for 5 minutes at 4°C two more times to ensure the removal of excess nucleases on the cell surface. Prior to the third wash step, the cells were counted for the final adjustment of cell density to $10^7$ cells/ml. The cells were pelleted by centrifugation at 1,200 rpm for 5 minutes at 4°C a third and final time. The liquid was decanted, and the cell pellet was resuspended with appropriate volumes of ice-cold DPBS without $Mg^{2+}/Ca^{2+}$. Ten 10 µl of viral RNA transcripts was added to 400 µl aliquot of Vero cells, immediately transferred to a pre-chilled 4 mm electroporation cuvette, and electroporated once at 225 volts for 25 msec using a BioRad GenePulser Xcell electroporation system. The electroporated cells were allowed to recover on ice for at least 10 minutes. Electroporated cells were retrieved by rinsing each cuvette with 800 µl of pre-warmed media three times and transferred to a T75 flask (Corning) containing 7-8 ml of pre-warmed MEM-α. All stocks of recombinant YFV were propagated at 37°C with 5% $CO_2$ for 7 days, when cytopathic effects were observed.

## C. Anti-YFV mAbs

***Sources of the two human anti-YFV mAbs.*** Two human anti-YFV mAbs were originally isolated from 17D vaccinees and generated in the form of recombinant human mAbs by the DeKosky group (DeKosky et al. 2013). One donor received two doses of YF-Vax in the USA, including a final boost 21 days prior to blood draw. The second donor was immunized three times in Brazil with the YFV 17DD substrain and once in the USA with the YF-Vax substrain approximately 21 days prior to blood draw. Consequently, mAbs acquired through the two subjects have been recently stimulated with one dose in the USA with YF-Vax.

The analysis of individual B cells from the two YFV 17D vaccinees yielded human anti-YFV mAbs (DeKosky et al. 2013). Virus-like particles (VLPs) of wt YFV BeH622493 strain were used to select for YFV-specific mAbs that recognize the E protein of wt YFV (Lima, Souza, and Castilho 2019). Two YFV type-specific human IgG1 mAbs were isolated: mAb-29 and mAb-32. These mAbs showed high neutralization potency against the YFV 17D strain. Throughout the experiments, the VRC01 isotype control human IgG mAb was used to ensure immune protection against YFV was not caused by the administration of non-specific antibodies (Wu et al. 2010). The VRC01 mAb recognizes the HIV envelope glycoprotein gp120 and has no known neutralizing activity against YFV.

***Mouse anti-YFV mAbs.*** To verify the antigenic structures of the recombinant YFV 17D and Asibi strains were analogous to the biological 17D and Asibi strains, the neutralizing activity of two mouse mAbs, mAb-117 and mAb-2D12, that preferentially bind to YFV Asibi strain were evaluated in $PRNT_{50}$ assays. A lyophilized mAb-117 (mAb-10.17a) from 2 ml of mouse ascitic fluid was reconstituted in 2 ml of sterile nuclease-free water followed by 4 ml of sterile 1x DPBS with $Ca^{2+}$ and $Mg^{2+}$. The mAb-2D12 (clone 2D12.A, EMD Millipore, Sigma Aldrich) was diluted 10-fold with L-15 media. Aliquots of mAb-117 and mAb-2D12 were heat-inactivated at 56°C for 30 minutes to inactivate complement proteins in the ascitic fluid. The heat-inactivated mAbs were stored at -20°C until further use.

## 2.3 Techniques for the quantitative analysis of infectivity of YFV and neutralization potency of human anti-YFV mAbs

### A. Plaque assay

To determine the infectivity of YFV used in the neutralization tests *in vitro* and passive protection studies in mice, plaque assay was performed using Vero76 cells. Formation of viral

plaques are due to the development of cytopathic effects among Vero76 cells infected with YFV. Each plaque is initiated by the infection with one infectious particle, followed by the spread to neighboring cells maintained in a semi-solid overlay media and the staining with MTT to distinguish the live and dead cells. Briefly, one day prior to infection, each well of 24-well plates were seeded with approximately $8x10^4$ cells suspended in 1 ml of outgrowth media. Plates were incubated overnight at 37°C to allow cells to adhere to the plate and form a monolayer. Virus samples were briefly thawed in a 37°C water bath and kept on ice. Stocks of respective YFV strains were serially diluted 10-fold with L-15 media or MEM-α media 5 times (i.e., $10^0$ to $10^{-5}$). Fifty microliters of diluted virus samples were inoculated into each well and adsorbed at 37°C for one hour prior to the addition of 1 ml L-15 overlay media containing 500 ml deionized water, 8 g methyl cellulose, 400 ml 2x L-15 media, 60 ml FBS, 20 ml antibiotics and L-glutamine mixture (100 U/ml penicillin, 100 µg/ml of streptomycin, and 2 mM of L-glutamine), and 100 ml of TPB. The plates were sealed with parafilm and incubated at 37°C for 7 days to allow the development of plaques.

After the 7-day plaque assay incubation period, the media was removed from each well and the cells were washed with 1 ml of sterile 1x DPBS. Approximately 1 ml of sterile 1x DPBS was added to each well followed by the addition of 3-(4,5-dimethylthiazol-2-yl)-2,5-diphenyltetrazolium bromide (MTT, 5 mg/ml solution in PBS) at 10% volume into each well. The cells incubated with the MTT solution for 2-3 hours at 37°C. Once the incubation period was over, the MTT solution was removed, and the plaques were counted using a light box for better visualization. The titers were calculated in plaque forming units (PFU)/ml using the following formula:

$$\frac{(Number\ of\ plaques)}{(10^{dilution})(0.050\ ml)} = PFU/ml$$

## B. 50% Plaque reduction neutralization test

To determine the neutralization potency of each mAb against the biological isolates of YFV, recombinant YFV strains, and the YFV chimeras, the $PRNT_{50}$ was performed using Vero76 cells. A constant amount of infectious virus (i.e., 50-100 PFU) is subjected to the neutralization of respective anti-YFV mAbs, followed by the inoculation onto a monolayer of Vero76 cells to allow the development of viral plaques. The 50% reduction of plaque numbers in wells treated with the mAbs in comparison with the control wells represents the log phase of each neutralization curve. This was used as the cutoff to compare the neutralization potency of each mAb against 1) the 17D vaccine strain, 2) the representative strains of four wt YFV genotypes, and 3) the recombinant YFV chimeras. Briefly, 24-well plates were seeded at the density of approximately $8x10^4$ Vero76 cells per well and incubated overnight at 37°C. Human anti-YFV mAb-29, mAb-32, and isotype control VRC01 (referred to as isotype control for the remainder of the dissertation) were removed from -80°C, briefly thawed in a 37°C water bath, and quickly spun down. Stocks of mAb-29, mAb-32, and the isotype control were generated by diluting to 100 μg/ml with L-15 media. Using a 96-well plate, 4-fold serial dilutions from 100 μg/ml to 0.00038147 μg/ml (10 total dilutions) were made using L-15 media to make a total of 60 μl of antibody sample at each dilution. Virus samples were briefly thawed in a 37°C water bath and diluted to approximately 1,500 PFU/ml in L-15 media. Sixty microliter of diluted virus was added to each well in the 96-well plate to make an equal volume of antibody and virus. A set of virus control wells containing 60 μl of L-15 media and 60 μl of diluted virus samples (no antibodies) were made. The antibody-mediated neutralization was tested by incubating the mixture of virus and mAbs at 37°C for 60 minutes. Towards the end of the incubation period, the L-15 media was removed from each well. Fifty microliter of virus/antibody mixture was added

to the corresponding well of Vero76 cells in duplicate. Three positive control wells were included in each plate by adding 50 µl of the virus only sample to three wells. Additionally, a negative control (L-15 media) was included for each plate. The inoculum adsorbed at 37°C for 60 minutes, with gentle agitation every 15 minutes. After the adsorption period, 1 ml of warmed 0.8% methyl cellulose overlay in L-15 media was added to each well. The plates were sealed with parafilm and incubated at 37°C for 7 days. After the 7-day incubation period, the staining of viral plaques followed the same procedures as described in Section 2.3.A. The neutralizing antibody titers were calculated based on a 50% or greater reduction in plaque numbers by dividing the plaque number in the well containing the virus/mAb mixture by the average of the three positive control wells, as shown in the formula below:

$$\frac{(Number\ of\ plaques)}{\begin{matrix}(Average\ number\ of\ plaques\ from \\ three\ positive\ control\ wells)\end{matrix}}\ x\ 100 = \%\ neutralization$$

## 2.4 Animal experiments and study design

The ability of each mAb to confer passive protection against YFV infection *in vivo* was evaluated in two mouse models of YF disease: the neurotropic disease model of the 17D and Asibi strains in CD-1 mice and the viscerotropic disease model in AG6 mice. The following experimental procedures and animal use were approved by the Kansas State University Institutional Animal Care and Use Committee (IACUC). All methods were conducted in accordance with the approved protocol and regulations. All animal work involving the manipulation of the 17D strain was conducted in an ABSL-2 laboratory. All animal work involving YFV Asibi was conducted in the ABSL-3 vivarium at the Biosecurity Research Institute. All experiments had an endpoint at day 14 post-infection, upon which surviving animals were euthanized according to the protocol.

## A. Neurotropic disease model of the 17D and Asibi strains in outbred CD-1 mice

While mice can generally succumb to neurotropic disease caused by the ic challenge with YFV, there have been considerable differences in the susceptibility to YFV reported between different mouse strains and even between different colonies within the same strain. Therefore, a preliminary study was first undertaken to determine the susceptibility of outbred CD-1 mice to ic injection of YFV 17D-204 at three doses. This was necessary to select the dose of 17D strain suited for the lethal challenge needed for the passive immunization experiments. A total of 15 four-week-old male outbred CD-1 mice (Charles River Laboratory) were randomly assigned into three groups ($n$=5) and housed in separate cages. Animals were injected by the ic route with $10^4$ PFU, $5x10^4$ PFU, or $10^5$ PFU of 17D strain and monitored for the onset of lethal neurotropic disease.

Prior to inoculation, mice were anesthetized with 4% isoflurane until the mouse was nonresponsive, recumbent, and had a slowed, even respiratory pattern. Anesthesia was maintained using a nose cone and 1%-2% isoflurane. Eye ointment was applied. The hair on the scalp of the mouse was clipped and the area was cleaned three times with sterile saline to remove debris and clipped hair. Mice were inoculated with a 0.5 ml syringe (27 Gauge x ½ - 0.4mm x 13mm, BD Biosciences) containing 30 µl of $10^4$ PFU, $5x10^4$ PFU, or $10^5$ PFU of YFV 17D strain diluted in DMEM media. The needle was inserted into the mouse's skull centered between the ears and off center to the side from the eyes. Once the virus was injected into the brain, the mouse was placed in a holding area until fully recovered from anesthesia. Mice were given oxygen and stimulated in the event they stopped breathing during the procedure. All mice recovered within a few minutes of the procedure and were placed back in the corresponding cage and monitored.

Mice were weighed daily and observed for signs of disease. Mice that were moribund or displayed neurological disease symptoms, e.g., hind-limb paralysis, were euthanized with $CO_2$. The confirmation of death was done by cervical dislocation. The brains were collected and prepared (see Section 2.4.C) followed by viral genome detection (see Section 2.4.D). **Figure 2.3** shows the probability of survival in CD-1 mice challenged at the three doses.

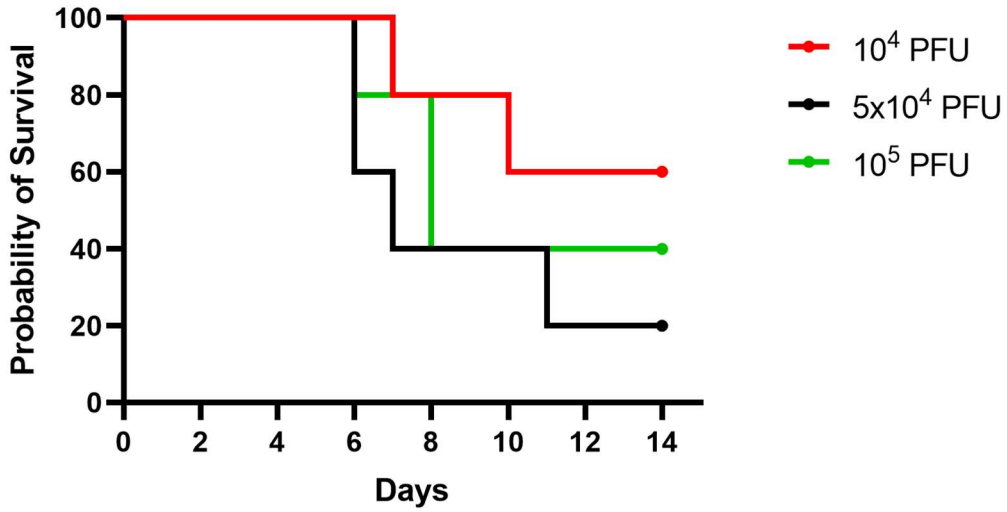


**Figure 2.3 Probability of survival in CD-1 mice challenged intracerebrally with $10^4$ PFU, $5x10^4$ PFU, or $10^5$ PFU of YFV 17D to determine the susceptibility of mice to YF infection.** CD-1 mice were challenged by the ic route with three doses of YFV 17D to determine the susceptibly for future passive protection studies. Mice in the $5x10^4$ PFU group reached 80% mortality. Probability of survival determined using Kaplan-Meier survival curve analysis.

A summary of the median survival time (MST) and mortality rate is shown in **Table 2.3**. There was no statistical difference in survival time between the three doses of YFV 17D (Kruskal-Wallis test followed by Dunn's multiple comparisons test, $p$=0.3640). Because the group that received $5x10^4$ PFU YFV 17D reached 80% mortality, this dosage was chosen for the passive protection study of the human anti-YFV mAbs in CD-1 mice against YFV 17D.

**Table 2.3 Mortality rate and median survival time (MST) of CD-1 mice challenged intracerebrally with YFV 17D strain to determine susceptibility.**
The percent mortality (dead/total) and median survival time (MST) in days post-infection of CD-1 mice challenged with $10^4$, $5x10^4$, or $10^5$ PFU of YFV 17D. There was no statistical difference in the survival time of mice among the three groups (Kruskal-Wallis followed by Dunn's multiple comparisons test, $p$=0.3640).

| | $10^4$ PFU | $5x10^4$ PFU | $10^5$ PFU |
|---|---|---|---|
| Mortality rate | 40% (2/5) | 80% (4/5) | 60% (3/5) |
| MST (days) | >14 | 7 | 8 |

It is worth noting that discrepancies observed during the susceptibility study of mice to YFV 17D may be partially due to the genetic background of these mice and the room to which they were bred at the manufacturing facility. Due to the variability in susceptibility of the mice, future studies using CD-1 mice from Charles River Laboratory were specifically requested from one breeding room.

To minimize the use of animals in ABSL-3 conditions, the first passive protection study was performed with the 17D strain in CD-1 mice using human anti-YFV neutralizing mAb-29 or mAb-32. A total of 15 four-week-old male outbred CD-1 mice (Charles River Laboratory) were randomly assigned into three groups ($n$=5): mAb-29, mAb-32, or the isotype control VRC-01, and housed in separate cages.

Twenty-four hours prior to challenge, mice were weighed and passively immunized with 1.0 mg/ml of mAb-29, mAb-32, or isotype control by the ip route. **Figure 2.4** summarizes the timeline for the passive protection studies. The antibodies were removed from -80°C, briefly thawed at 37°C in a water bath and kept on ice until use. All antibodies were diluted using sterile saline (1x DPBS, Corning). Up to 120 µl of antibodies were loaded in 26G 3/8 (0.45mm x 10mm, BD brand) x 1 ml syringes with an intradermal bevel needle, tuberculin sliptip.

Mice were anesthetized and prepared for ic injection using the same methods as previously described. The 17D strain was diluted in DMEM media to $5x10^4$ PFU in approximately 30 µl. All mice were monitored for up to 14 days post infection (d.p.i.) and the humane euthanasia was administered according to the same standards as previously described. The brains were collected and prepared (see Section 2.4.C) followed by viral genome detection (see Section 2.4.D).

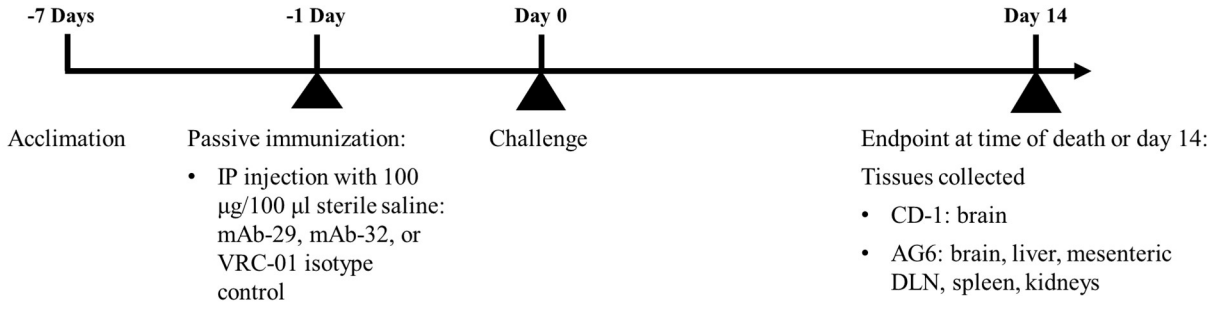


**Figure 2.4 Timeline for passive immunization and challenge studies in mice.** After acclimation, mice were passively immunized by the ip route with mAb-29, mAb-32, or the isotype control. On day zero, mice were challenged by the ic route with YFV 17D or Asibi, or by the ip route with YFV Asibi. Tissues were harvested at the time of death or euthanasia. The study concluded on day 14 post-infection.

As both mAbs conferred full protection against the 17D strain (Section 5.2), the protective efficacy of human anti-YFV neutralizing mAb-29 and mAb-32 against YF neurotropic disease using the wt Asibi strain was evaluated. A total of 18 four-week-old male (*n*=9) and female (*n*=9) outbred CD-1 mice (Charles River Laboratory) were weighed and evenly distributed into three groups (*n*=3 male and *n*=3 female per group) to receive the passive transfer of mAb-29, mAb-32, or the isotype control VRC01 mAb. Twenty-four hours prior to challenge, mice were weighed and passively immunized with approximately 1.0 mg/ml of mAb-29, mAb-32, or isotype control via the ip route as previously described and summarized in **Figure 2.4**. Mice were anesthetized and prepared for ic injection using the same methods as described. The

YFV Asibi strain was diluted in DMEM media to $5x10^4$ PFU/30 µl. Mice were weighed daily, observed for signs of disease, and humanely euthanized using the standards as described previously. The brains were collected and homogenized (see Section 2.4.C) and the viral load was determined (see Section 2.4.D).

### B. Passive protection of AG6 mice against YFV Asibi strain

The second model was used to determine the ability of each human anti-YFV neutralizing mAb to protect against viscerotropic disease induced by wt YFV in immunocompromised mice that lack type-I and type-II IFN receptors. AG6 mice were selected as a relevant model because they develop viscerotropic disease like severe human YF infection. Importantly, virus can be detected in the liver of AG6 mice, better resembling human YF viscerotropic disease. A total of 15 male (*n*=8) and female (*n*=7) AG6 mice (Jackson Laboratory) were distributed into three groups based on their sex, age, and weight, as summarized in **Table 2.4**. To avoid the skewed data on weight loss, the heaviest and lightest mice were grouped together, and mice with middle weights were grouped together.

**Table 2.4 Distribution and grouping of AG6 mice based on sex and age.**

| | Male (Age) | Female (Age) |
|---|---|---|
| Isotype control | 2 (7-weeks) | 3 (2x 7-weeks, 1x 6-weeks) |
| mAb-29 | 3 (7-weeks) | 2 (7-weeks) |
| mAb-32 | 3 (7-weeks) | 2 (7-weeks) |

Twenty-four hours prior to challenge, mice were weighed and passively immunized with approximately 120 µl of 1.0 mg/ml of mAb-29, mAb-32, or isotype control by the ip route as described in Section 2.4.A and summarized in **Figure 2.4**. Prior to the ip challenge, mice were anesthetized under 4% isoflurane. Mice were quickly removed from the isoflurane induction box

and inoculated using a 1.0 ml syringe slip tip with intradermal bevel needle (26 Gauge x 3/8, 0.45mm x 10mm, BD Biosciences) containing $2x10^4$ PFU/100 µl of YFV Asibi diluted in DMEM media. Mice were weighed daily and observed for signs of disease as described previously. If moribund or displayed neurological disease symptoms such as paralysis, they were euthanized with $CO_2$. The confirmation of death was done by cervical dislocation. The brain, kidneys, liver, spleen, and mesenteric DLNs were harvested and homogenized (see Section 2.4.C) followed by viral genome detection (see Section 2.4.D).

### C. Sample collection and preparation

For the duration of all the studies, mice were monitored twice daily, approximately 12 hours apart, with weight recordings at the morning check. When one mouse in the experiment started developing signs of disease, the observation checks were increased to three times daily, approximately 8 hours apart. Clinical signs of disease included weight loss greater than 20% relative to baseline, quiescent, paralysis in one or more limbs, hunched posture, ruffled fur, and non-ambulatory.

Tissue samples were collected to determine the tissue viral load in infected animals. The brain was harvested from CD-1 mice injected with YFV 17D or Asibi strain by the ic route and the brain, liver, mesenteric DLN, spleen, and kidneys were harvested from AG6 mice injected via the ip route with YFV Asibi strain. Upon death or euthanasia, the tissues were harvested and separated into two 2 ml Eppendorf tubes containing 1 ml of L-15 media and a single stainless-steel homogenizing bead and weighed individually. All tissues were stored at -80°C prior to further processing for analysis. Before RNA extraction, the tubes containing the tissues were thawed in a 37°C water bath and homogenized using a TissueLyser II system (Qiagen) at 26 Hz for four minutes. The samples were centrifuged at 10,000 rpm for 10 minutes and 250 µl of

supernatant was aliquoted into new 1.5 ml Eppendorf tubes. RNA inactivation was completed by adding a 1:3 mix of supernatant with Trizol LS (ThermoFisher). The mixture incubated for 15 minutes to allow complete dissociation of the nucleoproteins complex and an equal volume of ethanol was added and mixed thoroughly to inactive the virus. The sample was centrifuged at 5,000 rpm for 30 seconds and was ready for RNA extraction (see Section 2.4.D).

### D. Detection of viral genome

Two criteria were used to evaluate the protective efficacy of the human anti-YFV mAbs: mortality rates and tissue viral loads. The presence of YFV in tissues was detected using one-step quantitative reverse transcription PCR (RT-qPCR). Genome equivalents of YFV in tissues were determined using a previously published TaqMan one-step RT-qPCR assay targeting the genomic fragment encoding the NS5 protein (Chao, Davis, and Chang 2007). After tissue homogenization and inactivation of viral RNA with Trizol LS, viral RNA was extracted using the Direct-zol RNA Miniprep Kit (Zymo Research) according to the manufacturer's instructions. Briefly, approximately 650 µl of lysate containing Trizol LS was loaded onto a Direct-zol RNA miniprep column and spun at 13,500 rpm for 60 seconds. The procedure was repeated until approximately 2 ml of lysate was completely processed. Each column was washed with 400 µl of RNA wash buffer, digested with 75 µl of DNA digestion buffer and 5 µl of turbo DNase. The reaction incubated at room temperature for 15 minutes followed by the addition of 400 µl of RNA pre-wash and centrifugation at 13,500 rpm for 60 seconds. The flow through was discarded and the pre-wash step was repeated. Seven-hundred microliter of RNA wash buffer was added to the column followed by centrifugation at 13,500 rpm for 2 minutes to ensure complete removal of the buffer. The flow through was discarded and the column was centrifuged an additional 60 seconds. The column was transferred to a new RNase-free collection tube and the RNA was

eluted with 50 µl of nuclease-free water. The RNA was aliquoted into two sterile 1.5 ml Eppendorf tubes containing 25 µl each and stored at -80°C until needed for RT-qPCR.

For each sample reaction, the iTaq Universal Probe One-step reaction kit (Bio-Rad) was used to prepare 10 µl total reaction mixture containing 5 µl of 2X iTaq Universal Probes One-step Reaction mix, 0.25 µl iScript Reverse transcriptase, 0.5 µl of 10 µM mFU1 primer (5′-TACAACATGATGGGAAAGCGAGAGAAAAA-3′), 0.5 µl of 10 µM CFD2 primer (5′-GTGTCCCAGCCGGCGGTGTCATCAGC-3′), 0.2 µl of YFV NS5 probe (10 µM), 1.55 µl of nuclease-free water, and 2 µl of RNA sample was prepared. Reactions were performed with a Rotor-Gene system (Qiagen). The samples underwent reverse transcription at 50°C for 30 minutes, initial denaturation at 95°C for 3 minutes, and 40 cycles of denaturation at 95°C for 15 seconds followed by primer annealing at 48°C for 3 minutes.

A standard curve was generated by 10-fold serial dilution of RNA extract derived from the *in vitro* transcription of the infectious clone of the Asibi strain. For each RT-qPCR reaction set, a positive control using the RNA transcript and two negative controls containing only the mastermix with no viral RNA and a blank water control were included. Results were reported as genome copies per gram of tissue. Samples were considered positive when the Ct value was lower than 32.

## 2.5 Statistical analysis

The GraphPad Prism version 9.2.0 for Windows, GraphPad Software, San Diego, California, USA, www.graphpad.com, program was used for all statistical analysis and data graphical displays. The relative percent of infection and $PRNT_{50}$ titers were evaluated using the nonlinear fit least squares regression dose-response using the log of inhibitor verse the normalized response. The neutralizing curves were compared using one-way ANOVA followed

by Tukey's multiple comparisons test. In the passive protection studies, the average body weight (grams) between each of the human anti-YFV mAbs and the isotype control group were compared using mixed-effects analysis followed by Dunnett's multiple comparisons test. The non-parametric Kaplan-Meier survival analysis was used to determine the probability of survival of CD-1 and AG6 mice. The Kruskal-Wallis test followed by Dunn's multiple comparisons test was used to compare the survival rates of mice. The tissue viral loads from RT-qPCR experiments were calculated as RNA copies per gram of tissue. The viral loads in all mouse experiments were evaluated using ordinary one-way ANOVA followed by Dunnett's multiple comparisons test.

# Chapter 3 - Neutralizing activity of two human anti-YFV mAbs against the vaccine strain and four wild-type strains of YFV

## 3.1 Introduction

To demonstrate two anti-YFV mAbs isolated from 17D vaccinees are type-specific neutralizing antibodies, the neutralizing activity was determined against the 17D strain and four strains representing different genotypes of wt YFV. Human neutralizing antibody responses elicited by the 17D vaccine are type-specific (i.e., neutralize both 17D and wt strains of YFV), therefore, mAb-29 and mAb-32 will be proven to be relevant to antibody-mediated neutralization and protection against wt YFV in 17D vaccinees. To date, most type-specific neutralizing anti-YFV mAbs were produced in mice (Schlesinger, Brandriss, and Monath 1983; Buckley and Gould 1985; Barrett et al. 1989) and only a limited number of human anti-YFV mAbs have been generated (Daffis et al. 2005; Lu et al. 2019; Wec et al. 2020). Importantly, few available human anti-YFV mAbs prepared from 17D vaccinees have been proven to neutralize multiple genotypes of wt YFV. This leaves a significant gap in knowledge of how antibodies in 17D vaccinees neutralize and protect against different strains of wt YFV.

Available type-specific neutralizing anti-YFV mAbs have not been characterized by neutralization tests against different genotypes of wt YFV. Therefore, how antibodies raised against the 17D vaccine can neutralize and protect against all seven genotypes of wt YFV remains poorly understood. The neutralization potency of available type-specific anti-YFV mAbs are summarized in **Table 3.1**.

**Table 3.1 Neutralization activity of type-specific anti-YFV mAbs.**
The properties of YFV-derived type-specific neutralizing mAbs based on the species (human or mouse), immunogen, and genotype(s) neutralized.

| Mouse or human | Immunogen | mAb | Genotype(s) neutralized | References |
|---|---|---|---|---|
| Mouse | 17D-204 | **4E8**<br>**2C9**<br>**2E10** | 17D – yes<br>West Africa II – yes | (Schlesinger, Brandriss, and Monath 1983) |
| | | 2B8<br>5E3<br>2D12<br>3A3<br>4E1 | 17D – no<br>West Africa II – yes | |
| | | 3E9 | 17D – no<br>West Africa II – no | |
| Mouse | 17D-204 | **825** | 17D – yes<br>West Africa II – yes<br>South America I – yes | (Gould et al. 1985; Buckley and Gould 1985) |
| Mouse | 17D-204 | 863<br>871<br>979 | 17D-204 – no | (Gould et al. 1985) |
| Mouse | 17DD | B26<br>B39 | 17D – yes<br>17D-204 – yes | (Barrett et al. 1989) |
| Mouse | 17D-204 | 3B6<br>3F4<br>5B6<br>8H3 | 17D – no<br>West Africa II – no | (Adungo et al. 2016) |
| | WT E protein | 4A1<br>4C9<br>4H10<br>5H2 | 17D – no<br>West Africa II – no | |
| Human | WT YF infection | 5A | 17D – yes<br>West Africa I – yes<br>West Africa II – yes<br>East/Central Africa - yes<br>Angola – yes | (Daffis et al. 2005; Lu et al. 2019) |
| | | 7A<br>R3 | 17D – yes<br>West Africa II – yes | |

The earliest report of type-specific neutralizing anti-YFV mAbs was published by Schlesinger *et al.* using BALB/c mice immunized with the 17D vaccine produced by Connaught Laboratories (Schlesinger, Brandriss, and Monath 1983). The study generated one 17D-specific mAb and eight type-specific mAbs, providing the first evidence that type-specific antibodies constitute most of the neutralizing antibodies raised against the 17D vaccine. $PRNT_{90}$ titers showed that three type-specific anti-YFV mAbs, 4E8, 2C9, and 2E10, neutralize both the 17D strain and the wt Asibi strain. The remaining five mAbs, 2B8, 5E3, 2D12, 3A3, and 4E1, are type-specific by exhibiting HI activity against both the 17D and wt Asibi strains, but only eliciting neutralizing activity against the wt Asibi strain. Buckley and Gould *et al.* isolated four type-specific neutralizing mouse anti-YFV mAbs raised against the 17D-204 strain, identifying mAb-825 neutralization activity against both 17D and the West Africa II genotype (Gould et al. 1985; Buckley and Gould 1985). MAb-825 also had binding activity to South America I genotypes of wt YFV via indirect immunofluorescence. Similarly, Barrett *et al.* and Sil *et al.* developed four type-specific neutralizing mouse anti-YFV mAbs, B26, B39, S32, and S44, against both the 17D-204 strain and the 17DD strain (Barrett et al. 1989; Sil et al. 1992). However, only mAbs S32 and S44 were proven to neutralize both 17D and different strains of wt YFV, including Darka1279 and FVV strains in the West Africa II genotype and the 1899/81 strain in the South America II genotype (Sil et al. 1992). Mouse mAb-B39 exhibits YFV type-specific binding activity with 17D-204 and 17DD vaccine strains as well as wt Asibi and 1899/81 strains by indirect immunofluorescence, but only neutralizes 17D-204 (WHO strain specific) even though it was prepared against the 17DD-Brazil strain (Barrett et al. 1989). Collectively, there are only 25 type-specific neutralizing mouse anti-YFV mAbs available, as summarized in **Table 3.1**. Four of these mAbs (bolded in **Table 3.1**) are known to neutralize

both 17D and wt YFV, making them suited for the investigation of antibody-mediated neutralization of wt YFV in 17D vaccinees. Available mouse anti-YFV mAbs have only proven to neutralize the West African II and South American I genotypes of wt YFV, rendering our understanding of antibody-mediated neutralization against all seven genotypes of wt YFV incomplete.

The availability of type-specific neutralizing human anti-YFV mAbs is even more limited as technologies that support the isolation of human mAbs did not become widely available until the last two decades. Daffis *et al.* first reported the cloning and expression of three type-specific human anti-YFV mAbs isolated from two YF patients (Daffis et al. 2005). The three mAbs, 5A, 7A, and R3, neutralize 17D and wt YFV strains of West Africa I, II, East/Central Africa, and Angola genotypes (Daffis et al. 2005; Lu et al. 2019). Although mAb-5A and several human mAbs isolated from two 17D vaccinees were recently proven to target the overlapped antigenic structure (Lu et al. 2019; Wec et al. 2020), it has been well documented that wt YFV and 17D strains differ significantly in their antigenicity (Clarke 1960; Gould et al. 1989). To date, very few anti-YFV mAbs isolated from 17D vaccinees have been shown to neutralize different genotypes of wt YFV. Therefore, there is a fundamental need to examine the neutralizing activity of anti-YFV mAbs isolated from 17D vaccinees against different genotypes of wt YFV to provide the bases for understanding antibody-mediated neutralization of wt YFV in vaccinees. Furthermore, there are no side-by-side comparisons of neutralizing activity of human mAbs against multiple genotypes of wt YFV, especially against South American genotypes. Ultimately, this dissertation work aims to help fill in these knowledge gaps.

In this project, the ability of two anti-YFV mAbs to neutralize four strains of wt YFV was examined. The four wt YFV strains were selected to represent isolates from different

geographical regions. For example, the BA-55 strain belongs to the West Africa I genotype that causes urban outbreaks in Nigeria, Côte d'Ivoire, and Senegal. The West Africa II genotype represented by the Asibi strain is endemic to several countries including Ghana, Senegal, Burkina Faso, and Guinea. The JSS strain is representative of the South America I genotype, which can be found in Brazil (i.e., eastern part of the South American continent). The 1899/81 strain is a Peruvian isolate that belongs to the South America II genotype. All four strains of wt YFV were isolated from YF patients, representing wt YFV strains directly involved in the urban transmission cycle. Therefore, the strains selected are applicable to further our understanding of neutralizing mAbs against wt YFV strains with direct implications of human disease.

## 3.2 Results

To evaluate the neutralizing potencies of human mAb-29 and mAb-32, $PRNT_{50}$ was performed using four-fold serial dilutions of purified recombinant antibody preparations between $1.0x10^{5}$ and $3.8x10^{-1}$ ng/ml. The concentrations of respective mAbs that led to the 50% reduction in the plaque numbers produced by each of the four genotypes of wt YFV (i.e., $PRNT_{50}$ titers) was determined in Vero76 cells. Data points corresponding to the $PRNT_{50}$ titers are at the midpoint or more linear portion of the S-shaped neutralization curve and can be used to compare the neutralization potency of each mAb against different genotypes of wt YFV. To confirm the neutralization of the mAbs was not a result of non-specific binding, the neutralization of the isotype control antibody VRC01 was assessed in 17D and Asibi strains; no neutralizing activity was observed (see **Appendix A** – Neutralization curve of human anti-HIV mAb-VRC01 against YFV 17D and Asibi strains).

The $PRNT_{50}$ titers (ng/ml) of mAb-29 and mAb-32 against the 17D vaccine strain and four strains representing different genotypes of wt YFV is summarized in **Table 3.2**.

**Table 3.2 Neutralizing potency of human anti-YFV mAbs against the 17D vaccine and four strains of wild-type YFV.**
The $PRNT_{50}$ titers of mAb-29 and mAb-32 was determined against the 17D vaccine strain and strains representing four different genotypes of wt YFV in Vero76 cells.

| | **$PRNT_{50}$ (ng/ml)** | | | | |
|---|---|---|---|---|---|
| **mAbs** | **17D-204** (vaccine) | **Asibi** (West Africa II) | **BA-55** (West Africa I) | **1899/81** (South America II) | **JSS** (South America I) |
| mAb-29 | 32 | 285 | 22 | 32 | 176 |
| mAb-32 | 152 | 8,944 | 17 | 29 | 8,713 |

***Human anti-YFV mAb-29.*** The neutralization curve of mAb-29 is shown in **Figure 3.1**. Between the two anti-YFV mAbs, mAb-29 showed the highest neutralization potency against the 17D, Asibi, and JSS strains, as demonstrated by the lowest concentrations required to reach $PRNT_{50}$ titers (**Table 3.2**). No statistical difference was observed in the neutralization potency of mAb-29 against the four different genotypes of wt YFV (one-way ANOVA followed by Tukey's multiple comparisons test, $p$=0.8262), suggesting that mAb-29 may target several conserved residues in the E protein.

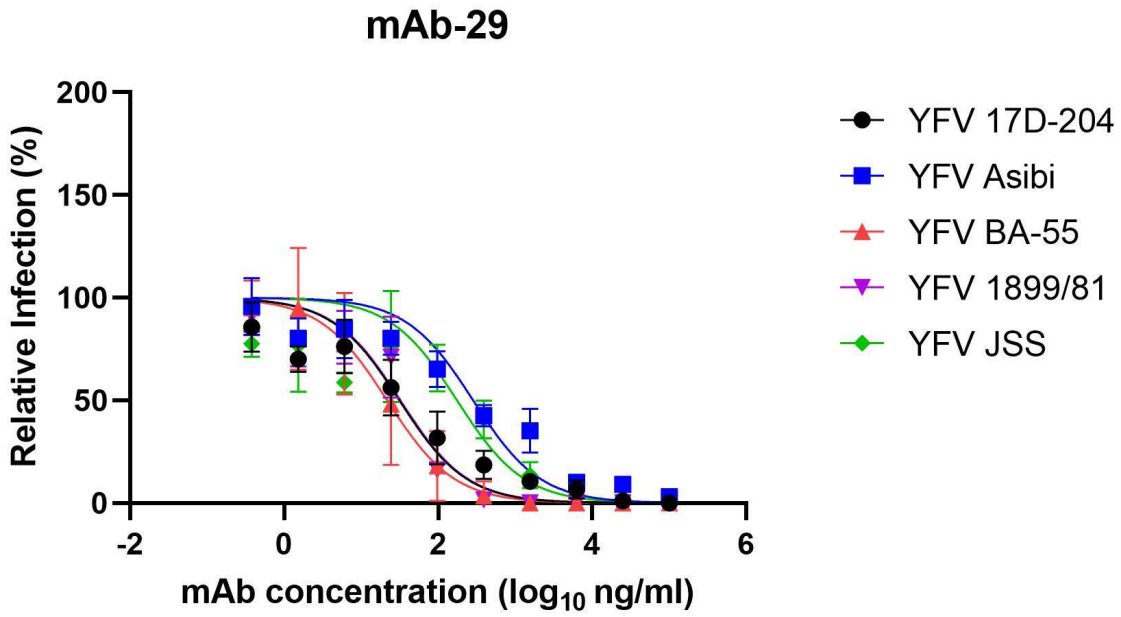


**Figure 3.1 Neutralization curve of human anti-YFV mAb-29 against 17D and four genotypes of wild-type YFV.**
The neutralizing activity of mAb-29 was evaluated by PRNT using four-fold serial dilutions against 17D and four strains representing different genotypes of wt YFV in Vero76 cells. There was no statistical difference in the neutralizing titers (one-way ANOVA followed by Tukey's multiple comparisons test, $p$=0.8262).

***Human anti-YFV mAb-32.*** The neutralization curve of mAb-32 is shown in **Figure 3.2**. A statistical difference in $PRNT_{50}$ titer of mAb-32 between the different strains of YFV was observed ($p$=0.0023) using one-way ANOVA. There was a 59-fold difference in $PRNT_{50}$ titers of mAb-32 against the 17D strain (152 ng/ml) and the Asibi strain (8,944 ng/ml) (**Table 3.2**). Interestingly, mAb-32 showed significant differences in the ability to neutralize different strains of wt YFV within the West African and South American clades. It is important to note that mAb-32 had a significantly lower $PRNT_{50}$ titer against the BA-55 strain compared to the Asibi strain (526-fold difference, one-way ANOVA followed by Tukey's multiple comparisons test, $p$=0.0149) because the sequence of the E protein only differs by 0.6% between the two strains. The neutralization potency of mAb-32 against the JSS and 1899/81 strains also differed by 300-fold, although there was a lack of statistical significance. Therefore, the intraclade differences in

the West African and South American isolates of wt YFV may represent the residues recognized by mAb-32. Furthermore, mAb-32 showed significant differences in the ability to neutralize different strains of wt YFV between the West African and South American clades. There was a 308-fold difference in $PRNT_{50}$ titer of mAb-32 against West African genotype II Asibi strain (8,944 ng/ml) and South American genotype II 1899/81 strain (29 ng/ml) (one-way ANOVA followed by Tukey's multiple comparisons test, $p$=0.0294). Lastly, mAb-32 had a significantly lower $PRNT_{50}$ titer against the West African genotype I BA-55 strain compared to the South American genotype I JSS strain (513-fold difference, one-way ANOVA followed by Tukey's multiple comparisons test, $p$=0.0267).

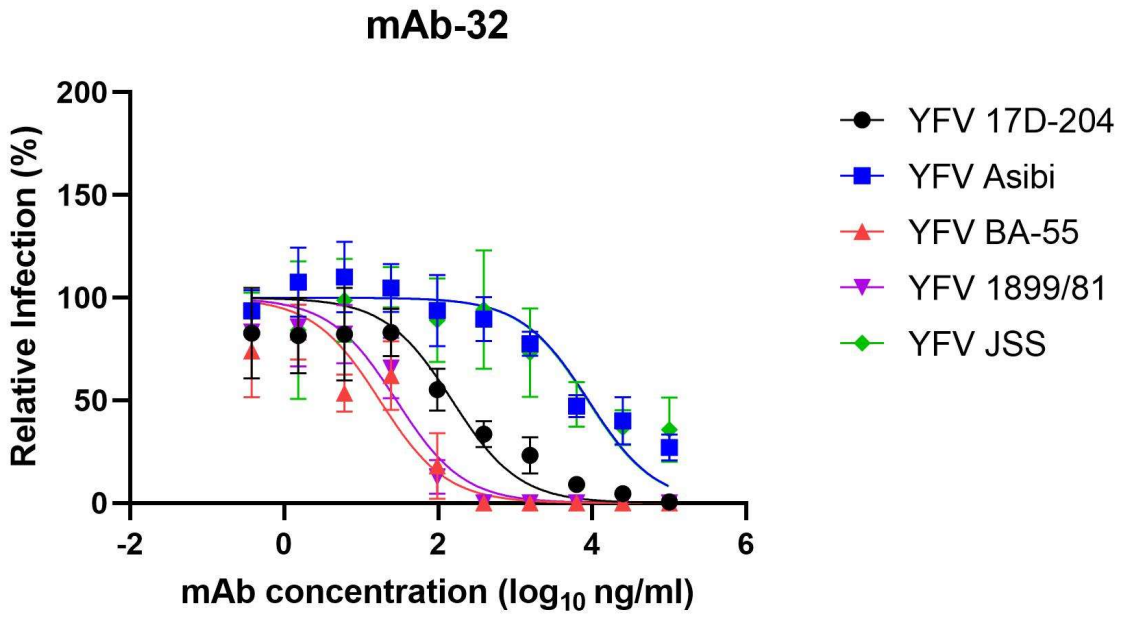


**Figure 3.2 Neutralization curve of human anti-YFV mAb-32 against 17D and four genotypes of wild-type YFV.**
The neutralizing activity of mAb-32 was evaluated by PRNT using four-fold serial dilutions against 17D and four strains representing different genotypes of wt YFV in Vero76 cells. A statistical difference in neutralizing titer of mAb-32 between the different strains of YFV was observed ($p$=0.0023) using one-way ANOVA.

## 3.3 Discussion

In summary, the $PRNT_{50}$ demonstrated both anti-YFV mAbs are type-specific neutralizing antibodies, however there are differences in the neutralization potency of each mAb against the 17D strain and wt YFV strains. Both mAbs showed a higher neutralization potency against the 17D strain compared to the Asibi strain. Since the 17D strain was the immunogen and there is a 2.4% amino acid divergence in the E protein between the two strains, this is sufficient to modulate the neutralizing activity of each mAb (**Table 3.3**). Differences in the amino acid residues and the domain in the E protein between the 17D strain and the four wt YFV strains is summarized in **Table 3.4**.

**Table 3.3 Amino acid divergence in the E protein sequences between 17D-204 and four genotypes of wt YFV.**

| | 17D-204 | West Africa I (BA-55) | West Africa II (Asibi) | South America I (JSS) | South America II (1899/81) |
|---|---|---|---|---|---|
| 17D-204 | | 15 aa | 12 aa | 27 aa | 27 aa |
| West Africa I (BA-55) | 3.0% | | 3 aa | 18 aa | 17 aa |
| West Africa II (Asibi) | 2.4% | 0.6% | | 17 aa | 17 aa |
| South America I (JSS) | 5.5% | 3.7% | 3.4% | | 17 aa |
| South America II (1899/81) | 5.5% | 3.4% | 3.4% | 3.4% | |

**Table 3.4 Differences in the amino acid residues of the E protein between the 17D-204 strain and four genotypes of wt YFV.**

The numbers listed in the top row correspond to the amino acid residues in the E protein. The E protein domains are boxed highlighted, red is EDI, yellow is EDII, and blue is EDIII. Amino acid residues not highlighted are located at the 3′ end of the E protein. Sequences were aligned using BioEdit.

| YFV Strain | Amino Acid Residues in the E Protein | | | | | | | | | | | | | | | | | | |
|---|---|---|---|---|---|---|---|---|---|---|---|---|---|---|---|---|---|---|---|
| | 52 | 56 | 62 | 67 | 83 | 90 | 148 | 154 | 170 | 173 | 191 | 200 | 207 | 243 | 268 | 270 | 271 | 272 | 282 |
| 17D-204 | R | V | N | H | A | N | K | T | V | I | G | T | R | R | T | D | N | N | S |
| BA-55 | G | A | N | H | A | N | K | T | A | T | G | K | R | R | T | D | N | N | S |
| Asibi | G | A | N | H | A | N | K | T | A | T | G | K | R | R | T | D | N | N | S |
| JSS | G | A | S | N | E | N | K | T | A | T | S | K | K | K | P | N | S | K | A |
| 1899/81 | G | A | S | H | A | H | N | A | A | T | S | K | R | K | T | G | S | N | S |
| | 299 | 305 | 318 | 325 | 331 | 335 | 343 | 344 | 360 | 380 | 407 | 416 | 421 | 426 | 430 | 436 | 450 | 459 | 468 |
| 17D-204 | I | F | V | S | R | I | A | I | D | R | V | T | S | F | V | T | N | A | T |
| BA-55 | M | S | V | P | K | I | A | I | D | T | A | A | S | L | I | T | S | A | T |
| Asibi | M | S | V | P | K | I | A | I | D | T | A | A | S | F | V | T | N | A | T |
| JSS | M | S | A | P | R | I | A | V | D | T | A | A | G | F | V | T | S | V | T |
| 1899/81 | M | S | A | P | R | M | S | V | E | T | A | A | S | F | V | M | S | A | M |

Variations in the neutralization potency of human anti-YFV mAbs against different genotypes of YFV allude to the amino acid divergence of the E protein, the major target of neutralizing antibodies. As summarized in **Table 3.3**, up to a 5.5% amino acid (27 amino acids) divergence in the E protein exists between the 17D vaccine strain and the two South American genotypes of wt YFV. The difference is consistent with the variation in the $PRNT_{50}$ titers of mAb-32. The JSS strain and the 1899/81 strain differ at E-67, E-83, E-90, E-154, E-207, E-268, E-270, E-272, E-282, E-335, E343, and E-360 residues in the ectodomain (**Table 3.4**). The amino acids may contain the putative residues that constitute the neutralizing epitope recognized by mAb-32. Further comparison of the E protein sequence between the Asibi strain and 1899/81 strain also showed a significantly different sensitivity to neutralization by mAb-32, as E-90, E-154, E-270, E-335, E-343, and E-360 residues that distinguish the JSS strain and the 1899/81 strain are among the 17 amino acids that distinguish the Asibi strain and the 1899/81 strain.

These mutations are distributed throughout the three distinct domains of the E protein (**Table 3.4**), indicating that mAb-32 may target a conformational epitope. This may explain why the Asibi strain and the BA-55 strain are significantly different in their sensitivity to neutralization by mAb-32 but are distinguished by three amino acids (E-426, E-430, and E-450) in the transmembrane domain of the E protein. Notably, the BA-55 and JSS strains, which had significantly different $PRNT_{50}$ titers tested with mAb-32, also share amino acid differences in the E-426 and E-430 residues. It is likely that mAb-32 may be binding to an antigenic structure which can be altered in presentation due to mutation(s) in both the ectodomain and the transmembrane domain of the E protein.

As the $PRNT_{50}$ titers of both anti-YFV mAbs against the 17D strain and the Asibi strain differed by at least four-fold, epitope characterization of the mAbs using a recombinant 17D strain (immunogen), Asibi strain, and Asibi/17D chimeras (Chapter 4) was conducted. Importantly, because mAb-29 and mAb-32 neutralized both the 17D and Asibi strains, it warranted the investigation of passive protection *in vivo* (Chapter 5).

# Chapter 4 - Characterization of YFV type-specific neutralizing epitopes on the envelope protein

## 4.1 Introduction

The YFV type-specific neutralizing epitopes using recombinant 17D and Asibi strains was characterized due to observing a greater than four-fold difference in $PRNT_{50}$ titer between the biological isolates of the 17D strain and the wt YFV Asibi-LSHTM strain with mAb-29 and mAb-32 (**Table 3.2**). Because the mAbs were isolated from 17D vaccinees and selected based on the reactivity of YFV virus-like particles, the YFV type-specific neutralizing epitope(s) are expected to be in the E protein, the major target of neutralizing antibodies. The E protein sequence of the 17D strain and the wt YFV Asibi-LSHTM strain differs by 13 amino acids. Ten of these residues can be investigated using the infectious clones developed by McElroy *et al.* (**Table 2.2**). Therefore, the recombinant 17D strain, Asibi strain, and four chimeras that contain individual E protein domains from respective viruses were produced using cDNA infectious clones and tested in $PRNT_{50}$ to characterize the YFV type-specific neutralizing epitope(s) recognized by human anti-YFV mAb-29 and mAb-32. The concentrations of each mAb corresponding to the $PRNT_{50}$ titer against recombinant YFV were compared to identify amino acids that constitute the neutralizing epitope(s) recognized by human antibodies raised against the 17D vaccine. Of significance, these experiments are the first characterization of YFV type-specific epitopes in the 17D vaccine strain and wt Asibi strain with human mAbs isolated from 17 vaccinees. Previously, the characterization of neutralizing epitopes in the YFV E protein was mainly undertaken using human polyclonal sera. To our best knowledge, only two recently published studies have examined the neutralizing epitopes targeted by human anti-YFV mAbs,

but there is a lack of detailed examination of amino acids that constitute the neutralizing epitopes in the E protein.

Available evidence suggests YFV type-specific neutralizing epitope(s) are mainly located in EDI and EDII. Human polyclonal sera preferentially recognize antigenic structures spanning the EDI-EDII (Vratskikh et al. 2013). The depletion of human antibodies using the recombinant EDI-EDII protein significantly reduced the neutralizing activity of polyclonal sera. This finding agreed with the recent report that YFV E-specific mAbs target epitopes within or proximal to the fusion loop on EDII whereas only a small fraction recognized epitopes in EDIII (Wec et al. 2020). However, this study stopped short of investigating the activity of each mAb to neutralize wt YFV. A significant gap in knowledge of how human antibodies raised against the 17D vaccine neutralizes wt YFV remains. Moreover, the critical antigenic structures in the 17D vaccine that elicit human neutralizing antibody responses are still poorly understood.

Antibody-mediated neutralization mainly targets neutralizing epitopes in the E protein and is important for protective immunity against wt YFV. Yellow fever virus type-specific neutralizing epitopes in the E protein are relevant to the protective immunity elicited by the 17D vaccine as serum neutralizing activity of 17D vaccinees are specific to YFV but no other flaviviruses. While a panel of YFV type-specific neutralizing mAbs are available (refer to **Table 3.1**), only three mouse and three human mAbs have been mapped to the E protein. The three mouse anti-YFV mAbs were used to prove that conformational epitope(s) in the E protein are involved in antibody-mediated neutralization of YFV. Neutralization escape mutants selected against anti-YFV mAb-2C9 contained amino acid substitutions at three discrete locations of the E protein, including E-N71, E-D72, and E-M125 residues (Lobigs et al. 1987). $PRNT_{50}$ with mouse mAbs B39 and 2E10 identified a neutralizing epitope that contains amino acids across

EDI and EDII (Ryman, Ledger, et al. 1997). Mab B39 recognizes E-D155 and E-T158 residues in the EDI and the E-N71 and E-D72 residues in EDII, which are also targeted by the mouse anti-YFV mAb 2E10. Epitope mapping using the three mouse anti-YFV mAbs shows that neutralizing epitopes in YFV E protein consists of amino acid residues across different domains, suggesting conformational epitopes in the 17D strain elicit neutralizing antibody responses in mice (**Figure 4.1)**. At least two neutralizing epitopes are targeted by mAbs B39, 2E10, and 2C9 and constitute amino acids conserved across the 17D-204 strain and wt YFV strains (**Table 3.4**). However, it is unclear whether mouse neutralizing anti-YFV mAbs raised against the 17D vaccine strain directly represent the neutralizing antibody responses in humans.

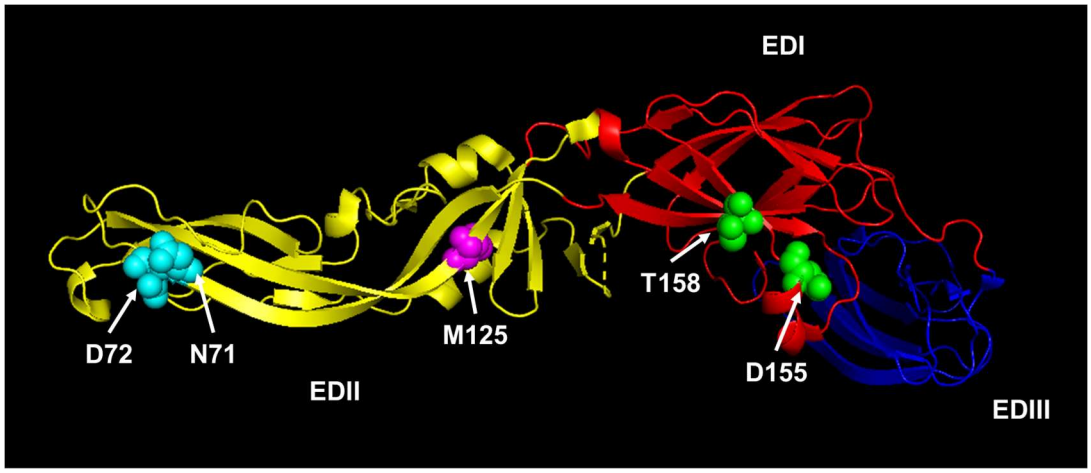


**Figure 4.1 Amino acid residues targeted by mouse YFV type-specific neutralizing mAbs.** Epitope mapping using three mouse anti-YFV mAbs shows that neutralizing epitopes in the YFV E protein consists of amino acid residues that span different domains. This suggests conformational epitopes in the YFV 17D vaccine strain are responsible for eliciting the neutralizing antibody responses in mice. Mouse anti-YFV mAb-2C9, mAb-B39, and mAb-2E10 share two common amino acid residues at N71 and D72 in the EDII, shown as cyan spheres. Additionally, mAb-2C9 has been mapped to M125 in the EDII, shown as magenta spheres; and mAb-B39 and mAb-2E10 both recognize D155 and T158 residues in the EDI, shown as green spheres. The three domains are labeled in red for EDI, yellow for EDII, and blue for EDIII. Image adapted from the Research Collaboratory for Structural Bioinformatics Protein Data Bank (RCSB PDB, rcsb.org) of PDB ID 6IW4, YFV-17D E protein monomer in pre-fusion conformation (Lu et al. 2019). Data files contained in the archive are free of all copyright restrictions.

The only available neutralizing epitope in the YFV E protein recognized by human antibodies was identified using three human mAbs isolated from patients, including mAbs 5A, 7A, and R3 (Daffis et al. 2005). The three mAbs were proven to target an overlapped antigenic structure in the E protein based on the sequence of neutralization escape mutants. MAb-R3 was mapped to E-426 and E-430 that are in the transmembrane domain of the E protein. MAb-7A was mapped to amino acid residues E-71, E-153, E-154, and E-155, which constitutes conformational epitopes across EDI and EDII. The results suggest the human mAbs bind to an epitope at the tip of the E dimer that are conformational and consist of residues across the EDI-EDII. The neutralizing epitope of mab-5A was mapped in the greatest detail using the crystal structure of YFV E protein. Mab-5A binds to the EDII region including E-65-74, E-81, E-84, E-87, E-101-104, and E-240-244 residues (Lu et al. 2019). The crystal structure revealed the antibody-antigen interaction of mAb-5A bound to the secreted E protein of YFV 17D in the pre- and post-fusion states, representing neutral and acidic conditions, respectively. As shown in **Figure 4.2**, during the pre-fusion state, mAb-5A recognizes a quaternary epitope containing the b strand (aa 65-72), the ij loop (aa 240-244), the bc loop (aa 73, 74, 81, 84, and 87), and the fusion loop (aa 99 and 101-104). Importantly, mAb-5A interacts with the 150 loop (aa 149) of EDI and k1 loop (aa 267) of EDII. In the post-fusion state, mAb-5A only binds to the exposed surface of EDII and the fusion loop (as in the pre-fusion state) but does not interact with the 150 loop of EDI or k1 loop of EDII (**Figure 4.2**). These data suggest that neutralizing antibodies raised against wt YFV may interfere with both viral attachment and fusion due to binding to dimeric forms of the E protein and the quaternary epitopes, respectively (Lu et al. 2019).

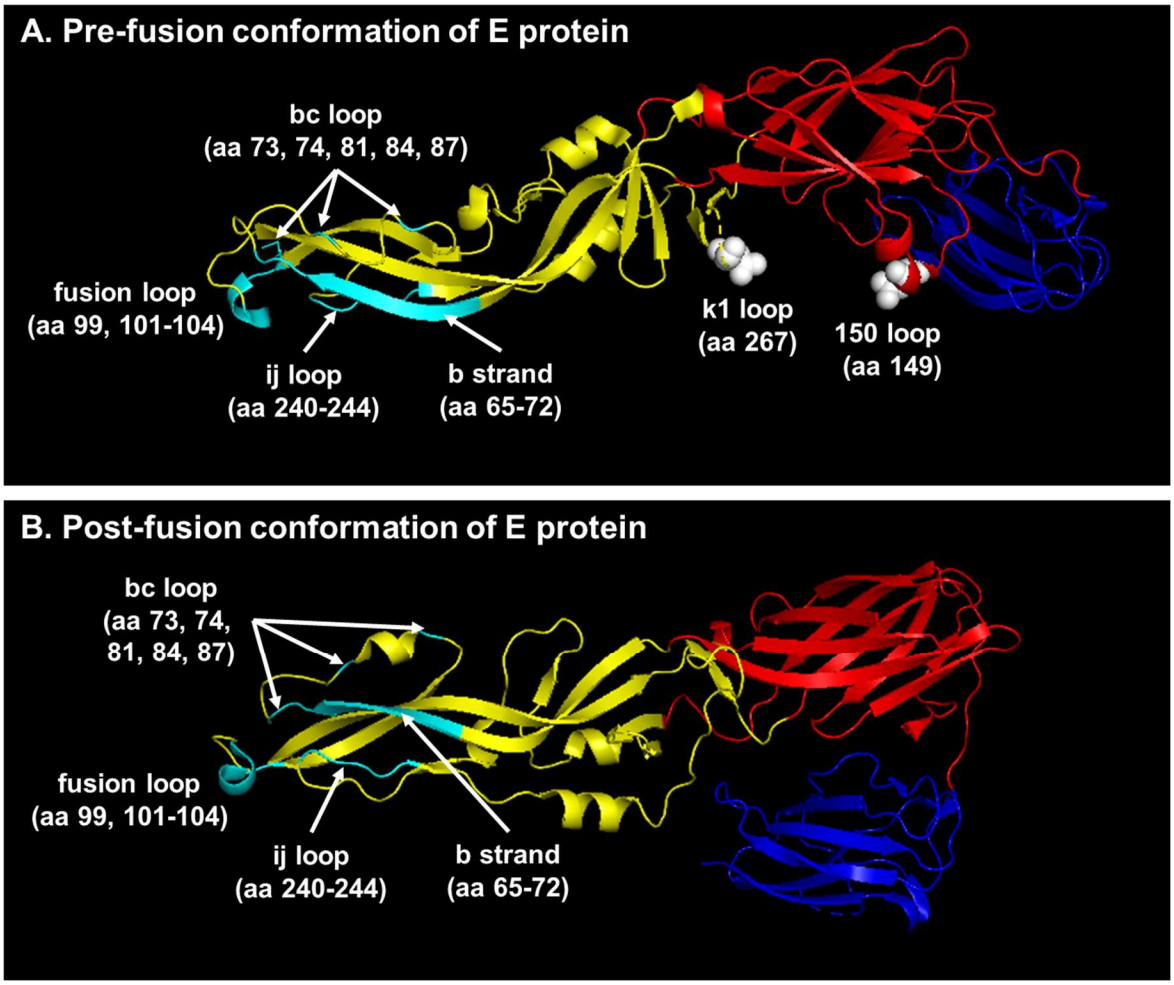


**Figure 4.2 Binding sites of mAb-5A in the pre- and post-fusion structure of YFV E protein.** MAb-5A targets amino acids in both EDI and EDII, suggesting the presence of a conformational neutralizing epitope for human antibodies in YFV E protein. EDII contains residues that leads to the binding of mAb-5A before (**A**) and after (**B**) membrane fusion, including the b strand (aa 65-72), the ij loop (aa 240-244), the bc loop (aa 73, 74, 81, 84, and 87), and the fusion loop (aa 99 and 101-104), shown in cyan color. Two residues are only accessible to mAb-5A in the pre-fusion conformation (**A**), including the 150 loop (aa 149) of EDI and k1 loop (aa 267) of EDII, shown as white spheres. The three domains are labeled in red for EDI, yellow for EDII, and blue for EDIII. Images adapted from the Research Collaboratory for Structural Bioinformatics Protein Data Bank (RCSB PDB, rcsb.org) of PDB ID 6IW4, YFV-17D E protein monomer in pre-fusion conformation (**A**) and PDB ID 6IW1, YFV-17D E protein monomer in post-fusion conformation (**B**) (Lu et al. 2019). Data files contained in the archive are free of all copyright restrictions.

Characterization of neutralizing epitopes recognized by human mAbs raised against the 17D vaccine was undertaken to aid in the understanding of antibody-mediated neutralization involved in protective immunity against wt YFV. Additionally, this information will help make

comparisons between neutralizing antibody responses elicited by vaccination or natural infection. Using the recombinant Asibi strain as the backbone, individual amino acid residues were mutated to swap ectodomains in the Asibi E protein with those of the 17D strain. These generated chimeras including Asibi-17D(EDI), Asibi-17D(EDII), Asibi-17D(EDI-EDII), and Asibi-17D(EDIII). It was important to include a chimera containing mutations across the EDI and EDII based on published literature showing known neutralizing confirmational epitopes that consist of residues across this region that binds within the 150-loop (Lu et al. 2019). The $PRNT_{50}$ titers of the two human anti-YFV mAbs against the recombinant 17D strain, Asibi strain, and the four chimeras were determined to identify residues that constitute the neutralizing epitope(s). Variations in the neutralizing potency of the chimeras can help delineate antigenic site(s) of the human anti-YFV mAbs.

## 4.2 Validating the antigenic structure of recombinant YFV 17D and Asibi strains are analogous to the biological isolates

As the infectious clones of the 17D-204 strain and the Asibi strain have not been extensively used for the characterization of neutralization epitopes, a pilot study was undertaken to demonstrate that the recombinant 17D and Asibi strains resemble the antigenic structures to the biological isolates and exhibit sensitivity to the neutralization by well characterized mAbs. This was confirmed using two mouse mAbs known to neutralize the Asibi strain at a higher potency (i.e., lower $PRNT_{50}$ titer) than the 17D strain. Mouse mAb-117 was shown by cross-immunofluorescence tests to be specific to wt YFV (Gould et al. 1989). The second anti-YFV mAb-2D12 (clone 2D12.A) is a mouse IgG2a antibody that interacts with the E protein of both the wt Asibi and vaccine strains, but preferentially neutralizes the Asibi strain. The neutralizing

titers of mAb-117 and mAb-2D12 against recombinant Asibi (rAsibi) and 17D (r17D) is summarized in **Table 4.1** and the neutralization curve is shown in **Figure 4.3**.

**Table 4.1 Neutralizing titers of mAb-117 and mAb-2D12 against recombinant strains of 17D and Asibi strains.**
The $PRNT_{50}$ titers of mAb-117 and mAb-2D12 was determined against recombinant 17D (r17D) and Asibi (rAsibi) strains in Vero76 cells to confirm antigenic structures.

| | $PRNT_{50}$ (ng/ml) | |
|---|---|---|
| | **mAb-117** | **mAb-2D12** |
| r17D | 1,535,478 | 172,610 |
| rAsibi | 18,630 | 1,179 |

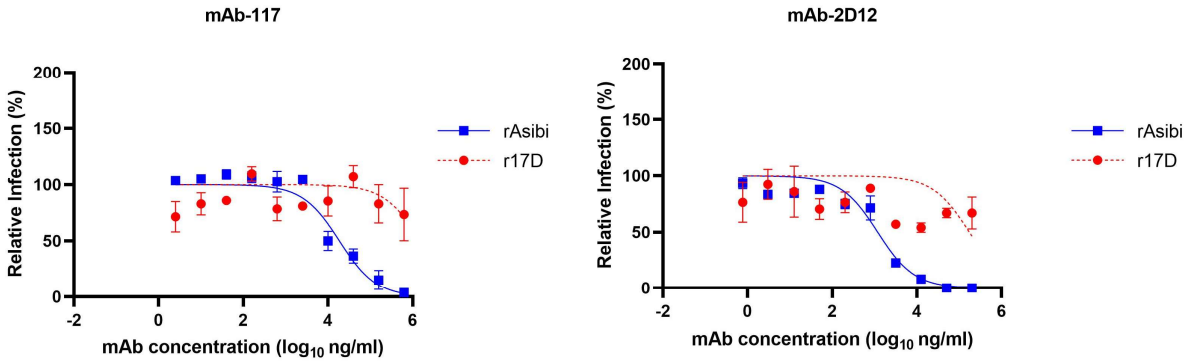


**Figure 4.3 Neutralization curve of mAb-117 and mAb-2D12 with recombinant strains of YFV 17D and Asibi strains.**
Mouse mAb-117 and mAb-2D12 confirmed the antigenic structures of the recombinant strains of Asibi (rAsibi) and 17D (r17D) strains were analogous to the biological isolates of these two YFV strains.

MAb-117 and mAb-2D12 preferentially bind and neutralize the wt Asibi strain. This aligns with what is observed with biological isolates of 17D and Asibi strains of YFV. These data confirmed the recombinant 17D and Asibi strains had similar antigenic structures to the biological isolates of respective YFV strains and can be used for the epitope characterization of mAb-29 and mAb-32.

## 4.3 Determination of locations of YFV type-specific neutralizing epitopes on the envelope protein recognized by two human anti-YFV mAbs

To evaluate the neutralizing potencies of human anti-YFV mAb-29 and mAb-32, $PRNT_{50}$ was performed using four-fold serial dilutions of purified recombinant antibody preparations between $1.0x10^5$ and $3.8x10^{-1}$ ng/ml. The concentrations of respective mAbs that led to the 50% reduction in the plaque numbers produced by the recombinant 17D strain, Asibi strain, and four chimeras (i.e., $PRNT_{50}$ titers) in Vero76 cells was determined. The $PRNT_{50}$ titers (ng/ml) of mAb-29 and mAb-32 against the recombinant 17D strain, Asibi strain, and four chimeras is summarized in **Table 4.2**.

**Table 4.2 Neutralizing potency of human anti-YFV mAbs against recombinant 17D and Asibi strains of YFV.**
The $PRNT_{50}$ titers of mAb-29 and mAb-32 was determined against the recombinant 17D strain, Asibi strain, and Asibi-17D chimeras in Vero76 cells.

| | **$PRNT_{50}$ (ng/ml)** | |
|---|---|---|
| | **mAb-29** | **mAb-32** |
| r17D-204 | 37 | 373 |
| rAsibi | 36 | 48 |
| rAsibi-17D(EDI) | 36 | 36 |
| rAsibi-17D(EDII) | 18 | 41 |
| rAsibi-17D(EDI-II) | 101 | 140 |
| rAsibi-17D(EDIII) | 30 | 34 |

***Human anti-YFV mAb-29.*** The neutralization curve of mAb-29 is shown in **Figure 4.4**. There was a lack of discernable difference in $PRNT_{50}$ titers of mAb-29 against recombinant strains of 17D and Asibi. The results indicate that the recombinant 17D and Asibi strains have a highly similar presentation of neutralizing epitope(s) recognized by mAb-29, leading to the lack of demonstrable difference in the $PRNT_{50}$ titer between the two strains. This was also consistent

with the comparable $PRNT_{50}$ titers between each chimera, except rAsibi-17D(EDI-II) that was approximately 3-fold higher in $PRNT_{50}$ titer compared to r17D and rAsibi, although no statistical difference was observed (one-way ANOVA followed by Tukey's multiple comparisons test).

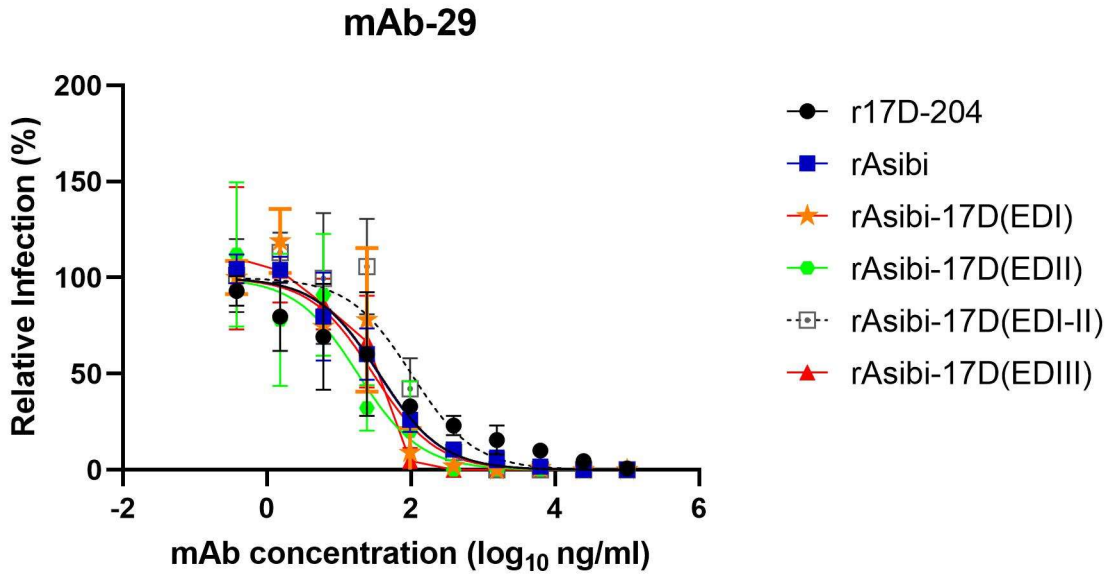


**Figure 4.4 Neutralization curve of mAb-29 and recombinant YFV 17D strain, Asibi strain, and Asibi-17D chimeras.**
The PRNT of four-fold serial dilutions of mAb-29 were determined against recombinant 17D strain, Asibi strain, and Asibi-17D chimeras in Vero76 cells. No statistical difference was observed in $PRNT_{50}$ titers among the recombinant strains and chimeras (one-way ANOVA followed by Tukey's multiple comparisons test).

***Human anti-YFV mAb-32.*** The neutralization curve of mAb-32 is shown in **Figure 4.5**. It is somewhat surprising that mAb-32 has a high neutralization potency against rAsibi, as demonstrable by the 8-fold reduction of $PRNT_{50}$ concentration compared to r17D. This is the opposite that is observed with biological isolates of 17D and Asibi strains and will be discussed further in the Discussion Section 4.4. There was a 3-fold difference in $PRNT_{50}$ titer between rAsibi and rAsibi-17D(EDI-II). A simultaneous substitution of the Asibi EDI-EDII region with the same region of 17D decreased sensitivity to the neutralization by mAb-32. Therefore, it is apparent that mAb-32 targets a conformational epitope across EDI and EDII. However, no

statistical difference in $PRNT_{50}$ titer among the recombinant strains and YFV chimeras was observed (one-way ANOVA followed by Tukey's multiple comparisons test).

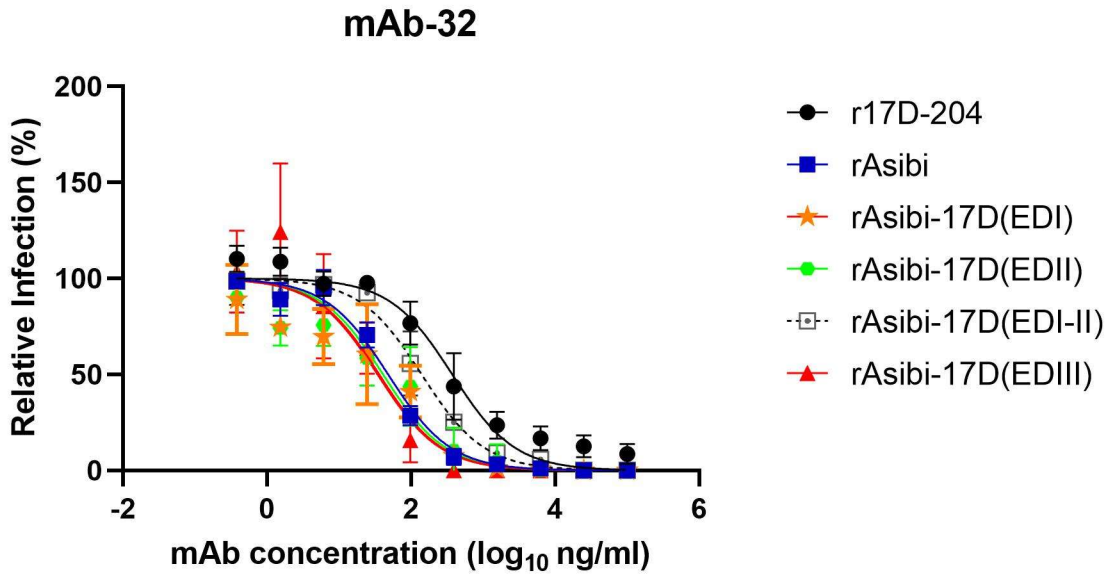


**Figure 4.5 Neutralization curve of mAb-32 and recombinant YFV 17D strain, Asibi strain, and Asibi-17D chimeras.**
The PRNT of four-fold serial dilutions of mAb-32 were determined against recombinant 17D strain, Asibi strain, and Asibi-17D chimeras in Vero76 cells. No statistical difference was observed in $PRNT_{50}$ titers among the recombinant strains and chimeras (one-way ANOVA followed by Tukey's multiple comparisons test).

## 4.4 Discussion

In conclusion, mutations introduced into a YFV Asibi infectious clone to generate chimeras with the EDI, EDII, EDI-EDII, or EDIII of 17D strain have determined the antigenic structures recognized by the human anti-YFV mAbs characterized in this study. Both mAb-29 and mAb-32 likely target antigenic structures across multiple domains of the YFV E protein and aligns with what is observed with biological isolates. The lack of a discernable difference in $PRNT_{50}$ titers of mAb-29 between the r17D and rAsibi strain was anticipated and agrees with the smallest difference in neutralization potency against the representative strains of four wt YFV genotypes among the human mAbs (**Table 3.2**). This suggests the epitopes on the r17D and

rAsibi strains are equally accessible, however, changing the EDI-EDII residues alters the presentation of the epitopes presented to the antibody and thus the binding pattern, leading to the three-fold difference in $PRNT_{50}$ titer. Therefore, mAb-29 still targets the E protein and likely targets a conformational structure in the EDI-EDII region. The chimera neutralization results in conjunction with data acquired from the neutralization potency against the four wt YFV genotypes may imply that mAb-29 targets a conserved epitope that is presented similarly across different genotypes of wt YFV. This epitope may be responsible for the binding of human antibodies proven to neutralize multiple genotypes of wt YFV.

The $PRNT_{50}$ titers of mAb-32 suggest this antibody may react with an interdomain epitope that consists of residues across EDI and EDII. This epitope has the apparent overlap with the neutralizing epitope recognized by human anti-YFV mAb-5A (Lu et al. 2019). As mentioned, mAb-32 neutralized the recombinant Asibi strain better than the recombinant 17D strain. The outcome contrasted with the observation made with $PRNT_{50}$ against the biological isolates of the wt Asibi-LSTMH strain and the 17D strain but can be further explained by the E protein sequence divergence between the Asibi strain derived from two different sources. The Asibi strain-LSHTM contains an E-D155R mutation compared to the Asibi strain-Yale used to construct the infectious clone (Davis et al. 2021). The E-D155R mutation is in the 150 loop of the YFV E protein, which is part of the neutralizing epitope for human mAbs. Therefore, it is highly likely that the E-D155R mutation between the Asibi strains derived from two different sources can modulate the binding of mAb-32. It is also important to note that Schlesinger *et al.* has reported anti-YFV mAbs raised against the 17D vaccine can neutralize the Asibi strain-Yale at a higher potency compared to the 17D strain (Schlesinger, Brandriss, and Monath 1983). The group suggested the preferential neutralization of the heterologous Asibi strain may indicate the

mAbs are reacting with similar or identical epitopes shared between the two strains, but the 17D strain is more restricted, resulting in decreased neutralization.

In conclusion, the epitope characterization showed the two human anti-YFV mAbs neutralize the recombinant 17D strain, Asibi strain, and four chimeras differently. Therefore, it is possible that each mAb recognizes a different neutralizing epitope, suggesting that there are multiple neutralizing epitopes in the E protein of YFV 17D strain. One of the two epitopes are presented differently between the 17D and wt YFV strains, leading to differences in $PRNT_{50}$ titers of mAb-32 against recombinant 17D and Asibi strains.

# Chapter 5 - Passive protection of human anti-YFV mAbs against neurotropic and viscerotropic diseases in mice

## 5.1 Introduction

The results of the neutralization tests and epitope characterization have proven that both mAbs belong to the type-specific neutralizing antibody group that are central to the protection of 17D vaccinees against wt YFV. The ability of each mAb to neutralize both 17D and wt YFV strains warrants the investigation of passive protection *in vivo*. In this project, the prophylactic passive immunization with each human anti-YFV mAb was undertaken to demonstrate the protection of mice against neurotropic and viscerotropic YF disease in an immunocompetent (CD-1) and immunocompromised (AG6) mouse model, respectively. This approach was employed due to the availability of mouse strains and the intense logistical requirement of mouse studies in ABSL-3 conditions. Although YFV does not cause neurotropic disease in humans, the neurotropic disease mouse model involves the ic challenge of readily available outbred mouse lines which can initially help identify mAbs that confer passive protection against either vaccine or wt strains of YFV in relatively large numbers. Subsequently, mAbs that confer passive protection can then be evaluated in the viscerotropic disease immunocompromised mouse models, which are costly and difficult to obtain.

The inoculation of YFV by the ic route in immunocompetent mice has repeatedly been proven as a robust model to investigate the passive protection of mAbs because uniform lethality can be achieved regardless of virus strain, age of mouse, or strain of mouse. In a comparative study by Barrett and Gould, outbred mice were inoculated with thirty-five different wt and vaccine strains of YFV by the ic or intranasal route at a dose of $10^4$ PFU (Barrett and Gould 1986). All mice succumbed to YF infection by the ic route of inoculation. The average survival

times (AST) of mice challenged with the wt and vaccine strains including FNV and various 17D substrains ranged from six to eleven days. Yellow fever virus administered intracerebrally is also uniformly lethal in immunocompetent mice regardless of age (Fitzgeorge and Bradish 1980). Finally, the 17D-204 strain ($10^4$ PFU) produced uniformed lethality in both outbred (TO and NIH Swiss) and inbred (C3H, DBA/2, C57BL/6, and Balb/C) mouse strains when administered by the ic route (Ryman, Xie, et al. 1997). Cumulatively, these results demonstrate the utility of the ic challenge method in the immunocompetent mouse model to assess the protective efficacy of neutralizing mAbs.

Protection against neurological disease by neutralizing antibodies is a sensitive technique to identify mouse anti-YFV mAbs that confer protection *in vivo*. Brandriss *et al*. showed immunocompetent BALB/c or Swiss (CD-1) mice are protected against ic challenge with 17D when passively immunized with mAbs twenty-four hours prior to challenge (Brandriss et al. 1986). Type-specific neutralizing antibodies 2C9, 4E8, and 2E10 conferred complete protection at both the highest dose of 400 μg per mouse and at 40 μg per mouse, but protection waned as the antibody concentration was decreased to 4 μg or 0.4 μg per mouse. Furthermore, mAb-2E10 conferred complete protection when 400 μg was administered by the ip route three days after ic challenge with YFV 17D. MAbs 2C9 and 4E8 afforded an 89% survival rate when given at 40 μg by the ip route four days after ic challenge with YFV 17D. These results suggest that neutralizing antibodies play a role in both preventing YF disease and in recovery from infection, as the antibodies neutralized under both prophylactic and therapeutic conditions (Brandriss et al. 1986).

Viscerotropic diseases that resemble human YF can be induced via the ip challenge of immunocompromised mice deficient in type-I and type-II IFN receptors challenged with wt YFV

strains. To date, two IFNAR$^{-/-}$-IFNGR$^{-/-}$ mouse lines infected with YFV have been shown to develop viscerotropic diseases. AG129 mice inoculated with $10^4$ PFU of YFV Asibi, Angola73, or 17D-204 by the subcutaneous route resulted in 100% mortality with an AST of 5.5, 5.8, and 10.1 d.p.i., respectively (Meier et al. 2009). Unlike the wt YFV strains that cause viscerotropic disease symptoms, inoculation of 17D-204 in AG129 mice display symptoms of neurological disease. Likewise, C57BL/6 mice lacking type-I and type-II IFN receptors (AGB6), the same mouse strain used in this study, infected subcutaneously with $10^4$ PFU of 17D-204 resulted in 100% mortality with an AST 10.75±0.5 d.p.i. (Lam et al. 2018). These mice experienced severe weight loss, liver and splenic stress, and signs of brain infection and neurological disease including hind limb paralysis, indicating that both viscerotropic and neurotropic diseases occurred. When infected with $10^4$ PFU of wt YFV Angola71 strain, AGB6 mice experienced severe weight loss and viscerotropic disease that required euthanasia, resulting in 100% mortality at 6 d.p.i. (Lam et al. 2018). These data show the IFNAR$^{-/-}$-IFNGR$^{-/-}$ mouse model is a valuable tool to evaluate the protective efficacy of neutralizing mAbs because they exhibit important characteristics of fatal human YF disease following wt YFV infection. These characteristics include uniform lethality from both vaccine and wt strains, and consistent production of viscerotropic disease symptoms induced by wt YFV.

There is limited data using the IFNAR$^{-/-}$-IFNGR$^{-/-}$ mouse model to evaluate the protective efficacy of neutralizing mAbs. Thibodeaux *et al*. passively immunized AG129 mice by the ip route with 127 μg of mouse mAb 2C9 or humanized 2C9-cIgG twenty-four hours prior to challenge with $2x10^5$ PFU of 17D-204 by the ip route (Thibodeaux, Garbino, Liss, Piper, Schlesinger, et al. 2012). The mice had increased AST compared to the control group and 95% of mice that received mAb-2C9 and 72% of mice that received mAb-2C9-cIgG survived

challenge against 17D-204 compared to a 4% survival rate in the control group. Even when the dose was decreased to 12.7 μg per mouse, prophylactic administration of mAb-2C9 and mAb-2C9-cIgG resulted in 80% and 100% survival, respectively. Corroborating these results, Calvert *et al*. challenged AG129 mice with 17D-204 by the ip route 24 hours after administration of 127 μg of mAb-864, 864-cIgG, or 2C9-cIgG by the ip route (Calvert et al. 2016). Although mAb-864 nor mAb-864-cIgG provided protection, mAb-2C9-cIgG had 80% survival rate. Altogether, these two studies demonstrated the utility of using the IFNAR$^{-/-}$-IFNGR$^{-/-}$ mouse model and the quantity of mAb to inoculate intraperitoneally to assess the protective efficacy of neutralizing anti-YFV mAbs.

To evaluate the protective efficacy of mAb-29 and mAb-32, a stepwise approach was taken to select the mAb(s) that provide protection prior to moving forward. First, outbred CD-1 mice were prophylactically immunized with one of the two mAbs or the isotype control and challenged by the ic route with the 17D vaccine strain. The same neurotropic disease model using CD-1 mice was used to assess the ability of each human anti-YFV mAb to protect against ic challenge using the wt Asibi strain. Finally, AG6 mice were passively immunized with either mAb-29, mAb-32, or the isotype control to evaluate the ability of each mAb to protect against viscerotropic disease induced by ip challenge with the wt YFV Asibi strain. Collectively, the passive immunization studies will identify neutralizing type-specific human anti-YFV mAbs raised against the 17D vaccine strain that can protect against viscerotropic disease caused by wt YFV infection.

## 5.2 Passive protection of outbred CD-1 mice with two human anti-YFV mAbs challenged with YFV 17D-204 strain by the intracerebral route

In the first mouse model, the prophylactic passive transfer of mAb-29 or mAb-32 were undertaken to determine the ability of each human anti-YFV mAb to protect against lethal neurological disease caused by the YFV 17D vaccine strain administered intracerebrally. Fifteen ($n$=5) male outbred CD-1 mice were passively immunized intraperitoneally with 100 μg of mAb-29, mAb-32, or the isotype control (timeline shown in **Figure 2.4**). Twenty-four hours later, mice were challenged intracerebrally with $5x10^4$ PFU of YFV 17D-204. This dosage was selected based on the 80% mortality rate achieved in the preliminary study (Section 2.4.A, **Figure 2.3** and **Table 2.3**). All mice had an initial decrease in body weight at 1 d.p.i. but remained bright, alert, and responsive (BAR). This was attributed to the stress of being anaesthetized and challenged. Euthanasia was carried out in accordance with the approved IACUC protocol.

***Isotype control VRC01 mAb.*** The individual body weight changes in mice passively immunized with the isotype control antibody are shown in **Figure 5.1**. One mouse lost 16% of weight from the baseline (day zero) one d.p.i., however, the mouse was BAR. Weight loss of mice that received the isotype control became apparent at 5 d.p.i. Two mice were euthanized due to hind limb paralysis at 6 d.p.i. The remaining mice in the isotype control group showed signs of neurological disease including involuntary twitching and/or hyperexcitement. At 7 d.p.i., the remaining mice were euthanized due to reaching a 20% weight loss from the baseline, and displaying signs of neurological disease (i.e., uncontrolled twitching and/or uncoordinated movements), severe depression, and hunched posture. Upon necropsy, the brains of mice in the isotype control group were unremarkable.

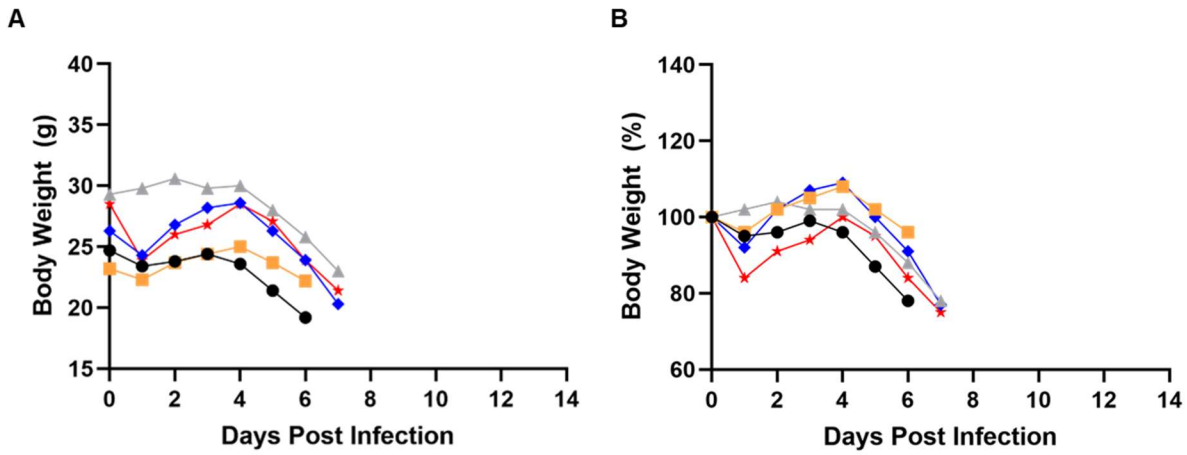


**Figure 5.1 Individual body weight changes of CD-1 mice passively immunized with the isotype control (VRC01) antibody followed by intracerebral challenge with YFV 17D strain.**
Five mice were passively immunized with 100 µg of the isotype control (VRC01) antibody. Twenty-four hours post-immunization, mice were challenged intracerebrally with $5x10^4$ PFU of YFV 17D. The body weight (g) was recorded daily for 14 days (**A**) and the percent body weight change from the baseline on day zero (**B**) was calculated.

***Human anti-YFV mAb-29.*** The individual body weight changes in mice passively immunized with mAb-29 are shown in **Figure 5.2**. Between 7 and 9 d.p.i., one mouse had observed weight loss, lethargy, and showed signs of bradykinesia (slower movements). However, the mouse began to recover, as observed with steady weight gain. The remaining mice that received mAb-29 had increased body weight and were apparently healthy for the duration of the study. At 14 d.p.i., mice passively immunized with mAb-29 had an average weight gain of 23%. None of the mice showed any signs of neurological disease. Upon necropsy, the brains of mice that received mAb-29 were unremarkable. A significant difference in body weight was observed starting at 6 d.p.i. ($p$=0.0075) compared to the isotype control group (mixed-effects analysis followed by Dunnett's comparisons test) (**Table 5.1**).

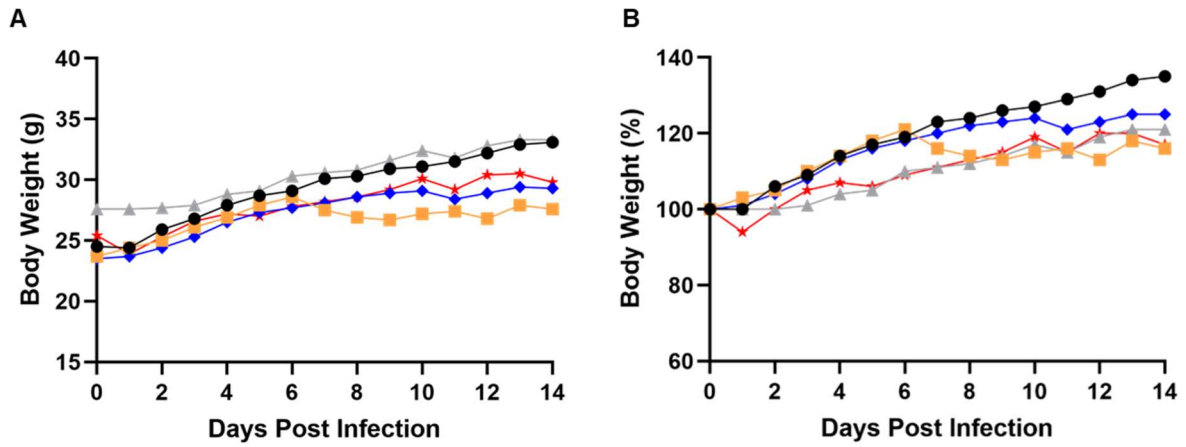


**Figure 5.2 Individual body weight changes of CD-1 mice passively immunized with mAb-29 followed by intracerebral challenge with YFV 17D strain.**
Five mice were passively immunized with 100 µg of mAb-29. Twenty-four hours post-immunization, mice were challenged intracerebrally with $5x10^4$ PFU of YFV 17D. The body weight (g) was recorded daily for 14 days (**A**) and the percent body weight change from the baseline (**B**) was calculated.

***Human anti-YFV mAb-32.*** The individual body weight changes in mice passively immunized with mAb-32 are shown in **Figure 5.3**. All mice had increased body weight and were apparently healthy for the entire study. At 14 d.p.i., mice passively immunized with mAb-32 had an average weight gain of 20%. None of the mice showed any signs of neurological disease. Upon necropsy, the brains of mice that received mAb-32 were unremarkable. A significant difference in body weight was observed starting at 6 d.p.i. ($p$=0.0079) compared to the isotype control group (mixed-effects analysis followed by Dunnett's comparisons test) (**Table 5.1**).

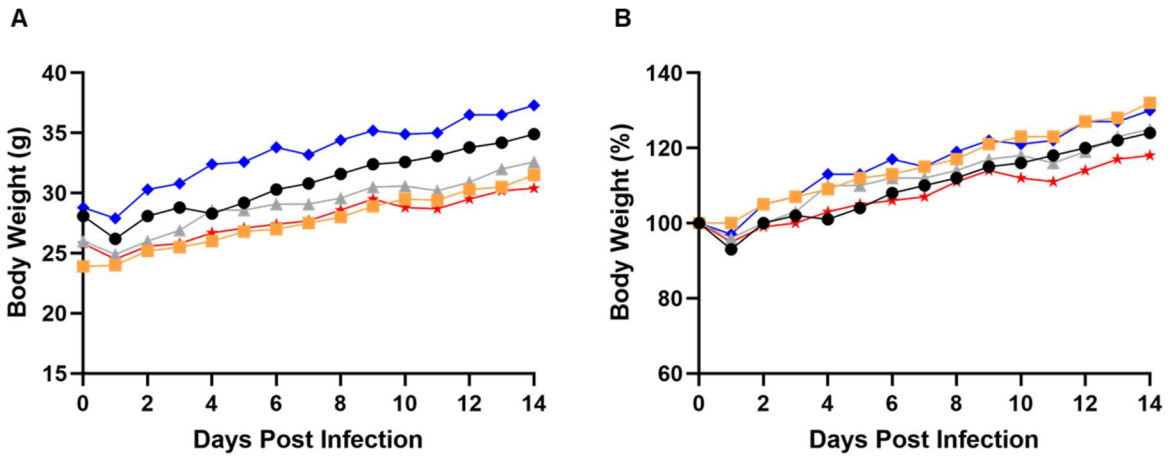


**Figure 5.3 Individual body weight changes of CD-1 mice passively immunized with mAb-32 followed by intracerebral challenge with YFV 17D strain.**
Five mice were passively immunized with 100 µg of mAb-32. Twenty-four hours post-immunization, mice were challenged intracerebrally with $5x10^4$ PFU of YFV 17D. The body weight (g) was recorded daily for 14 days (**A**) and the percent body weight change from the baseline (**B**) was calculated.

**Table 5.1 Body weight comparison between naïve and passively immunized mice challenged intracerebrally with YFV 17D strain.**
Mice were weighed daily. The average body weight (g) between the human anti-YFV mAbs and the isotype control group were compared. The time (days) begins on the day of challenge (day 0). The numbers in the table indicate *p*-values derived from mixed-effects analysis followed by Dunnett's multiple comparisons test.

| Time (days) | mAb-29 | mAb-32 |
|---|---|---|
| 0 | n.s. | n.s. |
| 1 | n.s. | n.s. |
| 2 | n.s. | n.s. |
| 3 | n.s. | n.s. |
| 4 | n.s. | n.s. |
| 5 | n.s. | n.s. |
| 6 | 0.0075 | 0.0079 |
| 7 | 0.0021 | 0.0015 |

n.s. = not significant

***Survival analysis and viral load results.*** The probability of survival by Kaplan-Meier curve analysis is shown in **Figure 5.4**. Passive immunization of mAb-29 or mAb-32 conferred full protection against ic challenge with the YFV 17D vaccine strain in outbred CD-1 mice.

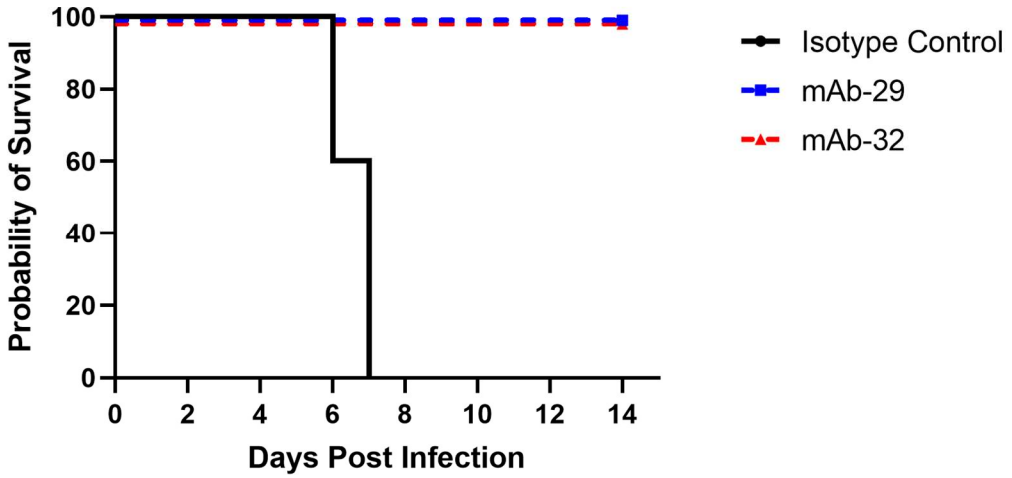


**Figure 5.4 Probability of survival in CD-1 mice passively immunized with the isotype control, mAb-29, or mAb-32 followed by intracerebral challenge with YFV 17D strain.** CD-1 mice passively immunized with 100 μg of the isotype control, mAb-29, or mAb-32 were challenged with $5x10^4$ PFU of YFV 17D intracerebrally. All mice that received a human anti-YFV mAbs survived challenge and were euthanized at 14 d.p.i. Probability of survival by Kaplan-Meier curve analysis.

As summarized in **Table 5.2**, all mice passively immunized with mAb-29 or mAb-32 survived the duration of the challenge study and were euthanized at 14 d.p.i. On the contrary, 100% of mice that received the isotype control mAb succumbed to YF infection with a median survival time (MST) of 7 d.p.i. Prophylactic passive immunization with either of the human anti-YFV mAbs significantly extended the MST of mice compared to the isotype control mAb (Kruskal-Wallis followed by Dunn's multiple comparisons test, $p$=0.0030).

**Table 5.2 Mortality rate and median survival time of passively immunized CD-1 mice challenged intracerebrally with YFV 17D strain.**
The percent mortality (dead/total) and median survival time (MST) in d.p.i. of CD-1 mice passively immunized with the isotype control, mAb-29, or mAb-32 followed by intracerebral challenge with $5x10^4$ PFU of YFV 17D. Passive immunization of mAb-29 or mAb-32 significantly extended the MST of mice compared to the isotype control mAb (Kruskal-Wallis followed by Dunn's multiple comparisons test, $p$=0.0030).

| | Isotype Control | mAb-29 | mAb-32 |
|---|---|---|---|
| Mortality rate | 100% (5/5) | 0% (0/5) | 0% (0/5) |
| MST (days) | 7 | >14 | >14 |

Upon death or euthanasia, the brains were harvested and underwent RT-qPCR to detect the presence of viral RNA. The brain viral loads are consistent with the full protection of passively immunized mice. No viral RNA was detected in the brains of mice passively immunized with mAb-29 or mAb-32. Viral RNA was detected in all the brains of mice in the isotype control group and averaged $4.40x10^7 \pm 5.84x10^7$ RNA copies per gram of brain tissue.

***Summary.*** Mice passively immunized with mAb-29 or mAb-32 were fully protected against lethal neurological disease caused by YFV 17D inoculated intracerebrally. No viral RNA was detected in the brains of mice immunized with either of the human anti-YFV mAbs. Since full protection was achieved against ic challenge with the 17D strain in CD-1 mice, both mAbs were selected for the passive protection studies against the wt Asibi strain of YFV.

## 5.3 Passive protection of outbred CD-1 mice with two human anti-YFV mAbs challenged with YFV Asibi strain by the intracerebral route

Two mouse models were used to investigate the passive protection of each human anti-YFV mAb against wt YFV. The prophylactic passive transfer of mAb-29 and mAb-32 was first undertaken in CD-1 mice challenged by the ic route with the wt Asibi strain of YFV. This approach evaluated the passive protection of each mAb against neurotropic disease caused by wt YFV because the Asibi strain is highly neurovirulent when administered intracerebrally. Eighteen ($n$=6 mice per group consisting of 3 males and 3 females) outbred CD-1 mice were passively immunized with 100 μg of mAb-29, mAb-32, or the isotype control by the ip route (timeline shown in **Figure 2.4**). Twenty-four hours later, mice were challenged intracerebrally with $5x10^4$ PFU of YFV Asibi. The same dosage of challenge at $5x10^4$ PFU allows for the comparison of passive protection between the 17D strain and the wt YFV Asibi strain. All mice had an initial decrease in body weight at 1 d.p.i. but remained BAR. This was attributed to the

stress of being anaesthetized and challenged. Euthanasia was carried out in accordance with the approved IACUC protocol.

***Isotype control VRC01 mAb.*** The individual body weight changes in mice passively immunized with the isotype control antibody are shown in **Figure 5.5**. At 3 d.p.i., five of the six mice showed signs of disease including weight loss, hunched posture, and circling. At 4 d.p.i., one mouse was found dead and four of the remaining mice were moribund. Of the four moribund mice, two displayed hind limb paralysis. All four mice were euthanized. The remaining mouse was BAR and had steady weight gain at 2 d.p.i. through the duration of the 14-day study and survived the challenge experiment. This mouse was considered an outlier. Omitting this mouse from the isotype control group resulted in an average weight loss of 24% from the baseline. By the end of the study at 14 d.p.i., the surviving mouse in the isotype control group had a 26% increase in weight from the baseline. All the brains were unremarkable during necropsy.

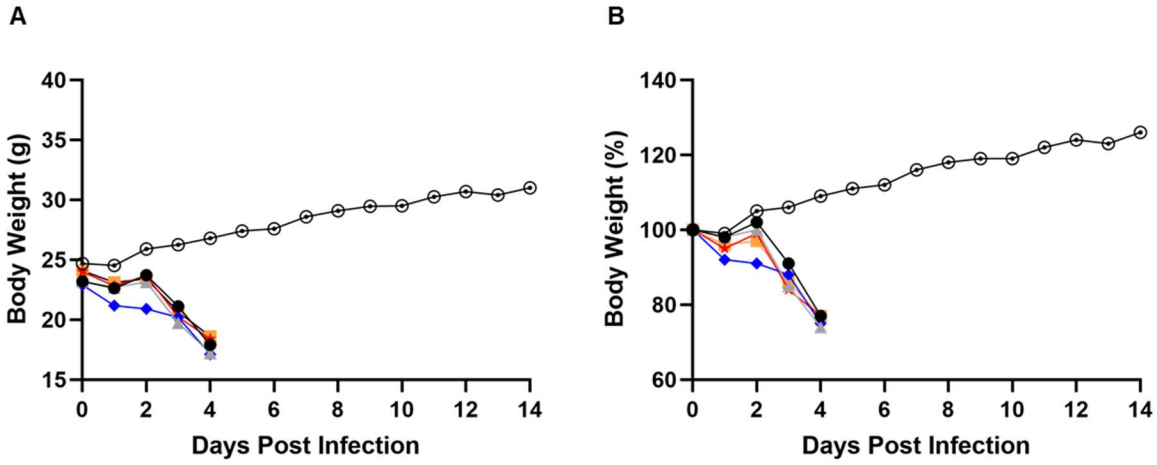


**Figure 5.5 Individual body weight changes of CD-1 mice passively immunized with the isotype control (VRC01) antibody followed by intracerebral challenge with YFV Asibi strain.**
Six mice were passively immunized with 100 µg of the isotype control (VRC01) antibody. Twenty-four hours post-immunization, mice were challenged intracerebrally with $5x10^4$ PFU of YFV Asibi. The body weight (g) was recorded daily for 14 days (**A**) and the percent body weight change from the baseline on day zero (**B**) was calculated.

***Human anti-YFV mAb-29.*** The individual body weight changes in mice passively immunized with mAb-29 are shown in **Figure 5.6**. At 3 d.p.i., mice showed symptoms of disease including weight loss. At 4 d.p.i., five of the six mice showed signs of severe disease including depression, limited and/or uncoordinated movements, or were moribund, and subsequently euthanized. The last mouse was euthanized at 5 d.p.i. due to being moribund. Mice in this group had an average weight loss from the baseline of 25%. No distinguishing features in the brain were observed during necropsy.

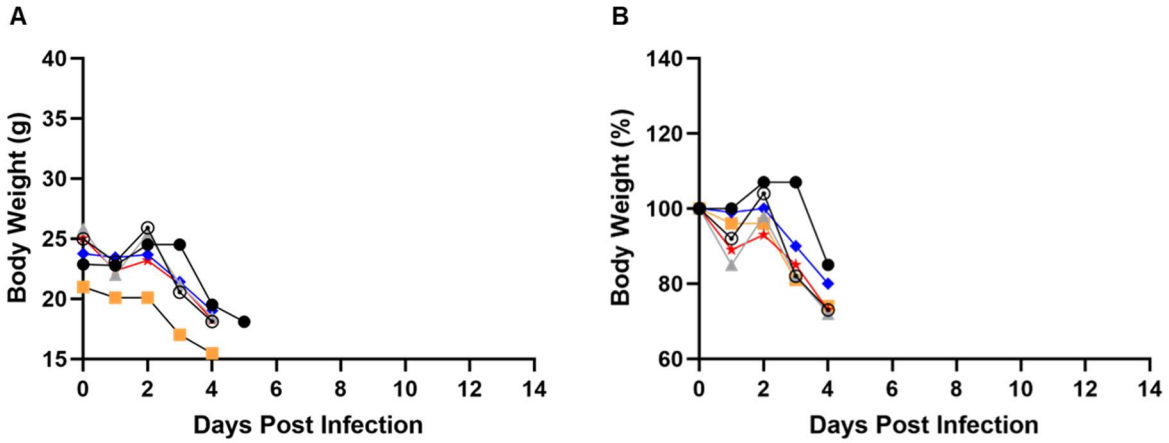


**Figure 5.6 Individual body weight changes of CD-1 mice passively immunized with mAb-29 followed by intracerebral challenge with YFV Asibi strain.**
Six mice were passively immunized with 100 µg of mAb-29. Twenty-four hours post-immunization, mice were challenged intracerebrally with $5x10^4$ PFU of YFV Asibi. The body weight (g) was recorded daily for 14 days (**A**) and the percent body weight change from the baseline on day zero (**B**) was calculated.

***Human anti-YFV mAb-32.*** The individual body weight changes in mice passively immunized with mAb-32 are shown in **Figure 5.7**. At 3 d.p.i., mice showed symptoms of disease including hunched posture, weight loss, depression, and minor neurological signs such as circling and involuntary twitching. Five of the six mice were moribund and subsequently euthanized. At 4 d.p.i., the last mouse was euthanized due to severe depression, minor neurological symptoms (i.e., circling), and falling below the 20% weight loss from baseline. Mice in this group had an

average weight loss from the baseline of 28%. The brains of these mice were unremarkable during necropsy.

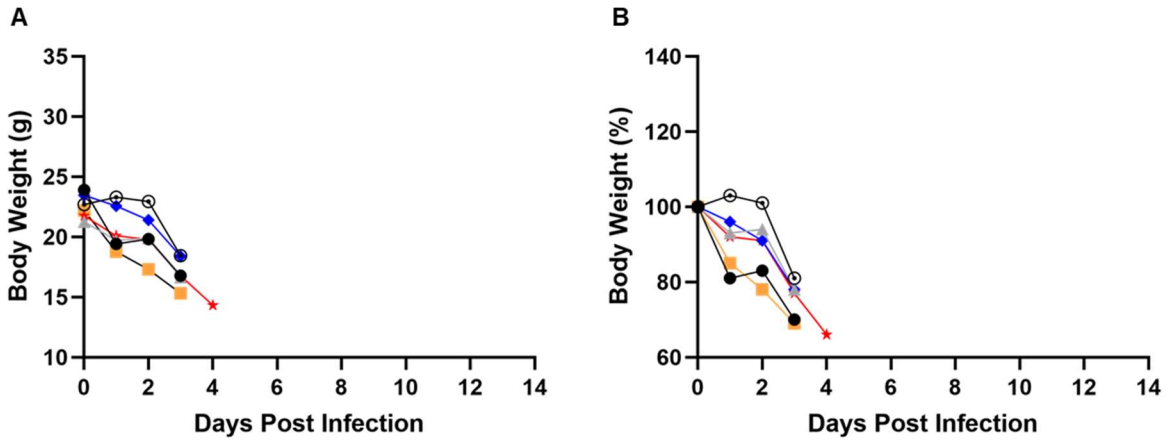


**Figure 5.7 Individual body weight changes of CD-1 mice passively immunized with mAb-32 followed by intracerebral challenge with YFV Asibi strain.**
Six mice were passively immunized with 100 µg of mAb-32. Twenty-four hours post-immunization, mice were challenged intracerebrally with $5x10^4$ PFU of YFV Asibi. The body weight (g) was recorded daily for 14 days (**A**) and the percent body weight change from the baseline on day zero (**B**) was calculated.

Interestingly, while some neurological signs (i.e., uncoordinated movements, circling, or involuntary twitching) were observed in mice that received mAb-29 or mAb-32, only mice that received the isotype control mAb displayed hind limb paralysis. There was no demonstratable weight gain in mice passively immunized with mAb-29 or mAb-32 compared to the control group (mixed-effects analysis followed by Dunnett's multiple comparisons test).

***Survival analysis and viral load results.*** The probability of survival by Kaplan-Meier curve analysis is shown in **Figure 5.8**. Mice were not protected against lethal YF infection following passive immunization of mAb-29 or mAb-32.

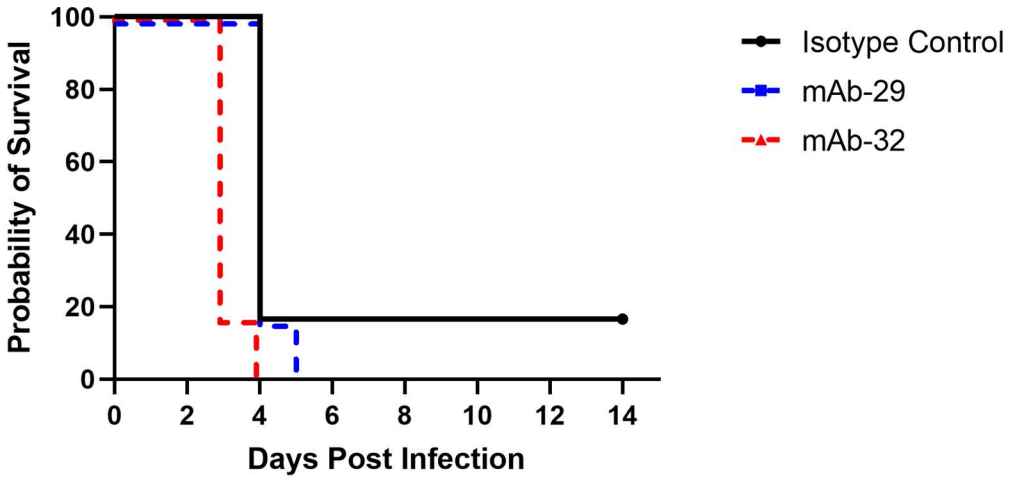


**Figure 5.8 Probability of survival in CD-1 mice passively immunized with the isotype control, mAb-29, or mAb-32 followed by intracerebral challenge with YFV Asibi strain.** CD-1 mice passively immunized with 100 μg of the isotype control, mAb-29, or mAb-32 were challenged with $5x10^4$ PFU YFV Asibi intracerebrally. Neither of the human anti-YFV mAbs conferred protection against lethal YF infection (Kaplan-Meier curve analysis).

As summarized in **Table 5.3**, neither of the human anti-YFV mAbs extended the survival time of mice compared to the control group (Kruskal-Wallis test followed by Dunnett's multiple comparisons test). The MST of mice was 4 d.p.i. in the isotype control and mAb-29 group and 3 d.p.i. in the mAb-32 group. The single mouse in the isotype control group that survived the Asibi challenge was euthanized at the end of the study at 14 d.p.i.

**Table 5.3 Mortality rate and median survival time of passively immunized CD-1 mice challenged intracerebrally with YFV Asibi strain.**
The percent mortality (dead/total) and median survival time (MST) in d.p.i. of CD-1 mice passively immunized with the isotype control, mAb-29, or mAb-32 followed by intracerebral challenge with $5x10^4$ PFU of YFV Asibi. Passive immunization of mAb-29 or mAb-32 did not extend the MST of mice compared to the isotype control group (Kruskal-Wallis test followed by Dunnett's multiple comparisons test).

| | Isotype Control | mAb-29 | mAb-32 |
|---|---|---|---|
| Mortality rate | 83% (5/6) | 100% (6/6) | 100% (6/6) |
| MST (days) | 4 | 4 | 3 |

Viral RNA was detected in the brains of all mice passively immunized with mAb-29 or mAb-32 (**Figure 5.9**). Viral RNA was also detected in all brains of mice that received the isotype control mAb except for the one mouse that survived the challenge.

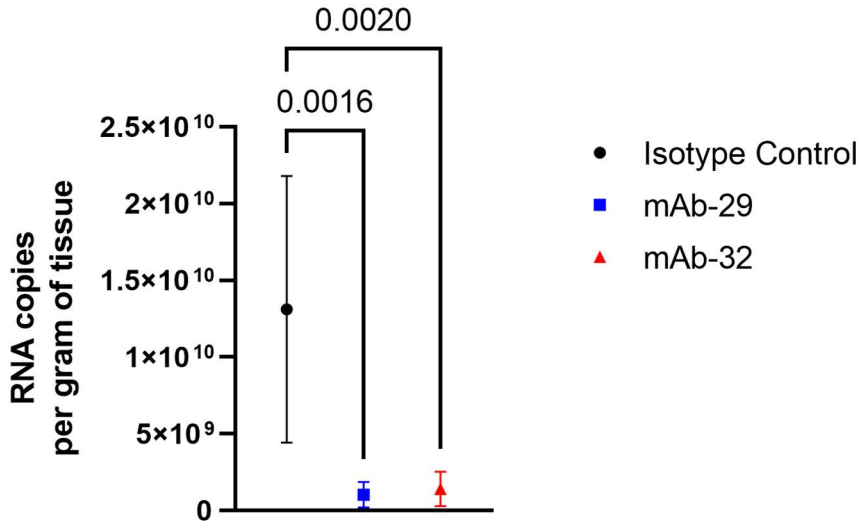


**Figure 5.9 Brain tissue viral loads of passively immunized CD-1 mice challenged intracerebrally with YFV Asibi strain.**
CD-1 mice passively immunized with 100 µg of the isotype control, mAb-29, or mAb-32 were challenged intracerebrally with YFV Asibi. At the time of death or euthanasia, the brains were harvested, and viral RNA was detected via RT-qPCR. A significant reduction in the brain viral load in mice passively immunized with mAb-29 ($p$=0.0016) or mAb-32 ($p$=0.0020) compared to the isotype control group was observed (one-way ANOVA followed by Dunnett's multiple comparisons test).

The average brain tissue viral load in the isotype control group ($n$=5) was $1.31x10^{10}$**±**$8.70x10^{9}$ RNA copies per gram of brain tissue. The brain viral loads of mice passively immunized with mAb-29 ($n$=6) or mAb-32 ($n$=6) averaged $1.03x10^{9}$±$8.33x10^{8}$ and $1.41x10^{9}$±$1.13x10^{9}$ RNA copies per gram of brain tissue, respectively. A significant reduction in the brain viral load of mice passively immunized with mAb-29 ($p$=0.0016) or mAb-32 ($p$=0.0020) compared to the isotype control group was observed (one-way ANOVA followed by Dunnett's multiple comparisons test).

***Summary.*** Mice passively immunized with the human anti-YFV mAbs were not protected against lethal neurological disease caused by YFV Asibi, however, both mAb-29 and mAb-32 reduced the viral load in the brain by approximately 13-fold and 9-fold, respectively. Therefore, passive immunization with mAb-29 or mAb-32 at 100 μg confers at least partial protection against neurotropic disease caused by ic challenge with the wt Asibi strain of YFV.

## 5.4 Passive protection of AG6 mice with two human anti-YFV mAbs challenged with YFV Asibi strain by the intraperitoneal route

There is limited research using the IFNAR$^{-/-}$-IFNGR$^{-/-}$ mouse model, especially AG6 mice, against lethal challenge with wt YFV by the ip route. Furthermore, no passive protection studies against the Asibi strain have been conducted. This is due to limited commercial availability of immunocompromised mice and the logistical constraints of conducting research in an ABSL-3. Therefore, this study served two purposes: to elucidate viscerotropic YF disease in the AG6 mouse model and evaluate the protective efficacy of two human anti-YFV mAbs against lethal wt Asibi infection.

Mice with the C57BL/6 background deficient in type-I IFN receptors (AB6) and both type-I and type-II IFN receptors (AGB6), and the AG129 mouse strain all succumb to lethal infection with wt YFV (Meier et al. 2009; Watson et al. 2016; Lam et al. 2018). These studies challenged mice subcutaneously in the footpad with $10^4$ PFU of YFV Asibi strain, $10^4$ PFU of YFV Angola71 strain, or $2x10^4$ PFU of Angola71 strain. The only ip challenge in the IFNAR$^{-/-}$-IFNGR$^{-/-}$ mouse model inoculated with $2x10^5$ PFU of YFV 17D-204 in AG129 mice (Thibodeaux, Garbino, Liss, Piper, Schlesinger, et al. 2012). Taken together, a dosage of $2x10^4$ PFU was selected to achieve at least 80% mortality in the control group.

Fifteen ($n$=5 per group) AG6 mice were passively immunized with 100 µg of mAb-29, mAb-32, or the isotype control by the ip route (timeline shown in **Figure 2.4**). Twenty-four hours later, mice were challenged intraperitoneally with $2x10^4$ PFU of YFV Asibi. All mice had an initial decrease in body weight at 1 d.p.i. but remained BAR. This was attributed to the stress of being anaesthetized and challenged. Euthanasia was carried out in accordance with the approved IACUC protocol.

***Isotype control VRC01 mAb.*** The individual body weight changes in mice passively immunized with the isotype control antibody are shown in **Figure 5.10**. At 2 d.p.i., mice in the isotype control group were BAR and either maintaining or had a minimal decrease in weight. All mice began showing signs of illness including dull coats and weight loss at 3 d.p.i. At 4 d.p.i., four of the five mice deteriorated rapidly and were euthanized. These mice had minimal weight loss in the morning but remained alert and responsive. However, a rapid onset of symptoms was observed within eight hours when the mice were moribund and developed signs of disease including hunched posture, ruffled fur, rapid breathing, involuntary twitching, and/or severe depression. One mouse had left hind paresis and another mouse excessively scratched near the abdominal area and thrashed into the bedding/cage, suggesting severe viscerotropic distress and discomfort. The fifth mouse showed signs of recovery and steadily started gaining weight. This mouse survived the duration of the study and was euthanized at 14 d.p.i. Upon necropsy, one mouse that had been euthanized at 4 d.p.i. had signs of hemorrhage including a darkened liver and intestines and an enlarged spleen, while the other mice were unremarkable, including the mouse that survived the challenge study.

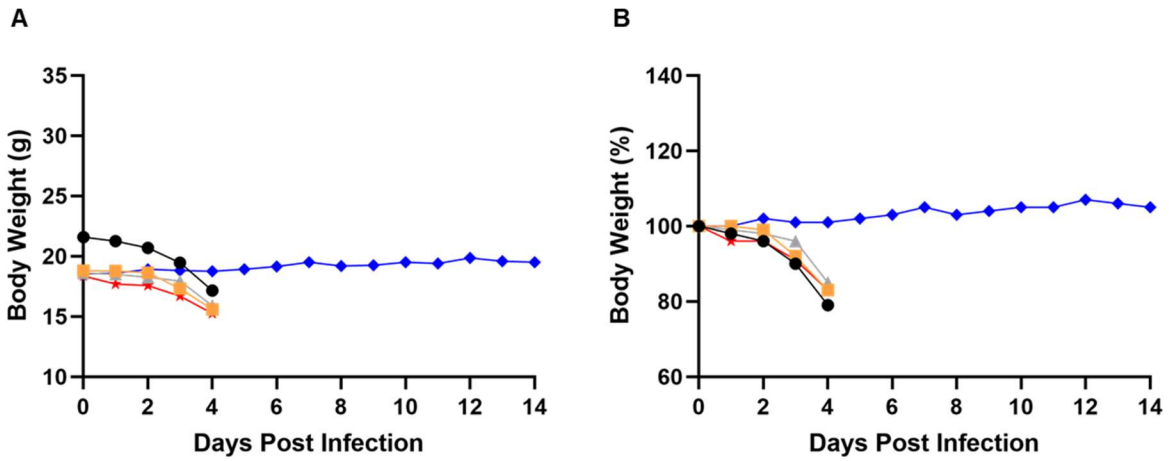


**Figure 5.10 Individual body weight changes of AG6 mice passively immunized with the isotype control (VRC01) antibody followed by intraperitoneal challenge with YFV Asibi strain.**
Five mice were passively immunized with 100 µg of the isotype control (VRC01) antibody. Twenty-four hours post-immunization, mice were challenged intraperitoneally with $2x10^4$ PFU of YFV Asibi. The body weight (g) was recorded daily for 14 days (**A**) and the percent body weight change from the baseline on day zero (**B**) was calculated.

***Human anti-YFV mAb-29.*** The individual body weight changes in mice passively immunized with mAb-29 are shown in **Figure 5.11**. Mice immunized with mAb-29 steadily gained or maintained weight and were BAR up to 3 d.p.i. At 4 d.p.i, three of the five mice developed weight loss, but all remained BAR. At 5 d.p.i., three mice displayed signs of disease including hunched posture, slow ambulation, and/or ruffled fur, and all mice had weight loss. At 6 d.p.i., four of the five mice were euthanized due to weight loss and being moribund. One mouse had right hind limb paralysis. The last mouse was BAR and gained weight at 7 d.p.i., however, at 10 d.p.i. the mouse developed weight loss and showed signs of discomfort including slower ambulation. At 11 d.p.i., the final mouse deteriorated rapidly in an 8-hour period and reached the criteria of euthanasia. This mouse and two others had no unique features and the organs appeared normal upon necropsy, however, two mice euthanized at 6 d.p.i. had signs of hemorrhage including a darkened spleen.

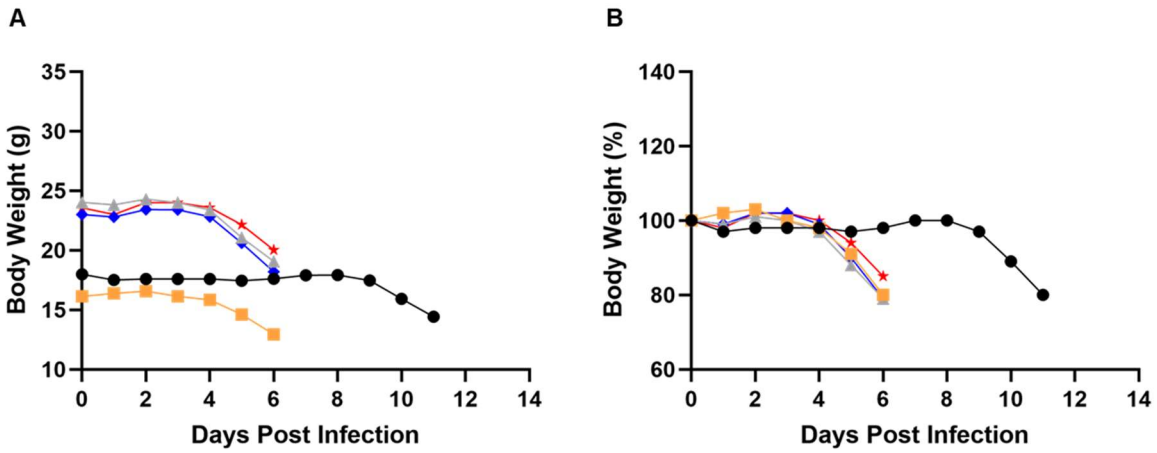


**Figure 5.11 Individual body weight changes of AG6 mice passively immunized with mAb-29 followed by intraperitoneal challenge with YFV Asibi strain.**
Five mice were passively immunized with 100 µg of mAb-29. Twenty-four hours post-immunization, mice were challenged intraperitoneally with $2x10^4$ PFU of YFV Asibi. The body weight (g) was recorded daily for 14 days (**A**) and the percent body weight change from the baseline on day zero (**B**) was calculated.

***Human anti-YFV mAb-32.*** The individual body weight changes in mice passively immunized with mAb-32 are shown in **Figure 5.12**. At 2 d.p.i., mice maintained or gained weight and were BAR. At 3 d.p.i. onwards, all mice steadily developed weight loss but remained BAR until 6 d.p.i., upon which two mice were moribund and euthanized. The remaining three mice had ruffled fur, slow ambulation, and/or abnormal posture possibly indicating neurological symptoms. Two mice were moribund and euthanized at 7 d.p.i. and the final mouse was euthanized at 8 d.p.i. Upon necropsy, one mouse euthanized at 6 d.p.i. showed signs of hemorrhage including a darkened liver, while the other four mice had indistinguishable features in the visceral cavity.

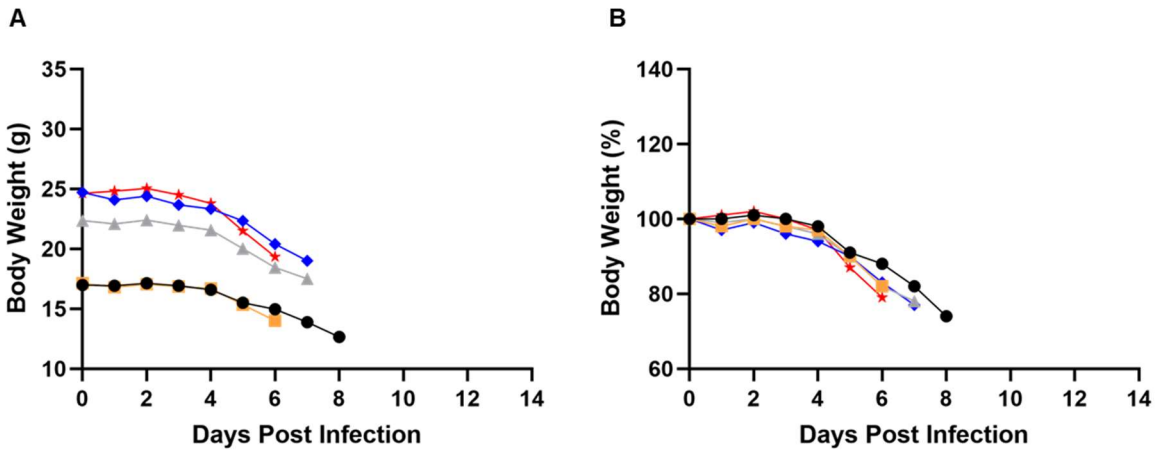


**Figure 5.12 Individual body weight changes of AG6 mice passively immunized with mAb-32 followed by intraperitoneal challenge with YFV Asibi strain.**
Five mice were passively immunized with 100 μg of mAb-32. Twenty-four hours post-immunization, mice were challenged intraperitoneally with $2x10^4$ PFU of YFV Asibi. The body weight (g) was recorded daily for 14 days (**A**) and the percent body weight change from the baseline on day zero (**B**) was calculated.

***Survival analysis and viral load results.*** There was no demonstratable weight gain in mice passively immunized with mAb-29 or mAb-32 compared to the isotype control group (mixed-effects analysis followed by Dunnett's multiple comparisons test). The probability of survival by Kaplan-Meier curve analysis is shown in **Figure 5.13**. Both mAb-29 ($p$=0.0358) and mAb-32 ($p$=0.0076) extended the MST of mice compared to the isotype control group to provide partial protection from lethal wt YFV infection (Kruskal-Wallis test followed by Dunn's multiple comparisons test). The MST of the isotype control, mAb-29, and mAb-32 groups were 4, 6, and 7 d.p.i., respectively (**Table 5.4**). The single mouse in the isotype control group that survived Asibi challenge was euthanized at the end of the study at 14 d.p.i.

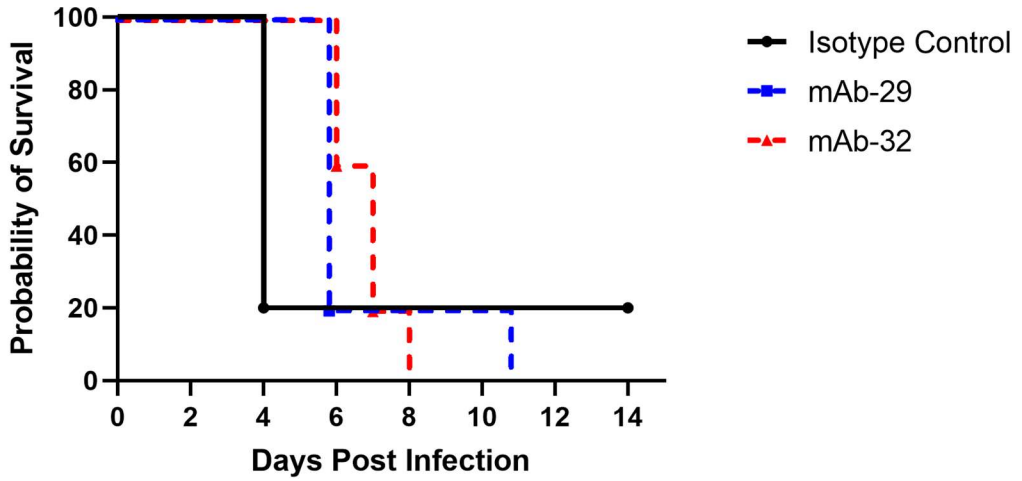


**Figure 5.13 Probability of survival in AG6 mice passively immunized with the isotype control, mAb-29, or mAb-32 followed by intraperitoneal challenge with YFV Asibi strain.** AG6 mice passively immunized with 100 µg of the isotype control, mAb-29, or mAb-32 were challenged intraperitoneally twenty-four hours later with $2x10^4$ PFU of YFV Asibi strain. Neither of the human anti-YFV mAbs conferred complete protection against lethal wt YF infection (Kaplan-Meier curve analysis).

**Table 5.4 Mortality rate and median survival time of passively immunized AG6 mice challenged intraperitoneally with YFV Asibi strain.**
The percent mortality (dead/total) and median survival time (MST) in d.p.i. of AG6 mice passively immunized with 100 µg of the isotype control, mAb-29, or mAb-32 followed by intraperitoneal challenge with $2x10^4$ PFU of YFV Asibi strain. There was a statistical difference in the survival time between mice passively immunized with mAb-29 ($p$=0.0358) or mAb-32 ($p$=0.0076) compared to the isotype control group (Kruskal-Wallis test followed by Dunn's multiple comparisons test).

| | Isotype Control | mAb-29 | mAb-32 |
|---|---|---|---|
| Mortality rate | 80% (4/5) | 100% (5/5) | 100% (5/5) |
| MST (days) | 4 | 6 | 7 |

Upon death or euthanasia, the brain, liver, spleen, kidneys, and mesenteric DLN was harvested, and RT-qPCR was performed. All the tissues from mice in all the groups contained viral RNA except for the single mouse in the isotype control group that survived the challenge experiment and is considered as an outlier. The brain, liver, spleen, kidney, and mesenteric DLN tissue viral loads in RNA copies per gram of tissue are shown in **Figure 5.14**.

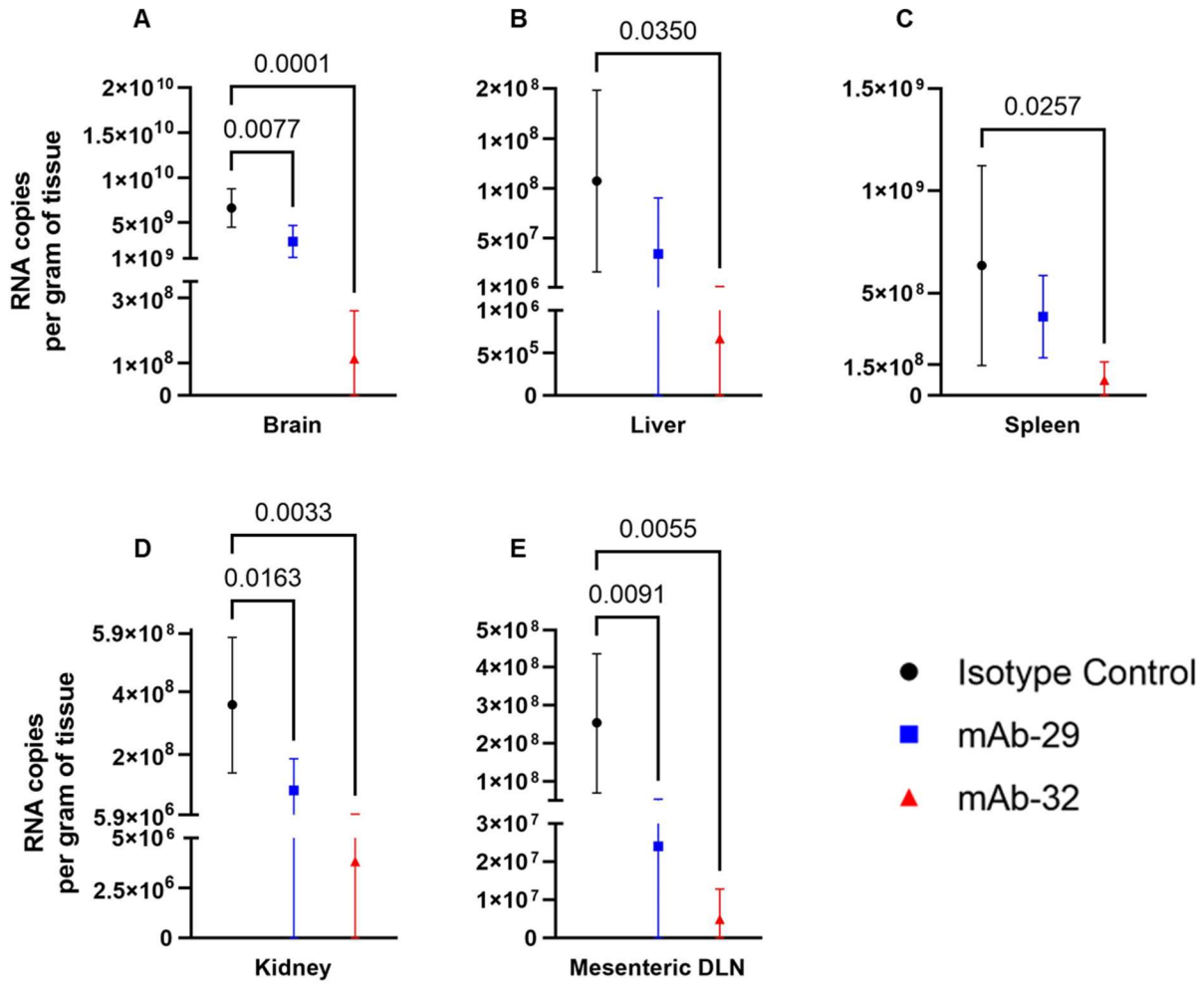


**Figure 5.14 Tissue viral loads of passively immunized AG6 mice challenged intraperitoneally with YFV Asibi strain.**
Twenty-four hours prior to intraperitoneal challenge with $2x10^4$ PFU of YFV Asibi strain, AG6 mice were passively immunized with 100 µg of the isotype control, mAb-29, or mAb-32. At the time of death or euthanasia, the brain (**A**), liver (**B**), spleen (**C**), kidneys (**D**), and mesenteric DLN (**E**) were harvested, and viral RNA was detected via RT-qPCR. Prophylactic passive immunization of mAb-29 significantly reduced the viral load in brain ($p$=0.0077), kidney ($p$=0.0163), and mesenteric DLN ($p$=0.0091) tissues. MAb-32 significantly reduced the viral load in brain ($p$=0.0001), liver ($p$=0.0350), spleen ($p$=0.0257), kidney ($p$=0.0033), and mesenteric DLN ($p$=0.0055) tissues. Viral load analyzed using one-way ANOVA followed by Dunnett's multiple comparisons test.

Using one-way ANOVA followed by Dunnett's multiple comparisons test, prophylactic passive transfer of mAb-29 and mAb-32 significantly reduced the viral load in multiple tissues compared to the isotype control group. Mab-29 significantly reduced the brain ($p$=0.0077), kidney ($p$=0.0163), and mesenteric DLN ($p$=0.0091) tissues compared to the isotype control

group. Mab-32 significantly reduced the viral load in all the tissue including the brain ($p$=0.0001), liver ($p$=0.0350), spleen ($p$=0.0257), kidneys ($p$=0.0033), and mesenteric DLN ($p$=0.0055) compared to the isotype control group. The average brain tissue viral load in mice passively immunized with mAb-29 or mAb-32 ($n$=5 mice per group) were $3.15x10^9 \pm 1.78x10^9$ and $6.96x10^6 \pm 1.48x10^8$ RNA copies per gram of tissue, respectively, compared to the isotype control ($n$=4) with a brain viral load of $6.16x10^9 \pm 2.14x10^9$ RNA copies per gram of tissue (**Figure 5.14.A**). The average liver viral load was $3.45x10^7 \pm 5.64x10^7$ and $6.67x10^5 \pm 1.14x10^6$ RNA copies per gram of tissue in mice passively immunized with mAb-29 or mAb-32 ($n$=5 mice per group), respectively, compared to $1.07x10^8 \pm 9.08x10^7$ RNA copies per gram of tissue in the isotype control group ($n$=4) (**Figure 5.14.B**). The spleen tissue viral load in mice passively immunized with mAb-29 or mAb-32 ($n$=5 mice per group) averaged $3.86x10^8 \pm 2.01x10^8$ and $7.50x10^7 \pm 8.90x10^7$ RNA copies per gram of tissue, respectively, compared to the isotype control ($n$=4) of $6.36x10^8 \pm 4.89x10^8$ RNA copies per gram of tissue (**Figure 5.14.C**). The kidney viral load in mice passively immunized with mAb-29 or mAb-32 ($n$=5 mice per group) averaged $8.45x10^7 \pm 1.01x10^8$ and $3.83x10^6 \pm 5.23x10^6$ RNA copies per gram of tissue, respectively, compared to the isotype control ($n$=4) of $3.59x10^8 \pm 2.18x10^8$ RNA copies per gram of tissue (**Figure 5.14.D**). Lastly, in mice that received the isotype control ($n$=4), the mesenteric DLN tissue viral load averaged $2.54x10^8 \pm 1.85x10^8$ RNA copies per gram of tissue, compared to $2.41x10^7 \pm 2.94x10^7$ and $4.88x10^6 \pm 8.00x10^6$ RNA copies per gram of tissue in mice immunized with mAb-29 or mAb-32 ($n$=5 mice per group), respectively (**Figure 5.14.E**).

***Summary.*** Prophylactic passive transfer of the anti-YFV mAbs partially protected AG6 mice against lethal viscerotropic disease caused by wt Asibi YFV. MAb-29 and mAb-32 significantly extended the MST compared to the isotype control group. Both mAb-29 and mAb-32 led to a

significant reduction of tissue viral loads in the brain, kidney, and mesenteric DLN. Additionally, mAb-32 significantly reduced the viral load in the liver and spleen. Collectively, these data prove that YFV type-specific neutralizing human mAbs confer protection against viscerotropic disease caused by the ip challenge of wt YFV Asibi strain.

## 5.5 Discussion

In conclusion, two human anti-YFV mAbs were proven to confer passive protection against neurotropic disease caused by the ic challenge of CD-1 mice with the 17D strain and wt YFV Asibi strain, and viscerotropic disease induced by the ip challenge of AG6 mice with wt YFV Asibi strain. Passive protection by the human anti-YFV mAbs increased the MST and decreased tissue viral loads in infected mice. In the neurotropic disease model using CD-1 mice, both mAbs were fully protective against ic challenge with the 17D vaccine strain. The human anti-YFV mAbs were further proven to partially protect against lethal neurological disease caused by wt YFV Asibi strain, as demonstrated with the significant reduction in brain viral load compared to the isotype control. Importantly, both mAb-29 and mAb-32 also provided partial protection against viscerotropic disease in AG6 mice caused by the wt Asibi strain as passively immunized mice had significantly longer MST compared to the isotype control. Furthermore, both human anti-YFV mAbs significantly reduced viral loads in the brain, kidneys, and mesenteric DLNs, and mAb-32 also significantly reduced viral loads in the liver and spleen, compared to the isotype control group. Passive protection by mAb-29 and mAb-32 demonstrates the involvement of YFV type-specific neutralizing antibodies in the protective immunity against wt YFV.

Although ic inoculation in mice does not recapitulate YF disease in humans as the virus is only detected in the central nervous system, this model is helpful to evaluate the protective

efficacy of antibodies prior to the immunocompromised mouse model using the 17D vaccine strain. Results from this study align with previous studies where mice inoculated by the ic route with 17D results in 100% lethality (Ryman et al. 1998). Even at the higher dose of $5x10^4$ PFU of 17D compared to $10^4$ PFU (Ryman, Xie, et al. 1997; Ryman et al. 1998; Mishra et al. 2020) or $2x10^4$ PFU (Lu et al. 2019) of 17D used in other studies, mAb-29 and mAb-32 conferred full protection in CD-1 mice. In addition to the higher dosage of inocula, the approach used in this dissertation research also achieved full protection against the 17D vaccine strain with human anti-YFV mAbs at a lower dosage than the passive protection previously achieved using mouse anti-YFV mAbs. For example, ascites fluid used for passive immunization has approximately $1.9\pm0.2$ mg $ml^{-1}$ of protein (antibody) and demonstrates protective efficacy against the 17D strain (Barrett et al. 1989). Passive transfer of 100 µl of ascites fluid is likely to deliver up to 200 µg of mAbs, which is 2-fold higher than the dosage described in this study. However, it is unclear if mAb-29 and mAb-32 can achieve full protection at an even lower dosage, as Brandriss *et al.* reported full protection of CD-1 mice against ic challenge using 17D by passively transferring type-specific mAbs 4E8 and 2E10 at 40 µg and 4 µg (Brandriss et al. 1986).

The full protection of CD-1 mice through prophylactic passive transfer of the human anti-YFV mAbs warrants further investigation of the protection after ic challenge with the 17D strain. Previously, 20 mg/kg of human anti-YFV mAb-5A by ip injection one d.p.i. completely protected mice challenged intracerebrally with YFV 17D (Lu et al. 2019). The average weight of CD-1 mice in this study was 25 grams, equating to a dosage of 4 mg/kg. While the prophylactic transfer was undertaken to investigate the role of each mAb in vaccine protection, the post-exposure passive transfer will further prove the potential utility of human anti-YFV mAbs as

candidate antiviral treatments in the rare but severe adverse event of YF vaccine-associated neurological disease.

The partial protection of CD-1 mice and AG6 mice is consistent with the lower neutralization potency of both human anti-YFV mAbs against wt YFV strains. Therefore, it is apparent that the dosage of 100 μg per mouse is insufficient to achieve full protection against the lethal neurotropic and viscerotropic diseases caused by the wt YFV Asibi strain. It has previously been demonstrated that the passive protection of hamsters by type-specific anti-YFV mAb-2C9-cIgC (humanized antibody) against the hamster-adapted Jimenez p.10 strain is dose-dependent, reaching an 80% survival rate at 380 μg per animal (Julander et al. 2014). It is likely that the passive transfer of mAb-29 and mAb-32 at a higher dosage is required to prevent lethal disease caused by the wt YFV Asibi strain in mice.

AG6 mice are a biologically relevant model to assess the protective efficacy of the anti-YFV mAbs because these mice develop viscerotropic disease that resembles human YF disease. The lethality of YFV is rapid in immunocompromised mice with the wt strain. A129 and AG129 mice subcutaneously inoculated with $10^4$ PFU of wt Asibi strain resulted in complete lethality with an AST of 6.4±0.8 and 5.5±0.0 d.p.i, respectively, with rapid viral dissemination in the spleen, brain, and importantly the liver, of A129 mice over six days (Meier et al. 2009). Similarly, AG6 mice in this study had an 80% mortality rate with an MST of 4 d.p.i and a significantly higher tissue viral load in the isotype control group compared to mAb-29 and mAb-32. In a study by Meier *et al.*, AG129 mice inoculated subcutaneously with wt Asibi virus did not develop signs of neurological disease such as paresis or paralysis (Meier et al. 2009). This was also reported in a study by Watson *et al.* where AB6 mice had rising levels of virus in the brain but did not present signs of neurological disease after subcutaneous challenge with wt

Angola71 YFV (Watson et al. 2016). On the contrary, in this study, AG6 mice inoculated intraperitoneally with wt Asibi strain did show signs of neurological disease including hind limb paresis in one mouse immunized with the isotype control at 4 d.p.i. and another mouse immunized with mAb-29 displayed hind limb paralysis at 6 d.p.i. While detectable virus in the brain was found in A129 mice following subcutaneous challenge with wt YFV Asibi strain at 6 d.p.i., no signs of neurological disease were observed (Meier et al. 2009).

Very few studies have evaluated the passive protection of mAbs in mice deficient for IFN-α/β and IFN-γ receptors to compare the effectiveness of these human anti-YFV mAbs. Julander *et al.* demonstrated partial protection of mAb-2C9-cIgC against the Jimenez p.10 strain by decreasing viral titers in the serum and liver and increasing the survival rate compared to the control group (Julander et al. 2014). Furthermore, Calvert *et al*. challenged AG129 mice with $2x10^5$ PFU of 17D by ip injection 24 hours after immunization with 127 μg of mAb-2C9-cIgC resulting in an 80% survival rate (Calvert et al. 2016). Although mAb-2C9-cIgC significantly reduced the brain viral load and extended the survival time compared to the control group, the antibody was only tested against the vaccine strain, the immunogen to which the antibody was generated. In this dissertation research, partial protection was observed using a non-adapted wt YFV strain.

A final factor to consider in this study was the ages of the AG6 mice when challenged with YFV Asibi. Due to the stringent breeding and phenotyping required of the AG6 mouse strain, mice used in this study were between six and seven weeks of age at the time of challenge. This should not influence the outcome in this experiment, however. In a study by Watson *et al.*, subcutaneous challenge of wt Angola71 YFV resulted in 100% mortality in AB6 mice at various ages including 5-weeks old, 8-weeks old, and one-year old (Watson et al. 2016). Lam *et al.*

challenged 6-week old AGB6 mice subcutaneously with $10^4$ PFU of either YFV Angola71 strain or 17D-204 strain, both resulting in 100% mortality (Lam et al. 2018). Finally, Calvert *et al*., challenged AG129 mice between 6 and 8 weeks of age with $2.0x10^5$ PFU of 17D that resulted in complete lethality (Calvert et al. 2016).

In conclusion, this study used the viscerotropic and two neurotropic YFV disease mouse models to demonstrate passive protection by mAb-29 and mAb-32. In the neurotropic CD-1 mouse, both mAb-29 and mAb-32 showed complete protection against ic challenge of 17D and partial protection against ic challenge with wt Asibi by significantly reducing the brain viral load compared to the isotype control group. In the viscerotropic disease model, mAb-29 and mAb-32 demonstrated partial protection against ip challenge with Asibi strain by extending the MST compared to the isotype control. Furthermore, mAb-29 and mAb-32 significantly reduced the viral load in the brain, kidneys, and mesenteric DLN, and mAb-32 also significantly reduced the viral load in the liver and spleen, compared to the isotype control group. For the first time, human YFV type-specific neutralizing antibodies have been proven to protect against viscerotropic disease induced by wt YFV infection in mice.

# Chapter 6 - Discussion

## 6.1 Overall conclusion

Yellow fever virus is a zoonotic virus that causes severe viscerotropic disease with a high mortality rate in immunologically naïve humans and New World primates. Although the live-attenuated 17D vaccine is highly effective in controlling YF in sub-Saharan Africa and tropical South America, larger demands during outbreaks and the inability to rapidly produce the vaccine in substantial quantities results in recurring YF vaccine shortages (Gaythorpe et al. 2021). Therefore, there is a growing interest in producing second-generation YF vaccines that can be manufactured using modern cell culture technologies. A better understanding of how the 17D vaccine protects against wt YFV is crucial because all candidate YF vaccines must be proven non-inferior to the 17D vaccine. It is well accepted neutralizing antibodies are the correlate of protection for the 17D vaccine (Mason et al. 1973). Neutralizing antibody responses elicited by the 17D vaccine are YFV type-specific and do not cross-react with other flaviviruses. However, the mechanism(s) of antibody-mediated neutralization against wt YFV in humans remains elusive. Thus, the characterization of two human anti-YFV mAbs aids in the understanding of how YFV type-specific neutralizing antibodies protect vaccinees against wt YF infection. This knowledge can then be translated to support the rational design of second-generation YF vaccines.

The objective of this dissertation research was to characterize two human anti-YFV mAbs isolated from 17D vaccinees to further our understanding on the mechanism(s) of antibody-mediated neutralization. The major findings of this project are as follows:

1. The quantification of the neutralizing potency of mAb-29 and mAb-32 against the 17D strain and the representative strains for four genotypes of wt YFV proved both mAbs exhibit YFV type-specific neutralizing activities.
2. The antigenic site(s) recognized by each mAb was delineated by examining the neutralizing potency against YFV chimeras that contain distinct E protein domains swapped between 17D and Asibi strains. A difference in neutralizing potencies was observed using mAb-32 against recombinant strains of 17D, Asibi, and the Asibi-17D(EDI-II) chimera, suggesting mAb-32 targets a conformational epitope across EDI and EDII. While mAb-29 did not exhibit the differential neutralization potencies against the recombinant 17D and Asibi strains, the replacement of EDI and EDII in the Asibi strain with the corresponding region from the 17D strain increased the $PRNT_{50}$ concentration of mAb-29. This observation suggests that mAb-29 targets E protein residues in EDI and EDII. Collectively, these results demonstrated that both human anti-YFV type-specific neutralizing mAbs interact with more than one domain in the E protein, thereby targeting conformational epitopes. Overall, this helps improve our understanding of how the presentation of YFV type-specific neutralizing epitopes are different among the genotypes of YFV, subsequently leading to variations in neutralization potency.
3. Prophylactic passive protection was determined by mAb-29 and mAb-32 in mice. Both mAbs conferred full protection against neurotropic disease caused by the 17D strain in CD-1 mice. MAb-29 and mAb-32 were further shown to partially protect against neurotropic and viscerotropic disease caused by the wt Asibi strain in CD-1 and AG6

mice, respectively. These results suggest that antibody-mediated neutralization contributes to the protective immunity elicited by the 17D vaccine.

Collectively, these data are helpful in addressing several unanswered questions of immune protection of 17D vaccinees against wt YFV and provide the basis to better understand protective neutralizing antibody responses against flaviviruses in humans.

## 6.2 YFV type-specific human mAbs neutralize genotypes of wild-type YFV endemic both in sub-Saharan Africa and tropical South America

A major finding of this project was to demonstrate human mAbs raised against the 17D vaccine neutralize multiple genotypes of YFV endemic in both South America and Africa. Differential neutralizing potencies of mAb-29 and mAb-32 between the 17D strain and four genotypes of wt YFV was expected, reflecting the amino acid divergence (up to 5%) in the E protein that can affect antigenicity. The ability of both mAbs to neutralize different genotypes of wt YFV provides an explanation for the ability of polyclonal sera of 17D vaccinees to neutralize wt YFV strains circulating in different geographic regions (Groot and Riberiro 1962; Monath 1971). Importantly, the antibody-mediated neutralization may involve clonal populations of antibodies that neutralize each of the seven genotypes of wt YFV at different potencies. These results warrant the further assessment of the neutralizing potency of these mAbs against the remaining three genotypes of wt YFV, including East Africa, East/Central Africa, and Angola genotypes. The three genotypes of wt YFV are phylogenetically distant from the four genotypes of wt YFV evaluated in this study (Mutebi et al. 2001). Collectively, this will lead to a better understanding of how protective immunity induced by the 17D vaccine can achieve the breadth of protection against all seven genotypes of wt YFV.

Recently, Haslwanter *et al*. showed the neutralization potency of YFV vaccine-induced human polyclonal antibody and mAb responses against two South American genotypes (YFV-ES-504, South America I genotype and YFV-Bolivia, South America II genotype) were substantially lower compared to wt African YFV strains (Haslwanter et al. 2021). This leads to the concern over a potential breakthrough of protective immunity elicited by the 17D vaccine in South America. However, it is clear the 17D vaccine is effective in controlling outbreaks of wt YFV in tropical South America and provides protection against other strains of South America I and II genotypes due to lowering the incidence of disease (Campi-Azevedo et al. 2019). Indeed, mAb-29 and mAb-32 neutralize South America II genotype as effectively as West Africa I genotype (**Table 3.2**). Mab-29 also reached $PRNT_{50}$ titer at 176 ng/ml against South America I genotype. The evidence presented in this study suggests that YFV type-specific neutralizing antibody responses elicited by the 17D vaccine can remain effective against both South America I and South America II genotypes of wt YFV.

## 6.3 Similarity of YFV and other flavivirus type-specific neutralizing epitopes

This work also highlighted both human anti-YFV mAbs recognize antigenic structures encompassing multiple domains of the E protein. Antibody-mediated neutralization of wt YFV in humans involves conformational epitopes in the E protein. It is highly likely that the divergent E protein sequences among different genotypes of wt YFV can alter the presentation of some neutralizing epitopes, leading to the differential neutralization potency of each mAb observed in this study. This finding is not unique to YFV as other flavivirus type-specific neutralizing epitopes recognized by human antibodies are known to constitute residues that encompass multiple domains of the E protein. Many neutralizing antibodies target conformational, surface-exposed epitopes that are accessible only on the intact virion and not soluble proteins

(VanBlargan, Goo, and Pierson 2016). Presentations of type-specific neutralizing epitopes can often be altered due to the amino acid divergence in the E protein among different genotypes of respective flaviviruses. Specific examples of intergenotype variation in the antibody-mediated neutralization are summarized below:

***Type-specific neutralizing epitopes in dengue virus.*** The phylogenetic examination of six DENV serotype 2 (DENV-2) genotypes identified up to a 6% genetic divergence in the E gene (Twiddy et al. 2002). The genetic differences are translated to the differential neutralization of potency of mAbs and polyclonal sera against different genotypes of DENV-2 (Martinez et al. 2020). The molecular basis for the intergenotype variation in antibody-mediated neutralization of DENV-2 has been further elucidated. A comparison of neutralizing epitopes of human mAbs raised reveals different presentations of antigenic structures in the E protein among different genotypes of DENV-2. Nivarthi *et al.* reported three of the four DENV-2 type-specific human mAbs, including mAbs 1662, 1671, and 1628, isolated from two individuals challenged with the attenuated rDEN2Δ30/Tonga/74 strain of the American genotype recognize quaternary epitopes in the E protein (Nivarthi et al. 2019). The DENV-2 type-specific neutralizing epitopes identified in this study mainly consist of amino acid residues in the EDI and/or EDII as none of the mAbs were reactive with recombinant EDIII. The epitopes recognized by mAbs 1615, 1662, and 1671 are highly accessible in the Tonga/74 strain, leading to an elevated level of neutralization at low concentrations. The same epitopes are restricted in the DENV-2 Cosmopolitan genotype, resulting in the low neutralization potency of mAbs 1662, 1628, 1615, and 1671 against the DENV-2 isolates from Singapore and Sri Lanka (Martinez et al. 2020). On the contrary, infection with DENV-2 Asian and Cosmopolitan genotypes elicits type-specific neutralizing antibody responses targeting the antigenic structures in the EDI and EDIII (Gallichotte et al.

2018). Human anti-DENV-2 mAb 3F9 raised against the Cosmopolitan genotype recognizes residues in the EDI, whereas human anti-DENV-2 mAb 2D22 and IL12 binds to complex quaternary epitopes that span the EDIII (Gallichotte et al. 2018; Martinez et al. 2020). The epitopes recognized by 3F9 and 2D22 are presented more similarly among different genotypes of DENV-2, as observed with similar $PRNT_{50}$ concentrations within one $\log_{10}$ µl/ml between genotypes (Martinez et al. 2020). Intriguingly, the same residues are also part of the DENV-2 type-specific neutralizing epitopes recognized by mouse mAbs 3H5 and ICL-2 (Pitcher et al. 2012). Both mouse anti-DENV-2 mAbs exhibit similar $PRNT_{50}$ concentrations across different genotypes, confirming the type-specific epitope in DENV-2 EDIII can have little variation in the presentation across different genotypes.

Although much less is known about the intergenotypic variation in the presentation of type-specific neutralizing epitopes among the three other serotypes of DENV, it is apparent that potential neutralizing human mAbs often target interdomain epitopes in the E protein. The potential neutralizing DENV-1 type-specific human mAb 14c10 targets a discontinuous epitope across two adjacent viral E proteins spanning all three domains of the E protein (Teoh et al. 2012). Similarly, the DENV-3 type specific human mAb 5J7 targets the conformational epitope in the EDI-EDII hinge region (de Alwis et al. 2012).

***Type-specific neutralizing epitopes in encephalitic flaviviruses.*** Type-specific neutralizing epitopes also play a significant role in eliciting human antibody responses against encephalitic flaviviruses, as observed with Japanese encephalitis virus (JEV) and WNV. Fernandez *et al*. generated a panel of human mAbs isolated from donors vaccinated with the inactivated JEV vaccine IXIARO (based on a genotype III strain) and characterized them based on the neutralization profile against different JEV genotypes, epitope binding, and protection *in vivo*

(Fernandez et al. 2018). Like the neutralization potency variation observed with the anti-YFV mAbs in this study, two human anti-JEV type-specific mAbs hJEV-69 and hJEV-75 had broad neutralizing potency against multiple JEV genotypes. Epitope characterization mapped mAb-hJEV-69 and mAb-hJEV-75 to conformational epitopes that interact with residues in EDIII or across EDI and EDII, respectively (Fernandez et al. 2018). Likewise, WNV-specific human mAbs CR4348 and CR4354 isolated from B-cells of convalescent patients target conformational epitopes in the E protein (Vogt et al. 2009). MAb CR4348 recognizes residues near the EDII dimer interface (Vogt et al. 2009). MAb CR4354 binds to a discontinuous epitope formed by protein segments at two independent positions from neighboring E molecules resulting in 120 amino acid binding sites (Kaufmann et al. 2010). This conformational epitope consists primarily of residues in EDI and along the EDI-EDII interface of the E protein. Interestingly, when Throsby *et al.* isolated 121 mAbs specific to the E protein of WNV from convalescent patients, the EDIII-targeting mAbs were more neutralizing compared to the EDII-binding mAbs (Throsby et al. 2006). However, only 8% of the total mAbs targeted EDIII whereas 47% of the total mAbs isolated bound to EDII. The more neutralizing antibodies including CR4274, CR4283, CR4271, and CR4353, bound to the same or overlapping conformational epitopes across residues in EDI (Throsby et al. 2006).

Results from this research suggests there are up to two YFV type-specific neutralizing epitopes present in the E protein. Or alternatively, each of the two mAbs recognize part of a large antigenic structure. Neutralizing antibodies involved in the protective immunity against wt YFV also recognize interdomain epitopes in the E protein. Multiple clones of neutralizing antibodies that target different interdomain epitopes collectively contribute to protection, as shown by mAb-

29 and mAb-32 conferring partial protection and binding to amino acids across the EDI and EDII.

## 6.4 Passive protection studies demonstrate the role of neutralizing human anti-YFV mAbs in vaccine protection and the potential application of human anti-YFV mAbs as candidate therapeutic antibodies

This dissertation research utilized a rigorous system to select neutralizing antibodies that are protective *in vivo* using a funnel approach, including outbred mice challenged with the 17D vaccine strain in ABSL-2 to passive protection against wt YFV in an ABSL-3. To our best knowledge, this is the first report of passive protection against viscerotropic disease caused by wt YFV infection by human anti-YFV mAbs raised against the 17D vaccine. The passive protection demonstrated with different mouse models increases the scientific rigor of this study. Anti-YFV mAb-29 and mAb-32 fully protected against neurotropic disease in CD-1 mice using YFV 17D. While neither of the anti-YFV mAbs provided full protection against the wt Asibi strain in the neurotropic or viscerotropic disease models with CD-1 and AG6 mice, respectively, partial protection was achieved by extending the MST and decreasing the tissue viral loads.

The partial protection against wt YFV in both CD-1 and AG6 mice is somewhat anticipated. Watson *et al.* reported that the passive transfer of immune serum from 17D-204 vaccinated AB6 mice to immunologically naïve AB6 mice only conferred partial protection against challenge with wt YFV Angola71 strain at $2x10^4$ PFU (Watson et al. 2016). However, complete protection against wt YFV Angola71 was achieved by transferring both immune sera and CD4+ T cells. This suggests that full protection is less likely to be achieved in the viscerotropic disease mouse model, especially in AG6 mice that lack both type I and type II IFN

receptors. To our best knowledge, no published study has reported full protection against wt YFV by the passive transfer of one single anti-YFV mAb.

Nevertheless, the reduction of tissue viral loads in mice challenged with wt YFV Asibi strain indicates a higher dosage of each mAb is required to achieve full protection. The further investigation of dose response is warranted and will prove that antibody-mediated neutralization is the mechanism of protection against wt YFV infection in humans. Results from this study also have significant implications for the development of human anti-YFV mAbs as candidate therapeutic antibodies. Both mAbs clearly protected against neurotropic disease caused by the 17D vaccine strain and can be evaluated as a candidate treatment for the rare but life-threatening disease caused by YF vaccine associated adverse events. It is important to note that genome sequences of viruses isolated from fatal cases of YF-AVD normally do not differ significantly from seed lot viruses used for manufacturing (von Lindern et al. 2006; de Menezes Martins, da Luz Fernandes Leal, and Homma 2015). Therefore, the two mAbs can potentially neutralize infectious viruses associated with YF-AVD. However, an effective therapeutic antibody against wt YFV infection must neutralize genetically diverse viral strains and show protection by post-exposure passive immunization. This echoes the importance of a dose escalation study in the passive transfer of each mAb and the evaluation of protective efficacy against different genotypes of wt YFV in the near future.

## 6.5 Future directions

Based on the neutralization potency of the human anti-YFV mAbs against multiple genotypes of wt YFV, further investigation of these mAbs against the remaining three genotypes is needed. This would help delineate how all seven genotypes of wt YFV are neutralized by mAbs raised against the 17D vaccine. Since variations in neutralization potency was observed, it

is likely the two mAbs recognize different YFV type-specific neutralizing epitopes or distinct parts of a single YFV type-specific neutralizing epitope. Additional work to generate and isolate neutralization escape mutants can further complement the neutralization tests against different genotypes of wt YFV. Key residues for antibody-mediated neutralization can be analyzed using bioinformatics tools to investigate whether these residues are in the motifs that are presented differently by seven genotypes of wt YFV.

Based on the partial protection observed with mAb-29 and mAb-32 by extending the survival time of AG6 mice and significantly reducing the tissue viral loads compared to the isotype control, and other *in vivo* studies using different flaviviruses, follow on studies evaluating polyclonal protection and dose response is warranted. This would help us understand why the 17D vaccine effectively protects against different genotypes of wt YFV. Even at a lower dose, mAb-29 and mAb-32 afforded partial protection. Therefore, increasing the concentration of the mAbs may provide greater protection against lethal infection in a neurotropic and viscerotropic model of wt YFV infection while still being safe in mice.

Lastly, future studies elucidating if there is a dose-dependent relationship with the human anti-YFV mAbs would indicate if antibody-mediated neutralization is the mechanism of protection of the 17D vaccine. Human mAbs with a high neutralization potency *in vitro* may be passively protective at a lower concentration *in vivo*. This relationship is expected to fluctuate based on the YFV genotype since variations in neutralization potency and passive protection was observed.

Together, findings from this dissertation research help expand our understanding of how human antibodies raised against a single immunization of the 17D vaccine strain can neutralize and protect against wt YFV infection. Two human anti-YFV type-specific mAbs demonstrated a

level of protection in a neurotropic and viscerotropic model of disease in mice, something that has not been previously shown. It was determined that YFV type-specific neutralizing epitopes are important for antibody-mediated neutralization of YFV. The rigorous and sensitive techniques using a funnel approach to assess antibodies in neurotropic and viscerotropic YF disease models will expedite the selection of human mAbs commendable of further testing in a NHP model. Lastly, this research will be important for the development of new YF vaccine candidates and therapeutics.

# References


Adungo, F., F. Yu, D. Kamau, S. Inoue, D. Hayasaka, G. Posadas-Herrera, R. Sang, M. Mwau, and K. Morita. 2016. 'Development and Characterization of Monoclonal Antibodies to Yellow Fever Virus and Application in Antigen Detection and IgM Capture Enzyme-Linked Immunosorbent Assay', *Clin Vaccine Immunol*, 23: 689-97.

Aitken, T. H., W. G. Downs, and R. E. Shope. 1977. 'Aedes aegypti strain fitness for yellow fever virus transmission', *Am J Trop Med Hyg*, 26: 985-9.

Akondy, R. S., M. Fitch, S. Edupuganti, S. Yang, H. T. Kissick, K. W. Li, B. A. Youngblood, H. A. Abdelsamed, D. J. McGuire, K. W. Cohen, G. Alexe, S. Nagar, M. M. McCausland, S. Gupta, P. Tata, W. N. Haining, M. J. McElrath, D. Zhang, B. Hu, W. J. Greenleaf, J. J. Goronzy, M. J. Mulligan, M. Hellerstein, and R. Ahmed. 2017. 'Origin and differentiation of human memory CD8 T cells after vaccination', *Nature*, 552: 362-67.

Akondy, R. S., P. L. Johnson, H. I. Nakaya, S. Edupuganti, M. J. Mulligan, B. Lawson, J. D. Miller, B. Pulendran, R. Antia, and R. Ahmed. 2015. 'Initial viral load determines the magnitude of the human CD8 T cell response to yellow fever vaccination', *Proc Natl Acad Sci U S A*, 112: 3050-5.

Akondy, R. S., N. D. Monson, J. D. Miller, S. Edupuganti, D. Teuwen, H. Wu, F. Quyyumi, S. Garg, J. D. Altman, C. Del Rio, H. L. Keyserling, A. Ploss, C. M. Rice, W. A. Orenstein, M. J. Mulligan, and R. Ahmed. 2009. 'The yellow fever virus vaccine induces a broad and polyfunctional human memory CD8+ T cell response', *J Immunol*, 183: 7919-30.

Ballinger-Crabtree, M. E., and B. R. Miller. 1990. 'Partial nucleotide sequence of South American yellow fever virus strain 1899/81: structural proteins and NS1', *J Gen Virol*, 71 ( Pt 9): 2115-21.

Barban, V., Y. Girerd, M. Aguirre, S. Gulia, F. Pétiard, P. Riou, B. Barrere, and J. Lang. 2007. 'High stability of yellow fever 17D-204 vaccine: a 12-year restrospective analysis of large-scale production', *Vaccine*, 25: 2941-50.

Baroian, O. V., and T. M. Lozinskaia. 1958. '[Some problems of yellow fever epidemiology]', *Vopr Virusol*, 3: 3-11.

Barrett, A. D., and S. Higgs. 2007. 'Yellow fever: a disease that has yet to be conquered', *Annu Rev Entomol*, 52: 209-29.

Barrett, A. D., and T. P. Monath. 2003. 'Epidemiology and ecology of yellow fever virus', *Adv Virus Res*, 61: 291-315.

Barrett, A. D. T., and E. A. Gould. 1986. 'Comparison of Neurovirulence of Different Strains of Yellow Fever Virus in Mice', *Journal of General Virology*, 67: 631-37.

Barrett, A. D. T., A. Pryde, A. R. Medlen, T. N. Ledger, J. E. Whitby, C. A. Gibson, M. DeSilva, D. J. Groves, D. J. Langley, and P. D. Minor. 1989. 'Examination of the envelope glycoprotein of yellow fever vaccine viruses with monoclonal antibodies', *Vaccine*, 7: 333-36.

Barrett, Alan D T. 2020. 'Yellow Fever Vaccine: The Conundrum of 2 Doses, One Dose, or One-Fifth Dose to Induce and Maintain Protective Immunity', *The Journal of Infectious Diseases*, 221: 1922-24.

Bauer, Johannes H, and Alexander F Mahaffv. 1930. 'The Susceptibility of African Monkeys to Yellow Fever', *American Journal of Hygiene*, 12.

Beaty, BJ, and THG Aitken. 1979. 'In vitro transmission of yellow fever virus by geographic strains of Aedes aegypti', *Mosquito News*, 39: 232-38.

Beck, A., R. B. Tesh, T. G. Wood, S. G. Widen, K. D. Ryman, and A. D. Barrett. 2014. 'Comparison of the live attenuated yellow fever vaccine 17D-204 strain to its virulent parental strain Asibi by deep sequencing', *J Infect Dis*, 209: 334-44.

Beck, Andrew S., Thomas G. Wood, Steven G. Widen, Jill K. Thompson, and Alan D. T. Barrett. 2018. 'Analysis By Deep Sequencing of Discontinued Neurotropic Yellow Fever Vaccine Strains', *Scientific Reports*, 8: 13408.

Beck, Andrew, Robert B. Tesh, Thomas G. Wood, Steven G. Widen, Kate D. Ryman, and Alan D. T. Barrett. 2013. 'Comparison of the Live Attenuated Yellow Fever Vaccine 17D-204 Strain to Its Virulent Parental Strain Asibi by Deep Sequencing', *The Journal of Infectious Diseases*, 209: 334-44.

Bradham, C. A., J. Plümpe, M. P. Manns, D. A. Brenner, and C. Trautwein. 1998. 'Mechanisms of hepatic toxicity. I. TNF-induced liver injury', *Am J Physiol*, 275: G387-92.

Brandriss, M. W., J. J. Schlesinger, E. E. Walsh, and M. Briselli. 1986. 'Lethal 17D yellow fever encephalitis in mice. I. Passive protection by monoclonal antibodies to the envelope proteins of 17D yellow fever and dengue 2 viruses', *J Gen Virol*, 67 ( Pt 2): 229-34.

Bredenbeek, P. J., E. A. Kooi, B. Lindenbach, N. Huijkman, C. M. Rice, and W. J. M. Spaan. 2003. 'A stable full-length yellow fever virus cDNA clone and the role of conserved RNA elements in flavivirus replication', *J Gen Virol*, 84: 1261-68.

Bryant, J. E., E. C. Holmes, and A. D. Barrett. 2007. 'Out of Africa: a molecular perspective on the introduction of yellow fever virus into the Americas', *PLoS Pathog*, 3: e75.

Bryant, J. E., P. F. Vasconcelos, R. C. Rijnbrand, J. P. Mutebi, S. Higgs, and A. D. Barrett. 2005. 'Size heterogeneity in the 3' noncoding region of South American isolates of yellow fever virus', *J Virol*, 79: 3807-21.

Bryant, J., H. Wang, C. Cabezas, G. Ramirez, D. Watts, K. Russell, and A. Barrett. 2003. 'Enzootic transmission of yellow fever virus in Peru', *Emerg Infect Dis*, 9: 926-33.

Bryant, Juliet E., and Alan D.T. Barrett. 2003. 'Comparative phylogenies of yellow fever isolates from Peru and Brazil', *FEMS Immunology & Medical Microbiology*, 39: 103-18.

Buckley, A., and E. A. Gould. 1985. 'Neutralization of yellow fever virus studied using monoclonal and polyclonal antibodies', *J Gen Virol*, 66 ( Pt 12): 2523-31.

Bugher, JC. 1951. 'The mammalian Host in Yellow Fever. In: Strode GK, editor. Yellow fever', *GK Mac Graw Hill Book Company Inc, New York*: 299-384.

Calisher, Charles H., Nick Karabatsos, Joel M. Dalrymple, Robert E. Shope, James S. Porterfield, Edwin G. Westaway, and Walter E. Brandt. 1989. 'Antigenic Relationships between Flaviviruses as Determined by Cross-neutralization Tests with Polyclonal Antisera', *Journal of General Virology*, 70: 37-43.

Calvert, Amanda E., Kandice L. Dixon, Joseph Piper, Susan L. Bennett, Brett A. Thibodeaux, Alan D. T. Barrett, John T. Roehrig, and Carol D. Blair. 2016. 'A humanized monoclonal antibody neutralizes yellow fever virus strain 17D-204 in vitro but does not protect a mouse model from disease', *Antiviral Research*, 131: 92-99.

Cammack, N., and E. A. Gould. 1986. 'Topographical analysis of epitope relationships on the envelope glycoprotein of yellow fever 17D vaccine and the wild type Asibi parent virus', *Virology*, 150: 333-41.

Campi-Azevedo, A. C., V. Peruhype-Magalhaes, J. G. Coelho-Dos-Reis, L. R. Antonelli, C. Costa-Pereira, E. Speziali, L. R. Reis, J. A. Lemos, J. G. L. Ribeiro, L. A. Bastos Camacho, M. L. de Sousa Maia, S. M. Barbosa de Lima, M. Simoes, R. de Menezes Martins, A. Homma, L. C. Cota Malaquias, P. L. Tauil, P. F. Costa Vasconcelos, A. P.

Martins Romano, C. M. Domingues, A. Teixeira-Carvalho, O. A. Martins-Filho, and Vaccine Collaborative Group for Studies of Yellow Fever. 2019. '17DD Yellow Fever Revaccination and Heightened Long-Term Immunity in Populations of Disease-Endemic Areas, Brazil', *Emerg Infect Dis*, 25: 1511-21.

Carbaugh, D. L., and H. M. Lazear. 2020. 'Flavivirus Envelope Protein Glycosylation: Impacts on Viral Infection and Pathogenesis', *J Virol*, 94.

Carrington, Christine VF, and Albert J Auguste. 2013. 'Evolutionary and ecological factors underlying the tempo and distribution of yellow fever virus activity', *Infection, Genetics and Evolution*, 13: 198-210.

Chang, GJ, Bruce C Cropp, Richard M Kinney, Dennis W Trent, and Duane J Gubler. 1995. 'Nucleotide sequence variation of the envelope protein gene identifies two distinct genotypes of yellow fever virus', *Journal of Virology*, 69: 5773-80.

Chao, D. Y., B. S. Davis, and G. J. Chang. 2007. 'Development of multiplex real-time reverse transcriptase PCR assays for detecting eight medically important flaviviruses in mosquitoes', *J Clin Microbiol*, 45: 584-9.

Chen, Yaping, Terry Maguire, Ronald E. Hileman, Jonathan R. Fromm, Jeffrey D. Esko, Robert J. Linhardt, and Rory M. Marks. 1997. 'Dengue virus infectivity depends on envelope protein binding to target cell heparan sulfate', *Nature Medicine*, 3: 866-71.

Clarke , D. H. 1960. 'ANTIGENIC ANALYSIS OF CERTAIN GROUP B ARTHROPOD-BORNE VIRUSES BY ANTIBODY ABSORPTION', *Journal of Experimental Medicine*, 111: 21-32.

Collins, Natalie D., Andrew S. Beck, Steven G. Widen, Thomas G. Wood, Stephen Higgs, Alan D. T. Barrett, Mary K. Estes, Carol Blair, and John Mackenzie. 2018. 'Structural and Nonstructural Genes Contribute to the Genetic Diversity of RNA Viruses', *MBio*, 9: e01871-18.

Cong, Y., M. A. McArthur, M. Cohen, P. B. Jahrling, K. B. Janosko, N. Josleyn, K. Kang, T. Zhang, and M. R. Holbrook. 2016. 'Characterization of Yellow Fever Virus Infection of Human and Non-human Primate Antigen Presenting Cells and Their Interaction with CD4+ T Cells', *PLoS neglected tropical diseases*, 10: e0004709.

Cook, S., and E. C. Holmes. 2006. 'A multigene analysis of the phylogenetic relationships among the flaviviruses (Family: Flaviviridae) and the evolution of vector transmission', *Archives of Virology*, 151: 309-25.

Daffis, S., R. E. Kontermann, J. Korimbocus, H. Zeller, H. D. Klenk, and J. Ter Meulen. 2005. 'Antibody responses against wild-type yellow fever virus and the 17D vaccine strain: characterization with human monoclonal antibody fragments and neutralization escape variants', *Virology*, 337: 262-72.

Daffis, Stephane, Kristy J. Szretter, Jill Schriewer, Jianqing Li, Soonjeon Youn, John Errett, Tsai-Yu Lin, Stewart Schneller, Roland Zust, Hongping Dong, Volker Thiel, Ganes C. Sen, Volker Fensterl, William B. Klimstra, Theodore C. Pierson, R. Mark Buller, Michael Gale, Jr., Pei-Yong Shi, and Michael S. Diamond. 2010. '2'-O methylation of the viral mRNA cap evades host restriction by IFIT family members', *Nature*, 468: 452-56.

Davis, Emily H., and Alan D. T. Barrett. 2020. 'Structure–Function of the Yellow Fever Virus Envelope Protein: Analysis of Antibody Epitopes', *Viral Immunology*, 33: 12-21.

Davis, Emily H., Jill K. Thompson, Steven G. Widen, and Alan D. T. Barrett. 2021. 'Genome Characterization of Yellow Fever Virus Wild-Type Strain Asibi, Parent to Live-Attenuated 17D Vaccine, from Three Different Sources', *Viruses*, 13: 1383.

Davis, N. C., and A. W. Burke. 1929. 'STUDIES ON SOUTH AMERICAN YELLOW FEVER : I. THE STRAINS OF VIRUS IN USE AT THE YELLOW FEVER LABORATORY IN BAHIA, BRAZIL', *Journal of Experimental Medicine*, 49: 975-84.

de Alwis, R., S. A. Smith, N. P. Olivarez, W. B. Messer, J. P. Huynh, W. M. Wahala, L. J. White, M. S. Diamond, R. S. Baric, J. E. Crowe, Jr., and A. M. de Silva. 2012. 'Identification of human neutralizing antibodies that bind to complex epitopes on dengue virions', *Proc Natl Acad Sci U S A*, 109: 7439-44.

De Brito, T., S. A. Siqueira, R. T. Santos, E. S. Nassar, T. L. Coimbra, and V. A. Alves. 1992. 'Human fatal yellow fever. Immunohistochemical detection of viral antigens in the liver, kidney and heart', *Pathol Res Pract*, 188: 177-81.

de Filippis, A.M.B., R.M.R. Nogueira, H.G. Schatzmayr, D.S. Tavares, A.V. Jabor, S.C.M. Diniz, J.C. Oliveira, E. Moreira, M.P. Miagostovich, E.V. Costa, and R. Galler. 2002. 'Outbreak of jaundice and hemorrhagic fever in the Southeast of Brazil in 2001: Detection and molecular characterization of yellow fever virus', *Journal of Medical Virology*, 68: 620-27.

de Menezes Martins, Reinaldo, Maria da Luz Fernandes Leal, and Akira Homma. 2015. 'Serious adverse events associated with yellow fever vaccine', *Human Vaccines & Immunotherapeutics*, 11: 2183-87.

Degallier, Nicolas, Amelia Travassos da Rosa, Jean-Pierre Hervé, J. F. S. Rosa, Pedro Vasconcelos, C. J. Silva, V. L. R. S. Barros, L. B. Dias, E. S. Rosa, and S. Rodrigues. 1992. 'A comparative study of yellow fever in Africa and South America'.

DeKosky, Brandon J., Gregory C. Ippolito, Ryan P. Deschner, Jason J. Lavinder, Yariv Wine, Brandon M. Rawlings, Navin Varadarajan, Claudia Giesecke, Thomas Dörner, Sarah F. Andrews, Patrick C. Wilson, Scott P. Hunicke-Smith, C. Grant Willson, Andrew D. Ellington, and George Georgiou. 2013. 'High-throughput sequencing of the paired human immunoglobulin heavy and light chain repertoire', *Nature Biotechnology*, 31: 166-69.

Deubel, V., J. P. Digoutte, T. P. Monath, and M. Girard. 1986. 'Genetic heterogeneity of yellow fever virus strains from Africa and the Americas', *J Gen Virol*, 67 ( Pt 1): 209-13.

Douam, F., and A. Ploss. 2018. 'Yellow Fever Virus: Knowledge Gaps Impeding the Fight Against an Old Foe', *Trends Microbiol*, 26: 913-28.

Elvidge, Suzanne. 2020. 'Developing the 17D yellow fever vaccine', *Nature Milestones*: S11.

Engelmann, F., L. Josset, T. Girke, B. Park, A. Barron, J. Dewane, E. Hammarlund, A. Lewis, M. K. Axthelm, M. K. Slifka, and I. Messaoudi. 2014. 'Pathophysiologic and transcriptomic analyses of viscerotropic yellow fever in a rhesus macaque model', *PLoS neglected tropical diseases*, 8: e3295.

Erickson, Andrea K., and Julie K. Pfeiffer. 2013. 'Dynamic viral dissemination in mice infected with yellow fever virus strain 17D', *Journal of Virology*, 87: 12392-97.

———. 2015. 'Spectrum of disease outcomes in mice infected with YFV-17D', *The Journal of general virology*, 96: 1328-39.

Falgout, B., M. Pethel, Y. M. Zhang, and C. J. Lai. 1991. 'Both nonstructural proteins NS2B and NS3 are required for the proteolytic processing of dengue virus nonstructural proteins', *J Virol*, 65: 2467-75.

Faye, M., N. Zein, C. Loucoubar, M. Weidmann, O. Faye, M. D. P. Cunha, P. M. A. Zanotto, A. Alpha Sall, and O. Faye. 2020. 'Biological Characteristics and Patterns of Codon Usage Evolution for the African Genotype Zika Virus', *Viruses*, 12.

Fernandez, E., N. Kose, M. A. Edeling, J. Adhikari, G. Sapparapu, S. M. Lazarte, C. A. Nelson, J. Govero, M. L. Gross, D. H. Fremont, J. E. Crowe, Jr., and M. S. Diamond. 2018. 'Mouse and Human Monoclonal Antibodies Protect against Infection by Multiple Genotypes of Japanese Encephalitis Virus', *MBio*, 9.

Ferreira, Clarissa de Castro, Ana Carolina Campi-Azevedo, Vanessa Peruhype-Magalhães, Christiane Costa-Pereira, Cleandro Pires de Albuquerque, Luciana Feitosa Muniz, Talita Yokoy de Souza, Ana Cristina Vanderley Oliveira, Olindo Assis Martins-Filho, and Licia Maria Henrique da Mota. 2018. 'The 17D-204 and 17DD yellow fever vaccines: an overview of major similarities and subtle differences', *Expert review of vaccines*, 17: 79-90.

Findlay, GM, and Ruby O Stern. 1935. 'The Essential Neurotropism of the Yellow Fever Virus', *Journal of Pathology and Bacteriology*, 41.

Finlay, CJ. 1912. 'Trabajos Selectos'.

Fitzgeorge, R., and C. J. Bradish. 1980. 'The In Vivo Differentiation of Strains of Yellow Fever Virus in Mice', *Journal of General Virology*, 46: 1-13.

Fox, John P, and Henrique A Penna. 1943. 'Behavior of 17D Yellow Fever Virus in Rhesus Monkeys. Relation to Substrain, Dose, and Neural or Extraneural Inoculation', *American Journal of Hygiene*, 38: 152-72.

Frierson, J. Gordon. 2010. 'The yellow fever vaccine: a history', *The Yale journal of biology and medicine*, 83: 77-85.

Furuichi, Yasuhiro, Alba LaFiandra, and Aaron J. Shatkin. 1977. '5′-Terminal structure and mRNA stability', *Nature*, 266: 235-39.

Gallichotte, Emily N., Thomas J. Baric, Boyd L. Yount, Jr., Douglas G. Widman, Anna Durbin, Steve Whitehead, Ralph S. Baric, and Aravinda M. de Silva. 2018. 'Human dengue virus serotype 2 neutralizing antibodies target two distinct quaternary epitopes', *PLOS Pathogens*, 14: e1006934-e34.

Gaythorpe, Katy A. M., Arran Hamlet, Kévin Jean, Daniel Garkauskas Ramos, Laurence Cibrelus, Tini Garske, and Neil Ferguson. 2021. 'The global burden of yellow fever', *Elife*, 10: e64670.

Germain, M., D. B. Francy, T. P. Monath, L. Ferrara, J. Bryan, J.-J. Salaun, G. Heme, J. Renaudet, C. Adam, and J.-P. Digoutte. 1980. 'Yellow Fever in the Gambia, 1978–1979: Entomological Aspects and Epidemiological Correlations', *Am J Trop Med Hyg*, 29: 929-40.

Gershman, M.D., J.E Staples. 2021. 'CH4 Yellow fever in US Centers for Disease Control and Prevention', *Yellow book*.

Gibney, Katherine B., Srilatha Edupuganti, Amanda J. Panella, Olga I. Kosoy, Mark J. Delorey, Robert S. Lanciotti, Mark J. Mulligan, Marc Fischer, and J. Erin Staples. 2012. 'Detection of anti-yellow fever virus immunoglobulin m antibodies at 3-4 years following yellow fever vaccination', *Am J Trop Med Hyg*, 87: 1112-15.

Gould, E. A., A. Buckley, A. D. Barrett, and N. Cammack. 1986. 'Neutralizing (54K) and non-neutralizing (54K and 48K) monoclonal antibodies against structural and non-structural yellow fever virus proteins confer immunity in mice', *J Gen Virol*, 67 ( Pt 3): 591-5.

Gould, E. A., A. Buckley, N. Cammack, A. D. Barrett, J. C. Clegg, R. Ishak, and M. G. Varma. 1985. 'Examination of the immunological relationships between flaviviruses using yellow fever virus monoclonal antibodies', *J Gen Virol*, 66 ( Pt 7): 1369-82.

Gould, E. A., A. Buckley, P. A. Cane, S. Higgs, and N. Cammack. 1989. 'Use of a Monoclonal Antibody Specific for Wild-type Yellow Fever Virus to Identify a Wild-type Antigenic Variant in 17D Vaccine Pools', *Journal of General Virology*, 70: 1889-94.

Groot, H. 1962. 'Serological reactions in Rhesus monkeys inoculated with the 17D strain of yellow fever virus', *Bull World Health Organ*, 27: 709-15.

Groot, H., and R. B. Riberiro. 1962. 'Neutralizing and haemagglutination-inhibiting antibodies to yellow fever 17 years after vaccination with 17D vaccine', *Bull World Health Organ*, 27: 699-707.

Hahn, C. S., J. M. Dalrymple, J. H. Strauss, and C. M. Rice. 1987. 'Comparison of the virulent Asibi strain of yellow fever virus with the 17D vaccine strain derived from it', *Proc Natl Acad Sci U S A*, 84: 2019-23.

Harrison, Stephen C. 2008. 'Viral membrane fusion', *Nat Struct Mol Biol*, 15: 690-98.

Haslwanter, Denise, Gorka Lasso, Anna Z. Wec, Nathália Dias Furtado, Lidiane Menezes Souza Raphael, Yan Sun, Stephanie Stransky, Núria Pedreño-Lopez, Alexandra Tse, Carolina Argondizo Correia, Zachary A. Bornholdt, Mrunal Sakharkar, Vivian I. Avelino-Silva, Crystal L. Moyer, David I. Watkins, Esper G. Kallas, Simone Sidoli, Laura M. Walker, Myrna C. Bonaldo, and Kartik Chandran. 2021. 'Genotype-specific Features Reduce the Susceptibility of South American Yellow Fever Virus Strains to Vaccine-Induced Antibodies', *bioRxiv*: 2021.08.22.457235.

Hindle, E. 1932. 'Yellow Fever: an Epidemiological and Historical Study of its Place of Origin', *Nature*, 130: 646-47.

Hombach, Joachim, Tom Solomon, Ichiro Kurane, Julie Jacobson, and David Wood. 2005. 'Report on a WHO consultation on immunological endpoints for evaluation of new Japanese encephalitis vaccines, WHO, Geneva, 2–3 September, 2004', *Vaccine*, 23: 5205-11.

Huang, Claire Y. H., Shawn J. Silengo, Melissa C. Whiteman, and Richard M. Kinney. 2005. 'Chimeric dengue 2 PDK-53/West Nile NY99 viruses retain the phenotypic attenuation markers of the candidate PDK-53 vaccine virus and protect mice against lethal challenge with West Nile virus', *Journal of Virology*, 79: 7300-10.

Hudson, N. P. 1928. 'The Pathology of Experimental Yellow Fever in the Macacus Rhesus: III. Comparison with the Pathology of Yellow Fever in Man', *The American journal of pathology*, 4: 419-30.9.

Hudson , N. Paul, and Cornelius B. Philip 1929. 'INFECTIVITY OF BLOOD DURING THE COURSE OF EXPERIMENTAL YELLOW FEVER', *Journal of Experimental Medicine*, 50: 583-99.

Igarashi, A. 1978. 'Isolation of a Singh's Aedes albopictus cell clone sensitive to Dengue and Chikungunya viruses', *J Gen Virol*, 40: 531-44.

James, Eddie A., Rebecca E. LaFond, Theresa J. Gates, Duy T. Mai, Uma Malhotra, and William W. Kwok. 2013. 'Yellow fever vaccination elicits broad functional CD4+ T cell responses that recognize structural and nonstructural proteins', *Journal of Virology*, 87: 12794-804.

Jennings, AD, CA Gibson, BR Miller, JH Mathews, CJ Mitchell, JT Roehrig, DJ Wood, F Taffs, BK Sil, and SN Whitby. 1994. 'Analysis of a yellow fever virus isolated from a fatal case of vaccine-associated human encephalitis', *Journal of Infectious Diseases*, 169: 512-18.

Julander, J. G., B. A. Thibodeaux, J. D. Morrey, J. T. Roehrig, and C. D. Blair. 2014. 'Humanized monoclonal antibody 2C9-cIgG has enhanced efficacy for yellow fever prophylaxis and therapy in an immunocompetent animal model', *Antiviral Res*, 103: 32-8.

Julander, Justin G., Dennis W. Trent, and Thomas P. Monath. 2011. 'Immune correlates of protection against yellow fever determined by passive immunization and challenge in the hamster model', *Vaccine*, 29: 6008-16.

Kato, H., O. Takeuchi, S. Sato, M. Yoneyama, M. Yamamoto, K. Matsui, S. Uematsu, A. Jung, T. Kawai, K. J. Ishii, O. Yamaguchi, K. Otsu, T. Tsujimura, C. S. Koh, C. Reis e Sousa, Y. Matsuura, T. Fujita, and S. Akira. 2006. 'Differential roles of MDA5 and RIG-I helicases in the recognition of RNA viruses', *Nature*, 441: 101-5.

Kaufmann, B., M. R. Vogt, J. Goudsmit, H. A. Holdaway, A. A. Aksyuk, P. R. Chipman, R. J. Kuhn, M. S. Diamond, and M. G. Rossmann. 2010. 'Neutralization of West Nile virus by cross-linking of its surface proteins with Fab fragments of the human monoclonal antibody CR4354', *Proc Natl Acad Sci U S A*, 107: 18950-5.

Kaufmann, Bärbel, and Michael G. Rossmann. 2011. 'Molecular mechanisms involved in the early steps of flavivirus cell entry', *Microbes Infect*, 13: 1-9.

Kleinert, Robin D.V., Eduardo Montoya-Diaz, Tanvi Khera, Kathrin Welsch, Birthe Tegtmeyer, Sebastian Hoehl, Sandra Ciesek, and Richard J.P. Brown. 2019. 'Yellow Fever: Integrating Current Knowledge with Technological Innovations to Identify Strategies for Controlling a Re-Emerging Virus', *Viruses*, 11: 960.

Klotz, O., and T. H. Belt. 1930. 'The Pathology of the Liver in Yellow Fiver', *The American journal of pathology*, 6: 663-88.1.

Konishi, E., and P. W. Mason. 1993. 'Proper maturation of the Japanese encephalitis virus envelope glycoprotein requires cosynthesis with the premembrane protein', *J Virol*, 67: 1672-5.

Koonin, Eugene V. 1991. 'The phylogeny of RNA-dependent RNA polymerases of positive-strand RNA viruses', *Journal of General Virology*, 72: 2197-206.

Kuhn, R. J., W. Zhang, M. G. Rossmann, S. V. Pletnev, J. Corver, E. Lenches, C. T. Jones, S. Mukhopadhyay, P. R. Chipman, E. G. Strauss, T. S. Baker, and J. H. Strauss. 2002. 'Structure of dengue virus: implications for flavivirus organization, maturation, and fusion', *Cell*, 108: 717-25.

Kümmerer, Beate M, and Charles M Rice. 2002. 'Mutations in the yellow fever virus nonstructural protein NS2A selectively block production of infectious particles', *Journal of Virology*, 76: 4773-84.

Lam, L. K. Metthew, Alan M. Watson, Kate D. Ryman, and William B. Klimstra. 2018. 'Gamma-interferon exerts a critical early restriction on replication and dissemination of yellow fever virus vaccine strain 17D-204', *npj Vaccines*, 3: 5-5.

Lataillade, Lucy de Guilhem de, Marie Vazeille, Thomas Obadia, Yoann Madec, Laurence Mousson, Basile Kamgang, Chun-Hong Chen, Anna-Bella Failloux, and Pei-Shi Yen. 2020. 'Risk of yellow fever virus transmission in the Asia-Pacific region', *Nature Communications*, 11: 5801.

Lazear, Helen M., Timothy J. Nice, and Michael S. Diamond. 2015. 'Interferon-λ: Immune Functions at Barrier Surfaces and Beyond', *Immunity*, 43: 15-28.

Lee, E., and M. Lobigs. 2008. 'E protein domain III determinants of yellow fever virus 17D vaccine strain enhance binding to glycosaminoglycans, impede virus spread, and attenuate virulence', *J Virol*, 82: 6024-33.

Lennette, Edwin H., and Alina Perlowagora. 1943. 'The Complement Fixation Test in the Diagnosis of Yellow Fever: Use of Infectious Mouse Brain as Antigen', *The American Journal of Tropical Medicine*, s1-23: 481-504.

Lepiniec, L., L. Dalgarno, V. T. Huong, T. P. Monath, J. P. Digoutte, and V. Deubel. 1994. 'Geographic distribution and evolution of yellow fever viruses based on direct sequencing of genomic cDNA fragments', *J Gen Virol*, 75 ( Pt 2): 417-23.

Li, H., S. Clum, S. You, K. E. Ebner, and R. Padmanabhan. 1999. 'The serine protease and RNA-stimulated nucleoside triphosphatase and RNA helicase functional domains of dengue virus type 2 NS3 converge within a region of 20 amino acids', *J Virol*, 73: 3108-16.

Li, W., and M. A. Brinton. 2001. 'The 3' stem loop of the West Nile virus genomic RNA can suppress translation of chimeric mRNAs', *Virology*, 287: 49-61.

Lima, T. M., M. O. Souza, and L. R. Castilho. 2019. 'Purification of flavivirus VLPs by a two-step chomatographic process', *Vaccine*, 37: 7061-69.

Liprandi, F. 1981. 'Isolation of plaque variants differing in virulence from the 17D strain of yellow fever virus', *J Gen Virol*, 56: 363-70.

Lloyd, Wray, and AF Mahaffy. 1936. 'Yellow fever virus encephalitis in African and Asiatic monkeys', *Am J Trop Med Hyg*, 1: 73-75.

Lloyd, Wray, Max Theiler, and N.I. Ricci. 1936. 'Modification of the virulence of yellow fever virus by cultivation in tissues in vitro', *Transactions of the Royal Society of Tropical Medicine and Hygiene*, 29: 481-529.

Lobigs, M., L. Dalgarno, J. J. Schlesinger, and R. C. Weir. 1987. 'Location of a neutralization determinant in the E protein of yellow fever virus (17D vaccine strain)', *Virology*, 161: 474-78.

Loo, Yueh-Ming, Jamie Fornek, Nanette Crochet, Gagan Bajwa, Olivia Perwitasari, Luis Martinez-Sobrido, Shizuo Akira, Michelle A. Gill, Adolfo García-Sastre, Michael G. Katze, and Michael Gale, Jr. 2008. 'Distinct RIG-I and MDA5 signaling by RNA viruses in innate immunity', *Journal of Virology*, 82: 335-45.

Lu, X., H. Xiao, S. Li, X. Pang, J. Song, S. Liu, H. Cheng, Y. Li, X. Wang, C. Huang, T. Guo, J. Ter Meulen, S. Daffis, J. Yan, L. Dai, Z. Rao, H. D. Klenk, J. Qi, Y. Shi, and G. F. Gao. 2019. 'Double Lock of a Human Neutralizing and Protective Monoclonal Antibody Targeting the Yellow Fever Virus Envelope', *Cell Rep*, 26: 438-46.e5.

Macdonald, Joanne, Jessica Tonry, Roy A. Hall, Brent Williams, Gustavo Palacios, Mundrigi S. Ashok, Omar Jabado, David Clark, Robert B. Tesh, Thomas Briese, and W. Ian Lipkin. 2005. 'NS1 protein secretion during the acute phase of West Nile virus infection', *Journal of Virology*, 79: 13924-33.

Macnamara, F. N. 1953. 'Reactions following neurotropic yellow fever vaccine given by scarification in Nigeria', *Trans R Soc Trop Med Hyg*, 47: 199-208.

Mares-Guia, Maria Angélica Monteiro de Mello, Marco A. Horta, Alessandro Romano, Cíntia D. S. Rodrigues, Marcos C. L. Mendonça, Carolina C. dos Santos, Maria C. Torres, Eliane S. M. Araujo, Allison Fabri, Everton R. de Souza, Roberta O. R. Ribeiro, Fabiana P. Lucena, Luiz C. A. Junior, Rivaldo V. da Cunha, Rita M. R. Nogueira, Patricia C. Sequeira, and Ana M. Bispo de Filippis. 2020. 'Yellow fever epizootics in non-human primates, Southeast and Northeast Brazil (2017 and 2018)', *Parasites & Vectors*, 13: 90.

Marfin, A. A., and T. P. Monath. 2008. 'Yellow Fever Virus.' in Brian W. J. Mahy and Marc H. V. Van Regenmortel (eds.), *Encyclopedia of Virology (Third Edition)* (Academic Press: Oxford).

Martinez, David R., Boyd Yount, Usha Nivarthi, Jennifer E. Munt, Matthew J. Delacruz, Stephen S. Whitehead, Anna P. Durbin, Aravinda M. de Silva, and Ralph S. Baric. 2020. 'Antigenic Variation of the Dengue Virus 2 Genotypes Impacts the Neutralization Activity of Human Antibodies in Vaccinees', *Cell Reports*, 33: 108226.

Mason, R. A., N. M. Tauraso, R. O. Spertzel, and R. K. Ginn. 1973. 'Yellow fever vaccine: direct challenge of monkeys given graded doses of 17D vaccine', *Appl Microbiol*, 25: 539-44.

McArthur, Monica A., Miguel T. Suderman, John-Paul Mutebi, Shu-Yuan Xiao, and Alan D. T. Barrett. 2003. 'Molecular characterization of a hamster viscerotropic strain of yellow fever virus', *Journal of Virology*, 77: 1462-68.

McArthur, Monica A., Shuliu L. Zhang, Li Li, Robert B. Tesh, and Alan D. T. Barrett. 2020. 'Molecular Characterization of Hamster-Adapted Yellow Fever Virus', *Vector Borne Zoonotic Dis*, 20: 222-27.

McElroy, K. L., Y. A. Girard, C. E. McGee, K. A. Tsetsarkin, D. L. Vanlandingham, and S. Higgs. 2008. 'Characterization of the antigen distribution and tissue tropisms of three phenotypically distinct yellow fever virus variants in orally infected Aedes aegypti mosquitoes', *Vector Borne Zoonotic Dis*, 8: 675-87.

McElroy, K. L., K. A. Tsetsarkin, D. L. Vanlandingham, and S. Higgs. 2005. 'Characterization of an infectious clone of the wild-type yellow fever virus Asibi strain that is able to infect and disseminate in mosquitoes', *J Gen Virol*, 86: 1747-51.

McElroy, Kate L., Konstantin A. Tsetsarkin, Dana L. Vanlandingham, and Stephen Higgs. 2006. 'Role of the yellow fever virus structural protein genes in viral dissemination from the Aedes aegypti mosquito midgut', *Journal of General Virology*, 87: 2993-3001.

Meertens, L., X. Carnec, M. P. Lecoin, R. Ramdasi, F. Guivel-Benhassine, E. Lew, G. Lemke, O. Schwartz, and A. Amara. 2012. 'The TIM and TAM families of phosphatidylserine receptors mediate dengue virus entry', *Cell Host Microbe*, 12: 544-57.

Meier, K. C., C. L. Gardner, M. V. Khoretonenko, W. B. Klimstra, and K. D. Ryman. 2009. 'A mouse model for studying viscerotropic disease caused by yellow fever virus infection', *PLoS Pathog*, 5: e1000614.

Melo-Lima, B. L., D. L. Espósito, B. A. da Fonseca, L. T. Figueiredo, P. Moreau, and E. A. Donadi. 2015. 'The Attenuated Live Yellow Fever Virus 17D Infects the Thymus and Induces Thymic Transcriptional Modifications of Immunomodulatory Genes in C57BL/6 and BALB/C Mice', *Autoimmune Dis*, 2015: 503087.

Méndez, M. R., C. H. Calisher, H. Kruger, F. Sipan, S. Sánchez, and J. S. Lazuick. 1984. 'A continuing focus of yellow fever in the Apurimac River Valley, Ayacucho, Peru, and the first isolation of yellow fever virus in that country', *Bull Pan Am Health Organ*, 18: 172-9.

Miller, B. R., T. P. Monath, W. J. Tabachnick, and V. I. Ezike. 1989. 'Epidemic yellow fever caused by an incompetent mosquito vector', *Trop Med Parasitol*, 40: 396-9.

Ministry of Health, Government of Kenya. 1996. 'Field Guide for Yellow Fever Surveillance', *Nairobi, Kenya*.

Mishra, N., R. Boudewijns, M. A. Schmid, R. E. Marques, S. Sharma, J. Neyts, and K. Dallmeier. 2020. 'A Chimeric Japanese Encephalitis Vaccine Protects against Lethal Yellow Fever Virus Infection without Inducing Neutralizing Antibodies', *MBio*, 11.

Monath, T. P. 1971. 'Neutralizing antibody responses in the major immunoglobulin classes to yellow fever 17D vaccination of humans', *Am J Epidemiol*, 93: 122-9.

———. 1999a. 'Facing up to re-emergence of urban yellow fever', *Lancet*, 353: 1541.

———. 2001. 'Yellow fever: an update', *Lancet Infect Dis*, 1: 11-20.
Monath, T. P., K. R. Brinker, F. W. Chandler, G. E. Kemp, and C. B. Cropp. 1981. 'Pathophysiologic correlations in a rhesus monkey model of yellow fever with special observations on the acute necrosis of B cell areas of lymphoid tissues', *Am J Trop Med Hyg*, 30: 431-43.
Monath, T. P., R. B. Craven, D. J. Muth, C. J. Trautt, C. H. Calisher, and S. A. Fitzgerald. 1980. 'Limitations of the complement-fixation test for distinguishing naturally acquired from vaccine-induced yellow fever infection in flavivirus-hyperendemic areas', *Am J Trop Med Hyg*, 29: 624-34.
Monath, T. P., I. Levenbook, K. Soike, Z. X. Zhang, M. Ratterree, K. Draper, A. D. Barrett, R. Nichols, R. Weltzin, J. Arroyo, and F. Guirakhoo. 2000. 'Chimeric yellow fever virus 17D-Japanese encephalitis virus vaccine: dose-response effectiveness and extended safety testing in rhesus monkeys', *Journal of Virology*, 74: 1742-51.
Monath, Thomas P. 1987. 'Yellow Fever: A Medically Neglected Disease. Report on a Seminar', *Reviews of Infectious Diseases*, 9: 165-75.
———. 1999b. 'YELLOW FEVER VIRUS (FLAVIVIRIDAE).' in Allan Granoff and Robert G. Webster (eds.), *Encyclopedia of Virology (Second Edition)* (Elsevier: Oxford).
Monath, Thomas P., Mark Gershman, J. Erin Staples, and Alan D. T. Barrett. 2013. '38 - Yellow fever vaccine.' in Stanley A. Plotkin, Walter A. Orenstein and Paul A. Offit (eds.), *Vaccines (Sixth Edition)* (W.B. Saunders: London).
Muñoz-Jordán, Jorge L., Gilma G. Sánchez-Burgos, Maudry Laurent-Rolle, and Adolfo García-Sastre. 2003. 'Inhibition of interferon signaling by dengue virus', *Proceedings of the National Academy of Sciences*, 100: 14333-38.
Mutebi, J. P., and A. D. Barrett. 2002. 'The epidemiology of yellow fever in Africa', *Microbes Infect*, 4: 1459-68.
Mutebi, J. P., R. C. Rijnbrand, H. Wang, K. D. Ryman, E. Wang, L. D. Fulop, R. Titball, and A. D. Barrett. 2004. 'Genetic relationships and evolution of genotypes of yellow fever virus and other members of the yellow fever virus group within the Flavivirus genus based on the 3' noncoding region', *J Virol*, 78: 9652-65.
Mutebi, J. P., H. Wang, L. Li, J. E. Bryant, and A. D. Barrett. 2001. 'Phylogenetic and evolutionary relationships among yellow fever virus isolates in Africa', *J Virol*, 75: 6999-7008.
Nasirudeen, A. M. A., Hui Hui Wong, Peiling Thien, Shengli Xu, Kong-Peng Lam, and Ding Xiang Liu. 2011. 'RIG-I, MDA5 and TLR3 synergistically play an important role in restriction of dengue virus infection', *PLoS neglected tropical diseases*, 5: e926-e26.
Neves, P. C., D. C. Matos, R. Marcovistz, and R. Galler. 2009. 'TLR expression and NK cell activation after human yellow fever vaccination', *Vaccine*, 27: 5543-9.
Nivarthi, Usha K., Huy A. Tu, Matthew J. Delacruz, Jesica Swanstrom, Bhumi Patel, Anna P. Durbin, Stephen S. Whitehead, Kristen K. Pierce, Beth D. Kirkpatrick, Ralph S. Baric, Ngan Nguyen, Daniel E. Emerling, Aravinda M. de Silva, and Sean A. Diehl. 2019. 'Longitudinal analysis of acute and convalescent B cell responses in a human primary dengue serotype 2 infection model', *EBioMedicine*, 41: 465-78.
Oliphant, T., G. E. Nybakken, S. K. Austin, Q. Xu, J. Bramson, M. Loeb, M. Throsby, D. H. Fremont, T. C. Pierson, and M. S. Diamond. 2007. 'Induction of epitope-specific neutralizing antibodies against West Nile virus', *J Virol*, 81: 11828-39.

Park, S. L., Y. S. Huang, A. C. Lyons, V. B. Ayers, S. M. Hettenbach, D. S. McVey, K. R. Burton, S. Higgs, and D. L. Vanlandingham. 2018. 'North American domestic pigs are susceptible to experimental infection with Japanese encephalitis virus', *Sci Rep*, 8: 7951.

Peltier, M. G. 1947. 'Yellow Fever Vaccination, Simple or Associated with Vaccination Against Smallpox, of the Populations of French West Africa by the Method of the Pasteur Institute of Dakar', *American journal of public health and the nation's health*, 37: 1026-32.

Pierson, Theodore C., Qing Xu, Steevenson Nelson, Theodore Oliphant, Grant E. Nybakken, Daved H. Fremont, and Michael S. Diamond. 2007. 'The stoichiometry of antibody-mediated neutralization and enhancement of West Nile virus infection', *Cell Host & Microbe*, 1: 135-45.

Pitcher, Trevor J., Gregory D. Gromowski, David W. C. Beasley, and Alan D. T. Barrett. 2012. 'Conservation of the DENV-2 type-specific and DEN complex-reactive antigenic sites among DENV-2 genotypes', *Virology*, 422: 386-92.

Post, Paulo R., Claudia N. D. Santos, Ricardo Carvalho, Ana C. R. Cruz, Charles M. Ricet, and Ricardo Galler. 1992. 'Heterogeneity in envelope protein sequence and N-Linked glycosylation among yellow fever virus vaccine strains', *Virology*, 188: 160-67.

Quaresma, J. A., V. L. Barros, E. R. Fernandes, C. Pagliari, C. Takakura, P. F. da Costa Vasconcelos, H. F. de Andrade, Jr., and M. I. Duarte. 2005. 'Reconsideration of histopathology and ultrastructural aspects of the human liver in yellow fever', *Acta Trop*, 94: 116-27.

Quaresma, J. A., V. L. Barros, C. Pagliari, E. R. Fernandes, H. F. Andrade, Jr., P. F. Vasconcelos, and M. I. Duarte. 2007. 'Hepatocyte lesions and cellular immune response in yellow fever infection', *Trans R Soc Trop Med Hyg*, 101: 161-8.

Quaresma, J. A., V. L. Barros, C. Pagliari, E. R. Fernandes, F. Guedes, C. F. Takakura, H. F. Andrade, Jr., P. F. Vasconcelos, and M. I. Duarte. 2006. 'Revisiting the liver in human yellow fever: virus-induced apoptosis in hepatocytes associated with TGF-beta, TNF-alpha and NK cells activity', *Virology*, 345: 22-30.

Quaresma, J. A., M. I. Duarte, and P. F. Vasconcelos. 2006. 'Midzonal lesions in yellow fever: a specific pattern of liver injury caused by direct virus action and in situ inflammatory response', *Med Hypotheses*, 67: 618-21.

Querec, Troy, Soumaya Bennouna, Sefik Alkan, Yasmina Laouar, Keith Gorden, Richard Flavell, Shizuo Akira, Rafi Ahmed, and Bali Pulendran. 2006. 'Yellow fever vaccine YF-17D activates multiple dendritic cell subsets via TLR2, 7, 8, and 9 to stimulate polyvalent immunity', *The Journal of experimental medicine*, 203: 413-24.

Querec, Troy D., Rama S. Akondy, Eva K. Lee, Weiping Cao, Helder I. Nakaya, Dirk Teuwen, Ali Pirani, Kim Gernert, Jiusheng Deng, Bruz Marzolf, Kathleen Kennedy, Haiyan Wu, Soumaya Bennouna, Herold Oluoch, Joseph Miller, Ricardo Z. Vencio, Mark Mulligan, Alan Aderem, Rafi Ahmed, and Bali Pulendran. 2009. 'Systems biology approach predicts immunogenicity of the yellow fever vaccine in humans', *Nature immunology*, 10: 116-25.

Reinhardt, B., R. Jaspert, M. Niedrig, C. Kostner, and J. L'Age-Stehr. 1998. 'Development of viremia and humoral and cellular parameters of immune activation after vaccination with yellow fever virus strain 17D: a model of human flavivirus infection', *J Med Virol*, 56: 159-67.

Rice, C. M., A. Grakoui, R. Galler, and T. J. Chambers. 1989. 'Transcription of infectious yellow fever RNA from full-length cDNA templates produced by in vitro ligation', *New Biol*, 1: 285-96.

Roehrig, J. T., J. Hombach, and A. D. Barrett. 2008. 'Guidelines for Plaque-Reduction Neutralization Testing of Human Antibodies to Dengue Viruses', *Viral Immunol*, 21: 123-32.

Roosendaal, Jojanneke, Edwin G Westaway, Alexander Khromykh, and Jason M Mackenzie. 2006. 'Regulated cleavages at the West Nile virus NS4A-2K-NS4B junctions play a major role in rearranging cytoplasmic membranes and Golgi trafficking of the NS4A protein', *Journal of Virology*, 80: 4623-32.

Ruiz-Linares, Andrès, Michèle Bouloy, Marc Girard, and Annie Cahour. 1989. 'Modulations of the in vitro translational efficiencies of Yellow Fever virus mRNAs: interactions between coding and noncoding regions', *Nucleic Acids Research*, 17: 2463-76.

Ryman, K. D., T. N. Ledger, G. A. Campbell, S. J. Watowich, and A. D. Barrett. 1998. 'Mutation in a 17D-204 vaccine substrain-specific envelope protein epitope alters the pathogenesis of yellow fever virus in mice', *Virology*, 244: 59-65.

Ryman, K. D., T. N. Ledger, R. C. Weir, J. J. Schlesinger, and A. D. Barrett. 1997. 'Yellow fever virus envelope protein has two discrete type-specific neutralizing epitopes', *J Gen Virol*, 78 ( Pt 6): 1353-6.

Ryman, K. D., H. Xie, T. N. Ledger, G. A. Campbell, and A. D. Barrett. 1997. 'Antigenic variants of yellow fever virus with an altered neurovirulence phenotype in mice', *Virology*, 230: 376-80.

Sarathy, Vanessa V., Mellodee White, Li Li, Jaclyn A. Kaiser, Gerald A. Campbell, Gregg N. Milligan, Nigel Bourne, and Alan D. T. Barrett. 2018. 'Characterization of a murine model of non-lethal, symptomatic dengue virus infection', *Scientific Reports*, 8: 4900.

Saron, W. A. A., A. P. S. Rathore, L. Ting, E. E. Ooi, J. Low, S. N. Abraham, and A. L. St John. 2018. 'Flavivirus serocomplex cross-reactive immunity is protective by activating heterologous memory CD4 T cells', *Sci Adv*, 4: eaar4297.

Sawyer, W. A. 1931. 'The Persistence of Yellow Fever Immunity', *Journal of Preventive Medicine*, 5: 413-28 pp.

Sawyer , W. A., S. F. Kitchen , Martin Frobisher , Jr., and Wray Lloyd 1930. 'THE RELATIONSHIP OF YELLOW FEVER OF THE WESTERN HEMISPHERE TO THAT OF AFRICA AND TO LEPTOSPIRAL JAUNDICE', *Journal of Experimental Medicine*, 51: 493-517.

Sawyer, W. A., and W. Lloyd. 1931. 'THE USE OF MICE IN TESTS OF IMMUNITY AGAINST YELLOW FEVER', *The Journal of experimental medicine*, 54: 533-55.

Sbrana, E., S. Y. Xiao, V. L. Popov, P. C. Newman, and R. B. Tesh. 2006. 'Experimental yellow fever virus infection in the golden hamster (Mesocricetus auratus) III. Clinical laboratory values', *Am J Trop Med Hyg*, 74: 1084-9.

Schlesinger, J. J., M. W. Brandriss, C. B. Cropp, and T. P. Monath. 1986. 'Protection against yellow fever in monkeys by immunization with yellow fever virus nonstructural protein NS1', *J Virol*, 60: 1153-5.

Schlesinger, J. J., M. W. Brandriss, and T. P. Monath. 1983. 'Monoclonal antibodies distinguish between wild and vaccine strains of yellow fever virus by neutralization, hemagglutination inhibition, and immune precipitation of the virus envelope protein', *Virology*, 125: 8-17.

Schlesinger, J. J., M. W. Brandriss, and E. E. Walsh. 1985. 'Protection against 17D yellow fever encephalitis in mice by passive transfer of monoclonal antibodies to the nonstructural glycoprotein gp48 and by active immunization with gp48', *J Immunol*, 135: 2805-9.

Schoggins, John W. 2019. 'Interferon-Stimulated Genes: What Do They All Do?', *Annual Review of Virology*, 6: 567-84.

Serrão de Andrade, Amanda Araújo, André E. R. Soares, Luiz Gonzaga Paula de Almeida, Luciane Prioli Ciapina, Cristiane Pinheiro Pestana, Carolina Lessa Aquino, Marco Alberto Medeiros, and Ana Tereza Ribeiro de Vasconcelos. 2021. 'Testing the genomic stability of the Brazilian yellow fever vaccine strain using next-generation sequencing data', *Interface focus*, 11: 20200063-63.

Shresta, S., K. L. Sharar, D. M. Prigozhin, P. R. Beatty, and E. Harris. 2006. 'Murine model for dengue virus-induced lethal disease with increased vascular permeability', *J Virol*, 80: 10208-17.

Sil, B. K., L. M. Dunster, T. N. Ledger, M. R. Wills, P. D. Minor, and A. D. Barrett. 1992. 'Identification of envelope protein epitopes that are important in the attenuation process of wild-type yellow fever virus', *J Virol*, 66: 4265-70.

Silva, M. L., M. A. Martins, L. R. Espírito-Santo, A. C. Campi-Azevedo, D. Silveira-Lemos, J. G. Ribeiro, A. Homma, E. G. Kroon, A. Teixeira-Carvalho, S. M. Elói-Santos, and O. A. Martins-Filho. 2011. 'Characterization of main cytokine sources from the innate and adaptive immune responses following primary 17DD yellow fever vaccination in adults', *Vaccine*, 29: 583-92.

Smithburn, KC, and Alexander J Haddow. 1949. 'The Susceptibility of African Wild Animals to Yellow Fever1', *Am J Trop Med Hyg*, 1: 389-423.

Smithburn, KC, and AF Mahaffy. 1945. 'Immunization against Yellow Fever. Studies on the Time of Development and the Duration of Induced Immunity', *American Journal of Tropical Medicine*, 25: 217-23.

Stevenson, Lewis D. 1939. 'Pathologic Changes in the Nervous System in Yellow Fever', *Arch. Pathol.*, 27: 249-66 pp.

Stiasny, Karin, and Franz X. Heinz. 2006. 'Flavivirus membrane fusion', *Journal of General Virology*, 87: 2755-66.

Stock, N. K., N. Boschetti, C. Herzog, M. S. Appelhans, and M. Niedrig. 2012. 'The phylogeny of yellow fever virus 17D vaccines', *Vaccine*, 30: 989-94.

Stock, Nina K., Hewád Laraway, Ousmane Faye, Mawlouth Diallo, Matthias Niedrig, and Amadou A. Sall. 2013. 'Biological and Phylogenetic Characteristics of Yellow Fever Virus Lineages from West Africa', *Journal of Virology*, 87: 2895-907.

Stokes, A., J. H. Bauer, and N. P. Hudson. 1928. 'The transmission of yellow fever to Macacus rhesus. 1928', *Rev Med Virol*, 11: 141-8.

Stone, D., A. C. Lyons, Y. S. Huang, D. L. Vanlandingham, S. Higgs, B. J. Blitvich, A. A. Adesiyun, S. E. Santana, L. Leiser-Miller, and S. Cheetham. 2018. 'Serological evidence of widespread exposure of Grenada fruit bats to chikungunya virus', *Zoonoses Public Health*, 65: 505-11.

Strode, G. K., Bugher J. C., Austin-Kerr J., Smith H. H., K. C. Smithburn, Taylor R. M., M. Theiler, Warren A. J., and L. Whitman. 1951. *Yellow Fever* (McGraw-Hill Book Co. Inc.: New York, Toronto & London).

Tassaneetrithep, B., T. H. Burgess, A. Granelli-Piperno, C. Trumpfheller, J. Finke, W. Sun, M. A. Eller, K. Pattanapanyasat, S. Sarasombath, D. L. Birx, R. M. Steinman, S. Schlesinger,

and M. A. Marovich. 2003. 'DC-SIGN (CD209) mediates dengue virus infection of human dendritic cells', *J Exp Med*, 197: 823-9.
Teoh, E. P., P. Kukkaro, E. W. Teo, A. P. Lim, T. T. Tan, A. Yip, W. Schul, M. Aung, V. A. Kostyuchenko, Y. S. Leo, S. H. Chan, K. G. Smith, A. H. Chan, G. Zou, E. E. Ooi, D. M. Kemeny, G. K. Tan, J. K. Ng, M. L. Ng, S. Alonso, D. Fisher, P. Y. Shi, B. J. Hanson, S. M. Lok, and P. A. MacAry. 2012. 'The structural basis for serotype-specific neutralization of dengue virus by a human antibody', *Sci Transl Med*, 4: 139ra83.
ter Meulen, J., M. Sakho, K. Koulemou, N. Magassouba, A. Bah, W. Preiser, S. Daffis, C. Klewitz, H. G. Bae, M. Niedrig, H. Zeller, M. Heinzel-Gutenbrunner, L. Koivogui, and A. Kaufmann. 2004. 'Activation of the cytokine network and unfavorable outcome in patients with yellow fever', *J Infect Dis*, 190: 1821-7.
Tesh, R. B., H. Guzman, A. P. da Rosa, P. F. Vasconcelos, L. B. Dias, J. E. Bunnell, H. Zhang, and S. Y. Xiao. 2001. 'Experimental yellow fever virus infection in the Golden Hamster (Mesocricetus auratus). I. Virologic, biochemical, and immunologic studies', *J Infect Dis*, 183: 1431-6.
Theiler, M. 1930a. 'SUSCEPTIBILITY OF WHITE MICE TO THE VIRUS OF YELLOW FEVER', *Science*, 71: 367.
Theiler, M., and H. H. Smith. 1937. 'THE EFFECT OF PROLONGED CULTIVATION IN VITRO UPON THE PATHOGENICITY OF YELLOW FEVER VIRUS', *The Journal of experimental medicine*, 65: 767-86.
Theiler, Max. 1930b. 'Studies on the Action of Yellow Fever Virus in Mice', *Annals of Tropical Medicine & Parasitology*, 24: 249-72.
Theiler, Max, Andrew Watson Sellards, and AW Sellards. 1928. 'The immunological relationship of yellow fever as it occurs in West Africa and in South America', *Annals of Tropical Medicine & Parasitology*, 22: 449-60.
Thibodeaux, B. A., N. C. Garbino, N. M. Liss, J. Piper, J. J. Schlesinger, C. D. Blair, and J. T. Roehrig. 2012. 'A humanized IgG but not IgM antibody is effective in prophylaxis and therapy of yellow fever infection in an AG129/17D-204 peripheral challenge mouse model', *Antiviral Res*, 94: 1-8.
Thibodeaux, Brett A., Nina C. Garbino, Nathan M. Liss, Joseph Piper, Carol D. Blair, and John T. Roehrig. 2012. 'A small animal peripheral challenge model of yellow fever using interferon-receptor deficient mice and the 17D-204 vaccine strain', *Vaccine*, 30: 3180-87.
Throsby, M., C. Geuijen, J. Goudsmit, A. Q. Bakker, J. Korimbocus, R. A. Kramer, M. Clijsters-van der Horst, M. de Jong, M. Jongeneelen, S. Thijsse, R. Smit, T. J. Visser, N. Bijl, W. E. Marissen, M. Loeb, D. J. Kelvin, W. Preiser, J. ter Meulen, and J. de Kruif. 2006. 'Isolation and characterization of human monoclonal antibodies from individuals infected with West Nile Virus', *J Virol*, 80: 6982-92.
Tomori, Oyewale. 1999. 'Impact of Yellow Fever on The Developing World.' in Karl Margniorosch, Frederick A. Murphy and Aaron J. Shatkin (eds.), *Adv Virus Res* (Academic Press).
Tretyakova, Irina, Brian Nickols, Rachmat Hidajat, Jenny Jokinen, Igor S. Lukashevich, and Peter Pushko. 2014. 'Plasmid DNA initiates replication of yellow fever vaccine in vitro and elicits virus-specific immune response in mice', *Virology*, 468-470: 28-35.
Tuboi, Suely Hiromi, Zouraide Guerra Antunes Costa, Pedro Fernando da Costa Vasconcelos, and Douglas Hatch. 2007. 'Clinical and epidemiological characteristics of yellow fever in

Brazil: analysis of reported cases 1998–2002', *Transactions of the Royal Society of Tropical Medicine and Hygiene*, 101: 169-75.
Twiddy, S Susanna, Jeremy J Farrar, Nguyen Vinh Chau, Bridget Wills, Ernest A Gould, Tamara Gritsun, Graham Lloyd, and Edward C Holmes. 2002. 'Phylogenetic relationships and differential selection pressures among genotypes of dengue-2 virus', *Virology*, 298: 63-72.
Vainio, Jari, Felicity Cutts, and World Health Organization. 1998. "Yellow fever." In.: World Health Organization.
Valentine, Matthew John, Courtney Cuin Murdock, and Patrick John Kelly. 2019. 'Sylvatic cycles of arboviruses in non-human primates', *Parasites & Vectors*, 12: 463.
van den Hurk, A. F., K. McElroy, A. T. Pyke, C. E. McGee, S. Hall-Mendelin, A. Day, P. A. Ryan, S. A. Ritchie, D. L. Vanlandingham, and S. Higgs. 2011. 'Vector competence of Australian mosquitoes for yellow fever virus', *Am J Trop Med Hyg*, 85: 446-51.
van der Schaar, Hilde M., Michael J. Rust, Chen Chen, Heidi van der Ende-Metselaar, Jan Wilschut, Xiaowei Zhuang, and Jolanda M. Smit. 2008. 'Dissecting the cell entry pathway of dengue virus by single-particle tracking in living cells', *PLOS Pathogens*, 4: e1000244-e44.
VanBlargan, Laura A., Leslie Goo, and Theodore C. Pierson. 2016. 'Deconstructing the Antiviral Neutralizing-Antibody Response: Implications for Vaccine Development and Immunity', *Microbiology and molecular biology reviews : MMBR*, 80: 989-1010.
Vasilakis, N., E. R. Deardorff, J. L. Kenney, S. L. Rossi, K. A. Hanley, and S. C. Weaver. 2009. 'Mosquitoes put the brake on arbovirus evolution: experimental evolution reveals slower mutation accumulation in mosquito than vertebrate cells', *PLoS Pathog*, 5: e1000467.
Vieira, W. T., L. C. Gayotto, C. P. de Lima, and T. de Brito. 1983. 'Histopathology of the human liver in yellow fever with special emphasis on the diagnostic role of the Councilman body', *Histopathology*, 7: 195-208.
Vignuzzi, M., J. K. Stone, J. J. Arnold, C. E. Cameron, and R. Andino. 2006. 'Quasispecies diversity determines pathogenesis through cooperative interactions in a viral population', *Nature*, 439: 344-8.
Vogt, Matthew R., Bastiaan Moesker, Jaap Goudsmit, Mandy Jongeneelen, S. Kyle Austin, Theodore Oliphant, Steevenson Nelson, Theodore C. Pierson, Jan Wilschut, Mark Throsby, and Michael S. Diamond. 2009. 'Human monoclonal antibodies against West Nile virus induced by natural infection neutralize at a postattachment step', *Journal of Virology*, 83: 6494-507.
von Lindern, Jana J., Sarah Aroner, Nicholas D. Barrett, Jason A. Wicker, C. Todd Davis, and Alan D. T. Barrett. 2006. 'Genome analysis and phylogenetic relationships between east, central and west African isolates of Yellow fever virus', *Journal of General Virology*, 87: 895-907.
Vratskikh, O., K. Stiasny, J. Zlatkovic, G. Tsouchnikas, J. Jarmer, U. Karrer, M. Roggendorf, H. Roggendorf, R. Allwinn, and F. X. Heinz. 2013. 'Dissection of antibody specificities induced by yellow fever vaccination', *PLoS Pathog*, 9: e1003458.
Wahala, W. M., C. Huang, S. Butrapet, L. J. White, and A. M. de Silva. 2012. 'Recombinant dengue type 2 viruses with altered e protein domain III epitopes are efficiently neutralized by human immune sera', *J Virol*, 86: 4019-23.

Wang, E., S. C. Weaver, R. E. Shope, R. B. Tesh, D. M. Watts, and A. D. Barrett. 1996. 'Genetic variation in yellow fever virus: duplication in the 3' noncoding region of strains from Africa', *Virology*, 225: 274-81.

Watson, A. M., L. K. Lam, W. B. Klimstra, and K. D. Ryman. 2016. 'The 17D-204 Vaccine Strain-Induced Protection against Virulent Yellow Fever Virus Is Mediated by Humoral Immunity and CD4+ but not CD8+ T Cells', *PLoS Pathog*, 12: e1005786.

Wec, Anna Z., Denise Haslwanter, Yasmina N. Abdiche, Laila Shehata, Nuria Pedreño-Lopez, Crystal L. Moyer, Zachary A. Bornholdt, Asparouh Lilov, Juergen H. Nett, Rohit K. Jangra, Michael Brown, David I. Watkins, Clas Ahlm, Mattias N. Forsell, Félix A. Rey, Giovanna Barba-Spaeth, Kartik Chandran, and Laura M. Walker. 2020. 'Longitudinal dynamics of the human B cell response to the yellow fever 17D vaccine', *Proceedings of the National Academy of Sciences of the United States of America*, 117: 6675-85.

Welsch, Sonja, Sven Miller, Ines Romero-Brey, Andreas Merz, Christopher K. E. Bleck, Paul Walther, Stephen D. Fuller, Claude Antony, Jacomine Krijnse-Locker, and Ralf Bartenschlager. 2009. 'Composition and three-dimensional architecture of the dengue virus replication and assembly sites', *Cell Host & Microbe*, 5: 365-75.

Wengler, G., and G. Wengler. 1991. 'The carboxy-terminal part of the NS 3 protein of the West Nile flavivirus can be isolated as a soluble protein after proteolytic cleavage and represents an RNA-stimulated NTPase', *Virology*, 184: 707-15.

Westaway, E. G., J. M. Mackenzie, M. T. Kenney, M. K. Jones, and A. A. Khromykh. 1997. 'Ultrastructure of Kunjin virus-infected cells: colocalization of NS1 and NS3 with double-stranded RNA, and of NS2B with NS3, in virus-induced membrane structures', *J Virol*, 71: 6650-61.

Wheelock, E. Frederick, and William A. Sibley. 1965. 'Circulating Virus, Interferon and Antibody after Vaccination with the 17-D Strain of Yellow-Fever Virus', *New England Journal of Medicine*, 273: 194-98.

Whitman, Loring. 1939. 'Failure of Aëdes Aegypti to Transmit Yellow Fever Cultured Virus (17D)', *The American Journal of Tropical Medicine*, s1-19: 19-26.

WHO, World Health Organization. 1986. "Prevention and control of yellow fever in Africa." In. Geneva: World Health Organization.

———. 2007. "Guidelines for plaque reduction neutralization testing of human antibodies to dengue viruses." In. Geneva: World Health Organization.

———. 2010. 'Expert Committee on Biological Standardization: Recommendations to Assure the Quality, Safety and Efficacy of Live Attenuated Yellow Fever Vaccines; Proposed replacement of: TRS 872, Annex 2 and Amendment to TRS 872, Annex 2, TRS (in press)'.

———. 2015. 'Vaccines and vaccination against yellow fever: WHO Position Paper, June 2013 - recommendations ', *Vaccine*, 33: 76-77.

Wieten, Rosanne W., Emile F. F. Jonker, Ester M. M. van Leeuwen, Ester B. M. Remmerswaal, Ineke J. M. Ten Berge, Adriëtte W. de Visser, Perry J. J. van Genderen, Abraham Goorhuis, Leo G. Visser, Martin P. Grobusch, and Godelieve J. de Bree. 2016. 'A Single 17D Yellow Fever Vaccination Provides Lifelong Immunity; Characterization of Yellow-Fever-Specific Neutralizing Antibody and T-Cell Responses after Vaccination', *PLoS One*, 11: e0149871-e71.

Wisseman, C. L., Jr., B. H. Sweet, M. Kitaoka, and T. Tamiya. 1962. 'Immunological studies with group B arthropod-borne viruses. I. Broadened neutralizing antibody spectrum

induced by strain 17D yellow fever vaccine in human subjects previously infected with Japanese encephalitis virus', *Am J Trop Med Hyg*, 11: 550-61.

Wu, Xueling, Zhi-Yong Yang, Yuxing Li, Carl-Magnus Hogerkorp, William R. Schief, Michael S. Seaman, Tongqing Zhou, Stephen D. Schmidt, Lan Wu, Ling Xu, Nancy S. Longo, Krisha McKee, Sijy O'Dell, Mark K. Louder, Diane L. Wycuff, Yu Feng, Martha Nason, Nicole Doria-Rose, Mark Connors, Peter D. Kwong, Mario Roederer, Richard T. Wyatt, Gary J. Nabel, and John R. Mascola. 2010. 'Rational design of envelope identifies broadly neutralizing human monoclonal antibodies to HIV-1', *Science (New York, N.Y.)*, 329: 856-61.

Xiao, Shu-Yuan, Hui Zhang, Hilda Guzman, and Robert B. Tesh. 2001. 'Experimental Yellow Fever Virus Infection in the Golden Hamster (Mesocricetus auratus). II. Pathology', *The Journal of Infectious Diseases*, 183: 1437-44.

Xie, Xuping, Shovanlal Gayen, CongBao Kang, Zhiming Yuan, and Pei-Yong Shi. 2013. 'Membrane topology and function of dengue virus NS2A protein', *Journal of Virology*, 87: 4609-22.

Yu, I. M., W. Zhang, H. A. Holdaway, L. Li, V. A. Kostyuchenko, P. R. Chipman, R. J. Kuhn, M. G. Rossmann, and J. Chen. 2008. 'Structure of the immature dengue virus at low pH primes proteolytic maturation', *Science*, 319: 1834-7.

Zhang, Xiaokang, Peng Ge, Xuekui Yu, Jennifer M. Brannan, Guoqiang Bi, Qinfen Zhang, Stan Schein, and Z. Hong Zhou. 2013. 'Cryo-EM structure of the mature dengue virus at 3.5-Å resolution', *Nat Struct Mol Biol*, 20: 105-10.

Zhang, Y., J. Corver, P. R. Chipman, W. Zhang, S. V. Pletnev, D. Sedlak, T. S. Baker, J. H. Strauss, R. J. Kuhn, and M. G. Rossmann. 2003. 'Structures of immature flavivirus particles', *EMBO J*, 22: 2604-13.

Zhou, Y., D. Ray, Y. Zhao, H. Dong, S. Ren, Z. Li, Y. Guo, K. A. Bernard, P. Y. Shi, and H. Li. 2007. 'Structure and function of flavivirus NS5 methyltransferase', *J Virol*, 81: 3891-903.

# Appendix A – Neutralization curve of human anti-HIV mAb-VRC01 against YFV 17D and Asibi strains

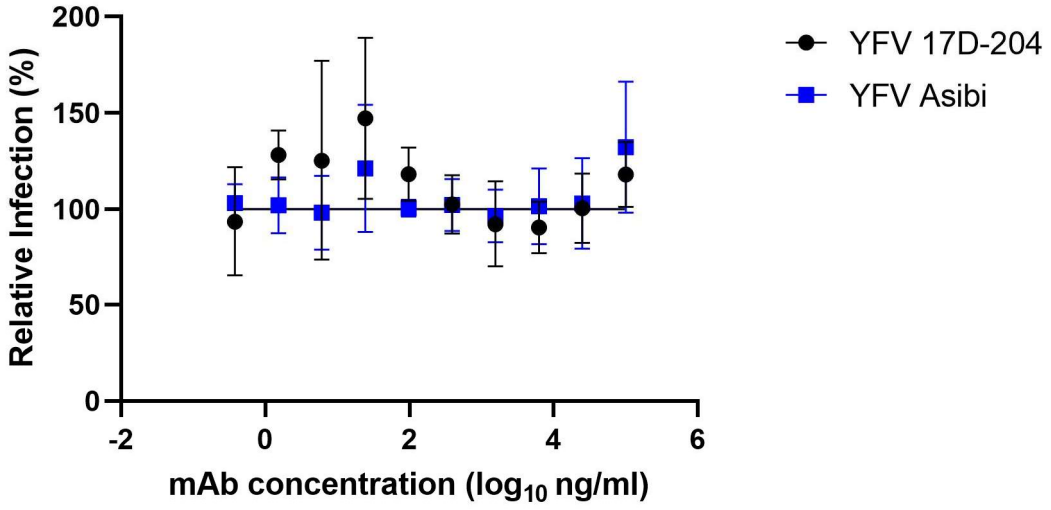


To confirm the neutralization of mAb-29 and mAb-32 were not a result of non-specific binding, the neutralization of the isotype control mAb-VRC01 was evaluated against YFV 17D and Asibi strains. $PRNT_{50}$ was conducted as summarized in Section 2.3.B. No neutralizing activity was observed.